AD-A073 223 UNIVERSITY OF SOUTHERN CALIFORNIA LOS ANGELES DEPT O--ETC F/G 20/5
INFRARED MOLECULAR LASERS PUMPED BY ELECTRONIC TO VIBRATIONAL E--ETC(U)
JUL 79 C WITTIG DAAG29-76-G-0124

UNCLASSIFIED ARO-13711.13-P NL

| OF |
AD
A073223

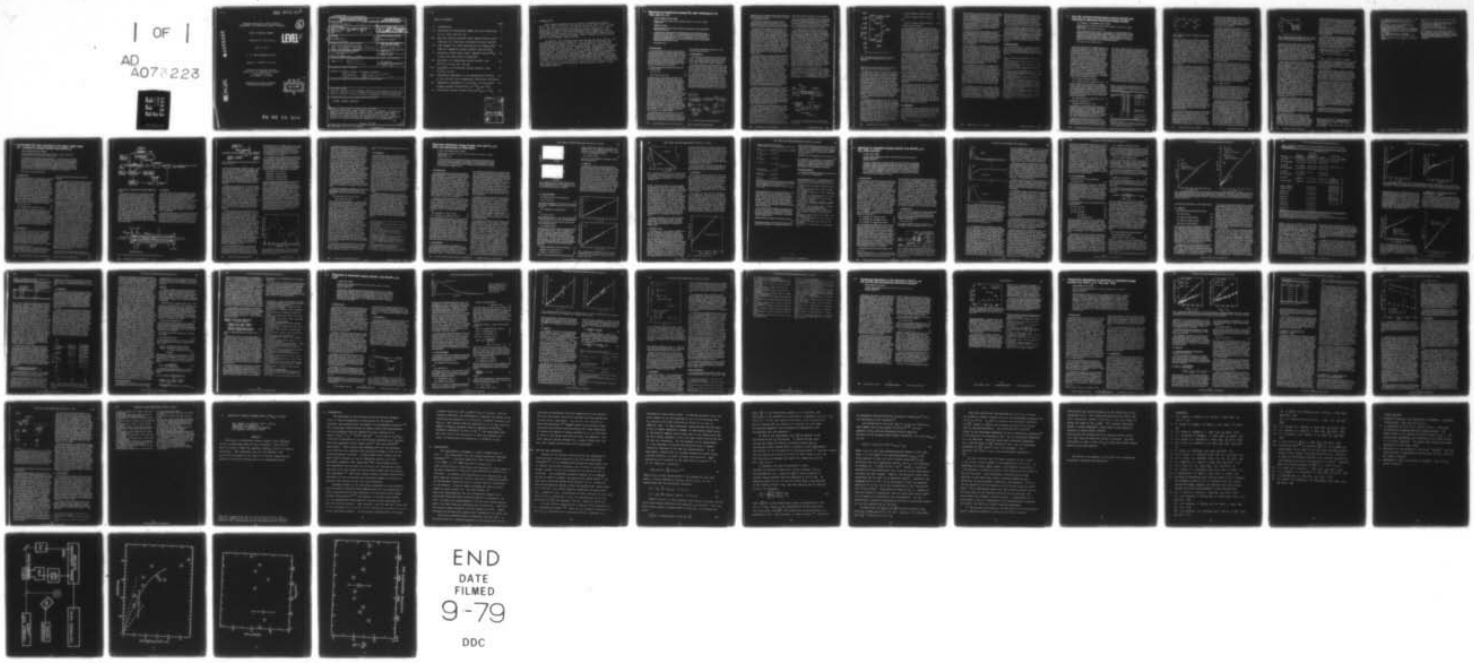

END
DATE
FILMED
9-79
DDC

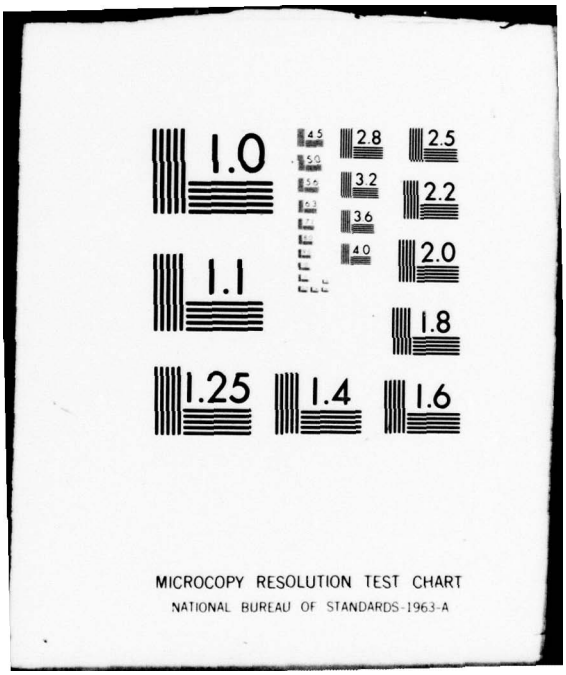
1.0
1.1
1.25
1.4
1.6
1.8
2.0
2.2
2.5
2.8
3.2
3.6
4.0
4.5
5.0
5.6
6.3
7.1
8.0
9.0
MICROCOPY RESOLUTION TEST CHART
NATIONAL BUREAU OF STANDARDS-1963-A

ARO 13711.13-P

INFRARED MOLECULAR LASERS PUMPED BY ELECTRONIC TO VIBRATIONAL ENERGY TRANSFER

(6)

FINAL TECHNICAL REPORT

prepared by Curt Wittig

LEVEL II

July 8, 1979

U. S. ARMY RESEARCH OFFICE

Grant no. DAAG29 76 G 0124

Electrical Engineering Dept.
University of Southern California
University Park
Los Angeles, CA 90007

AD A073223

DDC FILE COPY

APPROVED FOR PUBLIC RELEASE;
DISTRIBUTION UNLIMITED

Unclassified

SECURITY CLASSIFICATION OF THIS PAGE (When Data Entered)

REPORT DOCUMENTATION PAGE

READ INSTRUCTIONS BEFORE COMPLETING FORM

1. REPORT NUMBER: DAAG29-76-G-0124
2. GOVT ACCESSION NO.
3. RECIPIENT'S CATALOG NUMBER

4. TITLE (and Subtitle): Infrared Molecular Lasers Pumped by Electronic to Vibrational Energy Transfer,

5. TYPE OF REPORT & PERIOD COVERED: final report, 26 Jan 76-25 Jan 79
6. PERFORMING ORG. REPORT NUMBER

7. AUTHOR(s): Curt Wittig

8. CONTRACT OR GRANT NUMBER(s): DAAG29-76-G-0124

9. PERFORMING ORGANIZATION NAME AND ADDRESS: Electrical Engineering Dept. Univ. of Southern California, University Park, Los Angeles, CA 90007

10. PROGRAM ELEMENT, PROJECT, TASK AREA & WORK UNIT NUMBERS

11. CONTROLLING OFFICE NAME AND ADDRESS: U. S. Army Research Office, P. O. Box 12211, Research Triangle Park, NC 27709

12. REPORT DATE: July 8, 1979

13. NUMBER OF PAGES: 58 p.

14. MONITORING AGENCY NAME & ADDRESS (if different from Controlling Office): same as 11

15. SECURITY CLASS. (of this report): Unclassified

15a. DECLASSIFICATION/DOWNGRADING SCHEDULE: N/A

16. DISTRIBUTION STATEMENT (of this Report)

Approved for public release; distribution unlimited.

ARO 13711.13-P

17. DISTRIBUTION STATEMENT (of the abstract entered in Block 20, if different from Report)

18. SUPPLEMENTARY NOTES

The view, opinions, and/or findings contained in this report are those of the author(s) and should not be construed as an official Department of the Army position, policy, or decision, unless so designated by other documentation.

19. KEY WORDS (Continue on reverse side if necessary and identify by block number)

LASERS, ENERGY TRANSFER

20. ABSTRACT (Continue on reverse side if necessary and identify by block number)

Electronic-vibrational energy transfer studies are reported. IR lasers are pumped by these state specific transfer events, offering a large number of infrared laser transitions which were not available in the past. Cross sections for relevant processes were measured and the results interpreted in terms of the interaction potentials responsible for our observations.

361 560

DD FORM 1 JAN 73 1473 EDITION OF 1 NOV 65 IS OBSOLETE

Unclassified

TABLE OF CONTENTS

I. INTRODUCTION

This report summarizes our research on AFOSR Grant DAAG29 76 G 0124, which was active during the period 26 Jan. 1976 - 25 Jan. 1979. During this period, we studied several aspects of resonant electronic to vibrational (E→V) energy transfer processes. We developed a number of infrared molecular lasers pumped via these state specific processes, and we measured the energy transfer cross sections relevant to these systems. These results are described in detail in the chapters which follow.

In general, the research went well during the grant period. We encountered no obstacles which we were not able to overcome, and productivity was rather constant. Technologically, our greatest accomplishment was with the E→V pumped lasers; the greatest potential being with the Br^*-CO_2 system. This has been recommended by people both here and in the Soviet Union as a strong candidate for a solar pumped laser. Scientifically, we advanced the scientific community's knowledge of E→V processes substantially. Measuring absolute E→V cross sections and their temperature dependence was perhaps the most valuable contribution here, since simple quenching rate coefficients indicate little about the mechanisms of energy transfer. Fortunately, our data have been systematically compiled for publication during the past three years and are presented and discussed in detail in the following chapters.

11. Electronic-to-vibrational pumped CO_2 laser operating at 4.3, 10.6, and 14.1 μm*

Alan B. Petersen and Curt Wittig

Department of Electrical Engineering, University of Southern California, University Park, Los Angeles, California 90007

Stephen R. Leone

Chemistry Department, University of Southern California, University Park, Los Angeles, California 90007

(Received 20 October 1975)

A pulsed CO_2 laser is described in which the pumping mechanism is electronic-to-vibrational energy transfer from bromine atoms in the $4^2P_{1/2}$ state. Observation of stimulated emission in CO_2 gives detailed information on the specificity of the *E-V* process. The laser operates on the usual 10-μm transitions, as well as two new wavelengths regions near 4.3 and 14.1 μm. Pulse energies 112 mJ at 10.6 μm have been obtained by flash photolyzing 80 Torr of a 1:1 mixture of Br_2 and CO_2. Extension of this laser system to high-pressure sealed-off operation is discussed.

PACS numbers: 42.60.C

I. INTRODUCTION

In a recent publication[1] the authors reported the development of a number of molecular lasers using electronic-to-vibrational (E-V) energy transfer as a pumping mechanism. Electronically excited bromine atoms in the $4^2P_{1/2}$ state, referred to here as Br*, were used to selectively excite vibrational states in molecules, thereby producing the requisite population inversions. We have now undertaken a more detailed study of one of these E-V lasers, the Br*-CO_2 laser.

The laser system described below is based on the following processes:

$$Br_2 \xrightarrow{h\nu} Br + Br^*, \tag{1}$$

$$Br^* + CO_2 \rightarrow Br + CO_2^\dagger + \Delta E, \tag{2}$$

in addition to the various vibration-vibration (V-V) energy-exchange processes that follow process (2). Process (1) proceeds by conventional flash photolysis, leaving the CO_2 essentially unaffected. Process (2) is the near-resonant E-V step. The symbol † denotes vibrational excitation. The energy of Br* is 3685 cm^{-1} and CO_2 is excited to a vibrational state of comparable energy. The over-all rate constant for process (2) is known to be quite large[1] and is sufficiently fast and specific to generate population inversions and stimulated emission on a variety of vibrational-rotational transitions in CO_2. In particular, we have obtained laser action at 4.3, 10.6, and 14.1 μm. Lasing at 4.3 μm has been observed previously in Q-switched CO_2 lasers; however, this occurs on the (10^02)-(10^01) and (02^02)-(02^01) bands.[2] Stimulated emission on the (10^01)-(10^00) band of CO_2 has recently been observed by optical pumping of the upper level with a parametric oscillator.[3] To our knowledge, the 14.1-μm transition has not been seen previously in stimulated emission.

By observing these laser transitions, we have determined that the (10^01) and perhaps the (02^01) state receive a large fraction of the Br* excitation energy. This information was unavailable from previous fluorescence measurements.[1] Observation of stimulated emission in E-V systems involving other molecules may yield similar detailed information.

II. EXPERIMENTAL

The experimental apparatus is shown schematically in Fig. 1. It consists of a quartz laser tube and flashlamp, a glass vacuum system, and the appropriate infrared optical components and detection equipment.

The vacuum system is of a conventional nature, constructed of Pyrex and employing a single liquid-nitrogen trap and mechanical pump. Pressure is measured with mercury and oil manometers and a thermocouple gauge. Oil manometers are made with Dow Corning 704 silicone oil. A column of this oil is also maintained at the top of the mercury manometers to inhibit reaction of the mercury with Br_2. The thermocouple gauge is closed off from the system when corrosive gases are present. Vacuum of a few μm Hg are obtained routinely. Since bromine vapor attacks organic vacuum greases, permanent joints are made with black wax, while nonpermanent joints and stopcocks are greased with a fluorinated compound, DuPont KRYTOX 240 AD. The black wax is

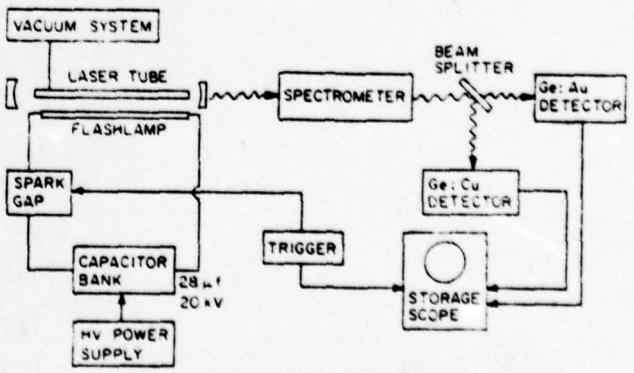

FIG. 1. Schematic diagram of experimental apparatus.

unaffected by Br_2 in moderate concentrations. Corrosive and toxic gases are condensed in the LN_2 trap and vented to a fume hood periodically.

Chemicals are purified in the following manner. Liquid bromine is repeatedly degassed at 77 °K, then distilled from trap to trap. Helium is passed through a trap at 77 °K and CO_2 is passed through a trap at 180 °K.

The laser tube and flashlamp are illustrated in Fig. 2. Both items are constructed of quartz tubing. The laser tube is 20 mm i.d. with active length 150 cm. A 2-mm-thick annular region around the tube contains an organic dye solution, while lasing gas mixtures fill the central section. The ends of the tube are fitted with O-ring joints and Viton O-rings. Various devices can be mated to these joints, as described below. The flashtube is 18 mm i.d. with arc length 150 cm. Argon flows through the lamp at a pressure of 30 Torr. Typical discharge energies are 3500 J. The photolysis flash has a rise time of 5 μsec and half-width of 40 μsec. The flashlamp and laser tube are mounted parallel to one another, separated by 4 cm and optically coupled with aluminum foil.

Molecular bromine has a strong continuous absorption from the near ultraviolet through the green portion of the spectrum, resulting in dissociation.[4] Photolysis in the region $450 \leq \lambda \leq 530$ nm results in equal amounts of excited- and ground-state atoms.[5] In order to improve the effectiveness of the flashlamp in producing Br^*, the laser tube is surrounded by a $2 \times 10^{-3} M$ solution of 7-diethylamino, 4-methyl coumarin dye. This dye transmits light of the desired wavelength and absorbs shorter wavelengths, fluorescing in the region near 480 nm.[6] Thus the lamp output over the range $330 \leq \lambda \leq 530$ nm is useful in producing Br^*, approximately doubling its effectiveness. In practice, we have found this effect reflected in the laser output, since use of a freshly prepared dye solution results in a CO_2 laser signal approximately twice that obtainable without the dye. The dye solution tends to degrade with repeated irradiation and must be replenished frequently.

As previously indicated, the construction of the laser allows for considerable flexibility. When measuring energy of the 4.3- and 10.6-μm output pulses, the ends of the main laser tube are sealed with KCl windows mounted at Brewster's angle, as in Fig. 2. Mirrors are either dielectric or gold coated and separated by 190 cm. Output coupling is through the dielectric mirror or with an intracavity beamsplitter. Energy measurements are performed by focusing the beam into a thermopile, either a Hadron Model 99 or Model 100.

When investigating the more detailed behavior of the 4.3- and 14.1-μm transitions, one end of the laser is sealed with a Brewster window as before. Laser output is coupled through a 0.5-mm hole in a gold-coated mirror ($R = 10$ m). At the other end, an intracavity absorption cell is employed, as shown in Fig. 2. The cell is constructed of Pyrex and stainless steel. Vacuum seals are made with rubber O rings or black wax. This device allows evacuation of a separate region, 23 cm long, between the Brewster window and the mirror. By introducing a few Torr of certain gases into this region, either of the CO_2 laser transitions can be suppressed.

The laser beam is sent through a 0.25-m Jarrell-Ash spectrometer equipped with a 50-line/mm grating blazed at 10 μm. The output of the spectrometer is viewed simultaneously by a Ge : Cu detector and a Ge : Au detector. The spectrometer can be removed from the system and a set of interference filters used in its place.

A simplified energy-level diagram of the $Br^* : CO_2$ system is shown in Fig. 3. We have investigated this system over a wide range of conditions, including laser gas composition and pressure, optical-cavity configuration, and flashlamp input. The traditional 10.4-μm band in CO_2 has been found to lase under almost all conditions, with varying strength and time behavior. Oscillation generally occurred near 945 cm^{-1} in the P branch of the 10.4-μm band. The maximum laser pulse energy obtained in this manner was 112 mJ in a pulse about 10 μsec wide beginning 8 μsec after the onset of the photolysis flash. Conditions were as follows: a cavity composed of a gold-coated total reflector ($R = 10$ m) and a flat AR-coated dielectric mirror (85% R at 10.6 μm); and a laser tube filled with a 1 : 1 mixture of Br_2 and CO_2, total pressure 80 Torr. Pulse energies were not very sensitive to gas pressure. Maintaining Br_2 and CO_2 in the same proportions, total pressure could be increased to 120 Torr with only a small loss in output energy. Although we have made no attempt at wavelength selection, it should be possible to obtain similar energies throughout the 9.4- and 10.4-μm bands.

When using gas mixtures more dilute in CO_2, stimulated emission at 4.3 μm was observed. This oscillation is also quite persistent over a more restricted range of conditions. In fact, this transition due to CO_2 has been observed in gas mixes containing Br_2 and OCS, with CO_2 as an impurity. The 4.3-μm oscillation occurs near

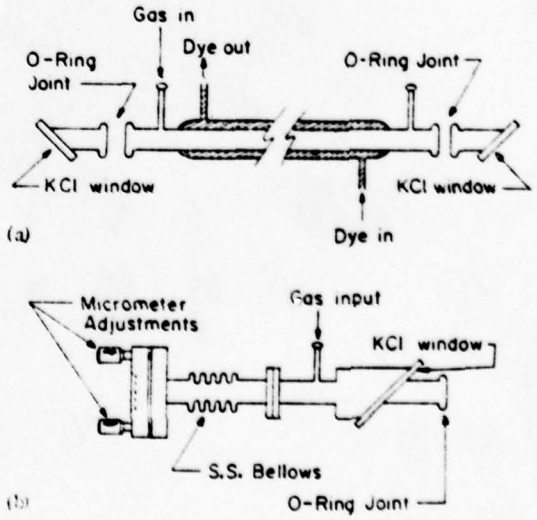

FIG. 2. (a) Quartz laser tube with dye jacket and Brewster-window end pieces. (b) Intracavity absorption cell with internal mirror mount.

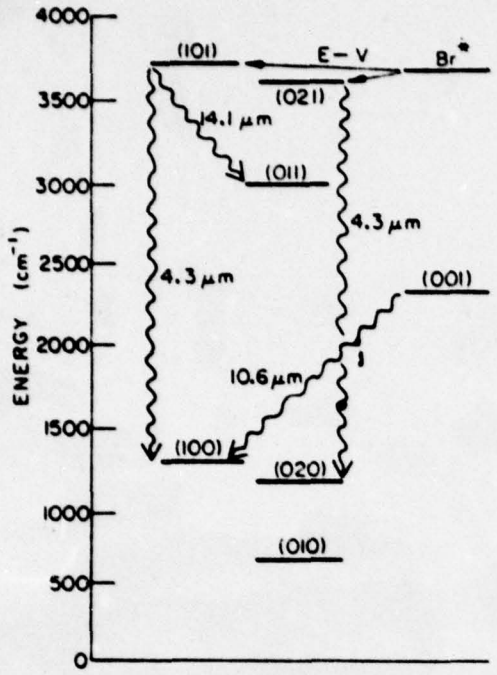

FIG. 3. Simplified energy-level diagram of the Br^*-CO_2 system showing E-V energy-transfer path and laser transitions.

2304 cm^{-1} and we have assigned it to the P branch of either the (10^01)-(10^00) or (02^01)-(02^00) band.

We performed a simple experiment to determine the lower state of this transition, using an extracavity absorption cell containing CO_2. The degree of absorption in this cell, combined with knowledge of approximate band strengths and other data, was sufficient to eliminate the (01^11)-(01^10) band as a possible assignment. Temperature dependence of the absorption indicated a lower-state energy near 1300 cm^{-1}. However, the accuracy of the experiment was not sufficient to determine the state exactly. A transition between the (02^21) and (02^20) states was ruled out because its band center would lie too far away from the observed frequency. Using the constants given by Herzberg,[7] we calculate this to be 2361 cm^{-1}. A precise wavelength measurement of the 4.3-μm transition should make possible a definite assignment.

The strongest laser output at 4.3 μm was ~0.1 mJ. This output pulse was generally 5 μsec wide, occurring between 10 and 15 μsec after the onset of the photolysis flash. An equal amount of energy could also be detected at 10.6 μm under these conditions. These results were obtained with an optical cavity composed of two gold-coated mirrors ($R = 2.6$ m and $R = \infty$) and a ZnSe beam-splitter providing output coupling of about 30%. The gas mixture contained 4 Torr Br_2, 4 Torr He, and 0.05 Torr CO_2. Gas fills containing more than 0.15 Torr CO_2 would not lase at 4.3 μm. We attribute this effect to depopulation of the upper laser level by intramolecular V-V energy transfer. Processes such as

$$CO_2(101) + CO_2(000) \rightarrow CO_2(100) + CO_2(001), \quad (3)$$

$$CO_2(021) + CO_2(000) \rightarrow CO_2(011) + CO_2(010), \quad (4)$$

and

$$CO_2(011) + CO_2(000) \rightarrow CO_2(001) + CO_2(010), \quad (5)$$

are known to proceed rapidly.[3]

Laser emission at 14.1 μm was also observed in dilute CO_2 mixtures. This transition, near 711 cm^{-1} has been assigned to the Q branch of the (10^01)-(01^11) band. The optimum gas fill was 5 Torr, containing 0.5 Torr Br_2, 0.15 Torr CO_2, and the balance He. Laser output usually occurred as a 4-μsec-wide pulse, 20 μsec after the onset of photolysis. The 14.1-μm transition lased well in optical cavities composed of externally mounted gold-coated reflectors using hole coupling. No lasing was observed when a dielectric mirror (90% R at 14.1 μm) was used as an output coupler. We were unable to make an energy measurement. However, by comparing 4.3- and 14.1 μm signals on the Ge:Cu detector, we estimate the 14.1-μm energy to be a few μJ.

Since the 4.3- and 14.1-μm transitions may share the same upper state and thus compete for the same inversion, we investigated the interaction of these two signals. With the intracavity absorption cell in place and evacuated, and employing a gas mixture between the optima for 14.1 and 4.3 μm, we observed stimulated emission at both of these wavelengths, as well as at 10.6 μm. Four Torr of CO_2 in the absorption cell suppressed the 4.3-μm emission, causing a sizeable increase in the 14.1-μm signal. Filling the cell with 10 Torr of HCN and 60 Torr of air stopped oscillation at 14.1 μm, with no noticeable effect on the 4.3-μm signal. HCN absorbs very strongly in the region $790 \gtrsim \nu \gtrsim 640$ cm^{-1}, but addition of air was necessary to broaden the rotational components and completely block the 14.1-μm oscillation. Lasing at 10.6 μm appeared to be unaffected when either of the other transitions was suppressed.

These results are consistent with the relative energy measurements at 4.3 and 14.1 μm. It appears that the 4.3-μm line, having a larger transition moment, requires a lower threshold inversion.[8] This is important since the pumping rate of the (10^01) state, although rapid, is still slower than nonradiative decay rates such as process (3).[1,3] For this reason, relatively little energy can be stored in the (10^01) state. This rapid intramolecular decay tends to populate the very long lived (001) state, making the 10.4-μm band a more efficient way to extract radiation from the gas.

III. DISCUSSION

Observation of a laser transition with the (10^01) state as its upper level confirms our previous belief that this state is a major recipient of the Br^* energy. The (10^01) and (02^01) states in CO_2 are Fermi resonant and, like the (10^00) and (02^00) states, are expected to undergo rapid collision-induced energy-sharing processes,[3] such as

$$CO_2(10^01) + M \rightleftarrows CO_2(02^01) + M, \quad (6)$$

Finzi,[3] however, has concluded that the rate for process (6) can be significantly slower than that for process (3), even with a large excess of inert gas such as argon. Further investigation will be required to determine if the $(02^{0}1)$ state is populated directly by E-V transfer, and, if not, the degree of its excitation via process (2) followed by process (6). In any case, it is likely that excitation of these states, followed by relaxation such as processes (3)–(5), is the dominant mechanism in populating the $(00^{0}1)$ state.

Our Br^{*}-CO_2 results, to date, suggest a number of device applications. Since photolysis light requires several passes through the gas mixture to be completely absorbed, a CO_2 laser with inherently homogeneous excitation of the gain medium can be constructed. Such a device might employ a flashlamp concentric with the laser medium and be useful where transverse mode purity is important.

The fact that Br atoms recombine to form Br_2 and the CO_2 is chemically inert in this system makes the gas mixtures reusable. In dilute CO_2 mixtures, we observe a slow degradation of 4.3- and 14.1-μm output on continued use of a single fill. We attribute this to air leaks and outgassing in the laser tube. Lasing at these wavelengths is particularly sensitive to the presence of H_2O and O_2, because these molecules quench Br^{*} very rapidly.[10] Lasing at 10.6 μm in high-pressure gas mixes shows no such degradation. For this reason, a sealed-off laser seems feasible.

Our experiments with gas mixtures containing 50% Br_2 and 50% CO_2 with no diluent, at pressures up to 120 Torr (limited essentially by the gas handling system and vapor pressure of Br_2) indicate that operation at 1 atm should be possible. Previous optical-gain measurements on the Br^{*}-CO_2 system[1] indicate that there is no loss of inversion when a large excess of helium is added to a Br_2:CO_2 mixture. We have the possibility, therefore, of a high-pressure sealed-off laser. Using various isotopic species of CO_2, such a device might provide optical gain and continuous tuning over many cm^{-1}.

The availability of relatively simple laser sources at new CO_2 wavelengths may be of importance by itself, in diagnostic experiments, for instance. Both the 4.3- and 14.1-μm transitions are sensitive to pumping rate and thus Br^{*} production rate. A flashlamp with a faster rise time and more efficient use of the photolysis light should improve performance at these wavelengths.

Photolysis of IBr also produces Br^{*}[11] and, since the absorption coefficient of IBr is greater than Br_2,[4] this may result in a net improvement. In our experiments, IBr-CO_2 mixtures have been at least as effective in producing CO_2 stimulated emission as comparable Br_2-CO_2 mixtures. However, IBr has the disadvantage of low vapor pressure (5 Torr) at room temperature.

Finally, observation of stimulated emission on the $(10^{0}1)$-$(01^{1}1)$ transition suggests the analogous Q-branch transition $(02^{0}1)$-$(01^{1}1)$ at 607 cm^{-1} (16.5 μm). A laser source in this region of the spectrum is of interest for such applications as isotope separation. By suppressing the 711-cm^{-1} oscillation it may be possible to induce lasing at this frequency. Although our initial attempts to do this have been unsuccessful, this point is worth pursuing.

ACKNOWLEDGMENT

The authors wish to thank J. F. Bott and R. Gross of the Aerospace Corporation, and M. Pitch and M. Buchwald of the Los Alamos Scientific Laboratory, for the loan of experimental equipment during the course of this work.

*Research supported by Energy Research and Development Agency.

[1] A. B. Petersen, C. Wittig, and S. R. Leone, Appl. Phys. Lett. 27, 305 (1975).
[2] D. R. Rao, L. O. Hocker, A. Javan, and K. Knable, J. Mol. Spectrosc. 25, 410 (1968).
[3] J. Finzi and C. B. Moore, J. Chem. Phys. 63, 2285 (1975).
[4] D. J. Seery and D. Britton, J. Phys. Chem. 68, 2263 (1964).
[5] K. R. Wilson, *Excited State Chemistry*, edited by J. N. Pitts, Jr. (Gordon and Breach, New York, 1970), p. 41.
[6] P. I. Petrovich and N. A. Borisevich, Izv. Akad. Nauk. SSSR Ser. Fiz. 27, 703 (1963).
[7] G. Herzberg, *Infrared and Raman Spectra* (Van Nostrand, New York, 1945), p. 276.
[8] See, for example, H. J. Kostkowski and L. D. Kaplan, J. Chem. Phys. 26, 1252 (1957); D. E. Burch, D. A. Gryvnak, and D. Williams, Appl. Opt. 1, 759 (1962). It is assumed that a transition between combination states [i.e., (101)-(100)] has approximately the same oscillator strength as the fundamental transition involving the same change in vibrational quanta [i.e., (001)-(000)].
[9] E. Weitz and G. Flynn, *Annual Review of Physical Chemistry*, edited by H. Eyring (Annual Reviews, Inc., Palo Alto, Calif., 1974), Vol. 25, p. 297.
[10] D. Husain and R. J. Donovan, *Advances in Photochemistry*, edited by J. N. Pitts (Wiley, New York, 1971), Vol. 8, p. 1.
[11] R. J. Donovan and D. Husain, Trans. Faraday Soc. 64, 2325 (1968).

III. H_2O, NO, and N_2O infrared lasers pumped directly and indirectly by electronic-vibrational energy transfer*

A. B. Petersen, L. W. Braverman, and C. Wittig

Department of Electrical Engineering, University of Southern California, University Park, Los Angeles, California 90007

(Received 8 March 1976; in final form 4 June 1976)

Pulsed infrared molecular lasers are reported in which pumping is via electronic-vibrational energy transfer from $Br(4^2P_{1/2})$. H_2O and NO lasers are pumped directly by E-V transfer and operate on a variety of transitions not previously seen in stimulated emission. The N_2O laser operates near 10.9 μm and is pumped by a two-step process involving E-V transfer to an intermediate molecule and subsequent V-V transfer from that molecule to N_2O. This latter technique extends the applicability of E-V pumping to molecules which do not interact directly with the electronically excited species.

PACS numbers: 42.60.Cz, 82.20.Rp, 34.50.−s

Electronic-vibrational (E-V) energy transfer is currently being investigated in the authors's laboratory as a means of pumping ir molecular lasers. Previous publications[1,2] have reported work on lasers pumped by E-V transfer from $Br(4^2P_{1/2})$, hereafter referred to as Br^*, to the molecules CO_2, N_2O, HCN, and C_2H_2. We have now obtained stimulated emission from H_2O and NO, where excitation is again derived by direct E-V transfer from Br^*. Most of the observed laser transitions in these molecules have not been previously reported. In addition, we have demonstrated an extension of the E-V pumping process, a type of "sensitization", whereby population inversion is obtained by sequential E-V and V-V transfers involving an intermediate molecule. This technique has been applied to the Br^*-N_2O system and should make laser action possible in molecular systems where *direct* E-V excitation does not result in population inversion.

The E-V process proceeds as follows:

$$Br^* + (\text{molecule } A) \xrightarrow{k_1} Br + (\text{molecule } A)^\dagger + \Delta E_1, \quad (1)$$

where † denotes vibrational excitation. In instances where k_1 is large, and vibrational excitation appears in a mode-specific manner, population inversions can result. This mechanism is operative in the Br^*-NO and Br^*-H_2O laser systems, as well as the laser systems we have described previously.[1,2] When k_1 does not meet these criteria a second molecule can be introduced to act as an intermediate:

$$Br^* + (\text{molecule } B) \xrightarrow{k_2} Br + (\text{molecule } B)^\dagger + \Delta E_2, \quad (2)$$

$$(\text{molecule } B)^\dagger + (\text{molecule } A) \xrightarrow{k_3}$$

$$(\text{molecule } B) + (\text{molecule } A)^\dagger + \Delta E_3. \quad (3)$$

It is possible to select molecule B such that both processes (2) and (3) are fast and specific. Population inversions in molecule A are generated in this manner. We have applied this principle to cases where molecule A is N_2O and molecule B is either HCl or CO_2. A list of laser transitions observed in the E-V–pumped H_2O, NO, and N_2O systems is given in Table I.

The general experimental technique has been described in Ref. 2. In the work reported here, two distinct laser configurations have been used. In the first device a quartz laser tube, 20 mm in inside diameter with an active length of 150 cm, is surrounded by a 2-mm annular region containing an appropriate dye solution. The ends of the tube are fitted with KBr or KCl Brewster windows. The center portion of the tube is filled with a static gas mixture prepared in a conventional Pyrex vacuum system. These mixtures, containing Br_2 and other species, are photolyzed with a linear quartz flashlamp 150 cm in length and mounted adjacent to the laser tube. The combination of flashlamp and dye solution results in the efficient production of photolysis light in the spectral region near 490 nm, where Br_2 dissociates to form equal amounts of Br and Br^*.[3] In most cases, the other molecular species in the gas mix are unaffected by the photolysis light. Gold-coated or dielectric mirrors are mounted at both ends of the laser tube to form an optical cavity. The second laser device is a triaxial arrangement similar to that found in a high-energy flashlamp-pumped dye laser.[4] The outer 0.7-mm annulus of this device is the flashlamp, the intermediate 2-mm annulus contains a flowing dye solution, and the

TABLE I. Laser transitions observed using E-V pumping. Tentative assignments for some of the H_2O transitions are given. NO and N_2O oscillate on various vibration-rotation lines of the bands indicated.

Laser species	Transition[a] (μm)	(cm^{-1})	Assignment
H_2O[b]	7.093	1410*	(020)-(010) 2_2-3_2
	7.204	1388	(020)-(010) 3_1-4_1
	7.285	1373*	
	7.297	1371	(020)-(010) 3_3-4_3
	7.390	1353	
	7.425	1347*	(020)-(010) 4_2-5_2
	7.453	1342	
	7.543	1326	
	7.590	1317*	
	7.709	1297*	(020)-(010) 6_5-7_7
	7.740	1292	(020)-(010) 6_4-7_4
	16.9	591*	
NO	~5.5	1817	(2, 1) band, P branch
N_2O	~10.9	920	(001)-(100) band, P branch

[a] Accuracy is ± 1 cm^{-1}.

[b] Transitions marked with an asterisk oscillate only in a non-frequency selective cavity, the other transitions oscillate only in a frequency selective cavity.

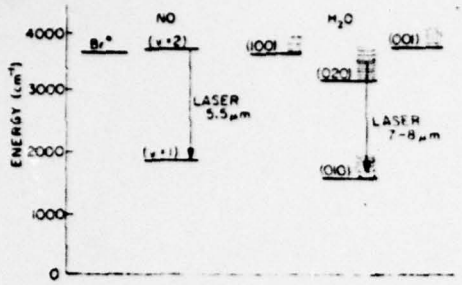

FIG. 1. Energy-level diagram for the Br*-NO and Br*-H_2O laser systems.

central 13-mm-diam section contains the lasing gas mixture. The active length is 48 cm. The ends of the device are fitted with BaF_2 Brewster windows. The flashlamp is driven by a commercial 400-J Marx bank (Phase R Co.). This flashlamp has a short rise time (0.5 μsec) and is more effective in producing laser oscillation in molecular systems where rapid vibrational energy transfer acts to degrade the specificity of process (1). In addition, the flashlamp-driver combination can be operated at 1 Hz, allowing for convenient tuning of the laser transitions by means of an intracavity grating. Stimulated emission from either device is sent through interference filters and a 0.25-m monochrometer, where it is detected by either a Ge:Au or Ge:Cu detector.

Gas mixtures containing Br_2, H_2O, and He produce laser emission at a variety of wavelengths in the 7–8-μm region and at 16.9 μm as listed in Table I. Typically, mixtures are composed of 50% Br_2 and from 3% to 50% H_2O, at total pressures of 5–25 Torr. The transitions marked with asterisks lase in a non-frequency-selective cavity at the lower H_2O concentrations. In the non-frequency-selective cavity the three shortest wavelength lines lase first, beginning at about the peak of the photolysis flash and lasting 1–2 μsec. The transitions at 1297 and 1317 cm^{-1} begin lasing immediately thereafter and have a duration of 5–10 μsec. At higher H_2O concentrations and higher flashlamp energies these two become dominant, the other three decrease in intensity, and the line at 16.9 μm appears. Using a gas mixture of 50% Br_2, 10% H_2O, and 40% He, at a total pressure of 20 Torr, we have observed separately each of the listed transitions between 7 and 8 μm. These results were obtained using the 48-cm device with an intracavity grating. The BaF_2 Brewster windows prevent lasing beyond 9 μm. By introducing optical components of known loss into the cavity, we estimate the round-trip gain of the five persistent lines at 20–30% per pass. Using a pyroelectric detector, we estimate the combined energy of the five strongest lines at 100–500 μJ.

A partial energy level diagram of the Br*-H_2O system is given in Fig. 1. Tentative assignments in the (020)-(010) band have been made for several of the H_2O transitions. Definite assignments for all the lines will require further experiments and more precise wavelength measurements. It appears that the strongest of the transitions, at 1297 cm^{-1}, is the same one previously observed in FIR H_2O lasers.[5] The upper level of this transition is near resonant with, and perturbed by, rotational states in (100) and (001). The respective amounts of stretching and bending excitation imparted to H_2O vis reaction (1) is an open question. Separate experiments which will answer this question are in preparation in our laboratory.

Photolysis of gas mixtures containing Br_2, NO, and He produces stimulated emission near 5.5 μm. A vibrational-energy-level diagram of the Br*-NO laser system appears in Fig. 1. Strongest laser output occurs with a gas mix composed of 50% Br_2, 45% He, and 5% NO, at a total pressure of 5 Torr in the 150-cm device and 20 Torr in the 48-cm device. Lasing occurs in a pulse ~1 μsec wide, slightly after the peak of the photolysis flash. Lasing occurs near 1817 cm^{-1}, with the precise frequency varying from pulse to pulse. This makes accurate frequency measurements difficult. However, the mean value, 1817 cm^{-1}, corresponds roughly to the center of the *P* branch of the NO(2,1) band. We have established, by other means, that lasing is indeed occurring on the (2,1) band as a result of *E-V* excitation. Using the same technique employed in the Br*-H_2O system, we estimate gain in the 48-cm device at 5% per pass. Output pulse energies from the Br*-NO laser were somewhat less than those obtained from the Br*-H_2O system.

The details of the NO laser are complex, and considerable effort has been devoted to determining the laser species, the laser transitions, and the pumping mechanism(s). The main complication arises from the fact that Br_2 and NO react spontaneously to form NOBr when allowed to come to equilibrium in the presence of room light. Such a mixture, when put in the laser tube, *does not* lase on the first photolysis flash, but *does* lase on subsequent flashes. We attribute this behavior to the photolytic production of a large density of Br atoms, which undergo the following reaction[6]:

$$Br + NOBr \rightarrow NO + Br_2. \quad (4)$$

Thus, the effect of the first photolysis flash is to regenerate a portion of the original NO. Nitric oxide and molecular bromine form a stable mixture once inside the laser tube, since room light is excluded by an enclosure. Our hypothesis is further supported by the fact that identical 10:1:10 mixtures of Br_2, NO, and He, when prepared with the room lights off, lase on the first flash, as well as subsequent flashes.

Previously, NO has been observed to lase on vibrational transitions following flash photolysis of NOCl.[7,8] Only laser transitions in the (6,5) and higher bands have been reported. Basco and Norrish[9] have shown that vibrational excitation of the NO fragment can result from photodissociation of NOCl and NOBr. However, very little photolysis and no vibrational excitation occur when photolysis light is limited to $\lambda > 300$ nm. In our device, absorption by the dye solution restricts the light to $\lambda > 450$ nm, and photodissociation of NOBr is unimportant in the production of vibrationally excited NO. To further establish that *E-V* excitation of NO is the laser pumping mechanism, gas mixtures of 4 Torr He and 0.2 Torr NOBr or 0.2 Torr NOCl were photolyzed. Experimental conditions were maintained the

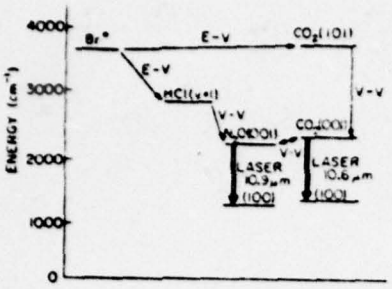

FIG. 2. Simplified energy-level diagram of the Br^*-N_2O laser system. Energy transfer processes are shown, which are important in the indirect pumping of N_2O via HCl or CO_2.

same as in previous experiments, but these mixtures, containing no excess of Br_2, did not lase. Referring to Fig. 1, it can be seen that $NO(v=2)$ and Br^* are very close in energy, while the energy of $NO(v=3)$ will lie almost 1900 cm^{-1} above Br^*. For this reason, E-V excitation of NO by Br^* can only be significant for $v \leq 2$. Since the 5.5-μm stimulated emission from our device shows no appreciable attenuation, when passed through a 4-cm long cell containing 6 Torr of NO, we conclude that lasing is occurring on the (2,1) band.

Earlier experiments with N_2O [1] have shown that direct E-V transfer from Br^* to N_2O results in a small amount of optical gain, ~0.001 cm^{-1}, on the usual (001)-(100) laser transitions. Using the 150-cm device, we have been unable to obtain laser oscillation using gas mixes that contain *only* Br_2, N_2O, and a buffer. However, by combining Br_2, CO_2, and N_2O we obtain stimulated emission from both CO_2 and N_2O. As shown in Fig. 2, E-V transfer selectively excites the ν_3 mode of CO_2. This excitation is rapidly shared through V-V processes with the ν_3 mode of N_2O. To further explore this indirect E-V pumping mechanism, or "sensitization", HCl was substituted for CO_2 in the gas mixtures. The energy-level scheme of this system is also shown in Fig. 2. E-V excitation of HCl is extremely rapid,[10] while V-V transfer from HCl to N_2O is believed to be fast. Thus, HCl is an effective intermediate in this two-step pumping process. Using the 150-cm device, gas mixtures of 5 Torr Br_2, 1 Torr HCl, 3 Torr N_2O, and 16 Torr He produce N_2O laser pulses of several mJ near 10.9 μm.

In all fairness, it should be pointed out that direct E-V excitation from Br^* has failed to produce stimulated emission in a number of molecules. We have tried D_2O, SO_2, OCS, CS_2, and CH_4 at various times without success. Although the quenching of Br^* has been measured and found to be rapid[11-13] for all of these species except SO_2, lack of specific E-V transfer and/or deleterious intramolecular energy transfer processes may prevent laser oscillation.

Our experimental results contribute to an understanding of some aspects of E-V transfer. Laser emission on the (2,1) band of NO, resulting from E-V transfer, further points out the importance of energy resonance in this process. Quenching of Br^* by NO is very rapid,[11] and our results indicate that excitation of $v=2$ is a major deactivation channel. Previous studies have shown that more than one quantum can be *efficiently* excited by E-V exchange for the cases $Br^* + CO_2$ [1,2] and $I^* + HF$.[14] It will be interesting to study E-V transfer from I^* to NO. This process is near resonant for $\Delta v = 4$, and quenching of I^* by NO is also rapid.[11] Quenching of Br^* by O_2 is efficient,[15] and it may be that the paramagnetic nature of NO and O_2 is important in quenching spin-orbit states such as Br^* and I^*. Further experiments will be required to resolve these and other questions.

Our results are also of technological significance, since the Br^*-H_2O laser represents the first simple line tunable laser source operating between 7 and 8 μm. The dense vibration-rotation spectrum of H_2O in this region suggests that greater tunability is possible. E-V excitation of H_2O may also generate population inversions on the FIR H_2O laser transitions.

Stimulated emission from NO in the Br^*-NO system is rather weak. Processes such as

$$NO(v=2) + NO(v=0) - 2\ NO(v=1) - 28\ cm^{-1} \quad (5)$$

and

$$NO(v=1) + NO(v=0) - 2\ NO(v=0) + 1876\ cm^{-1} \quad (6)$$

are very rapid[16] and it is probable that kinetic processes involving NO will limit this system to low-pressure low-power operation. Nevertheless, an NO laser operating on the (2,1) band may be a useful probe for vibrationally excited NO.

The sensitization technique, particularly utilizing a diatomic such as HCl, further increases the generality of E-V transfer as a laser pumping mechanism. Using this technique, it should be possible to obtain stimulated emission from a variety of molecules which do not interact directly with the electronically excited atom.

As a final note, we would like to point out that E-V laser systems are not necessarily limited to pulsed operation. We have collinearly propagated a cw CO_2 probe laser and a 1-W 488-nm Ar laser through a low-pressure gas cell (3.5 mm in diameter × 20 cm) containing Br_2 and CO_2, and observed 2–3% gain at 10.6 μm. The measured gain is within an order of magnitude of the theoretical maximum, taking into account the pumping rate and loss rate due to spontaneous emission, vibrational deactivation, diffusion, etc. No other fundamental limitations were detected. By using a higher pumping rate,[17] it would be straightforward to obtain oscillation at CO_2 laser frequencies, and it may also be possible to obtain cw operation at other molecular frequencies.

The authors acknowledge many enlightening discussions with S.R. Leone, and the loan of equipment by J. Bott, R. Gross, and M.D. Levenson.

*Research supported by the U.S. Energy Resource Development Agency, and by the U.S. Army Research Office.

[1] A.B. Petersen, C. Wittig, and S.R. Leone, Appl. Phys. Lett. 27, 305 (1975).
[2] A.B. Petersen, C. Wittig, and S.R. Leone, J. Appl. Phys. 47, 1051 (1976).

[3]K.R. Wilson, *Excited State Chemistry*, edited by J.N. Pitts, Jr. (Gordon and Breach, New York, 1970), p. 41.
[4]T. Morrow and H.T.W. Price, Opt. Commun. 10, 133 (1974).
[5]B. Hartmann, B. Kleman, and G. Spangstedt, IEEE J. Quantum Electron. QE-4, 296 (1968).
[6]The rate constant of this reaction is expected to be large by analogy with the reaction $NOCl + Cl \rightarrow NO + Cl_2$, which has been studied [W.G. Burns and F.S. Dainton, Trans. Faraday Soc. 48, 52 (1952)].
[7]M.A. Pollack, Appl. Phys. Lett. 9, 94 (1966).
[8]C.R. Guiliano and L.D. Hess, J. Appl. Phys. 38, 4451 (1967).
[9]N. Basco and R.G.W. Norrish, Proc. Roy. Soc. A 268, 291 (1962).
[10]S.R. Leone and F.J. Wodarczyk, J. Chem. Phys. 60, 314 (1974).
[11]D. Husain and R.J. Donovan, Adv. Photochem. 8, 1 (1971).
[12]S.R. Leone, Ph.D. thesis (University of California, Berkeley, 1974) (unpublished).
[13]V. Kushawaha and C. Wittig (unpublished).
[14]F.J. Wodarczyk and P.B. Sackett, Chem. Phys. 12, 65 (1976).
[15]R.J. Donovan and D. Husain, Chem. Rev. 70, 489 (1970).
[16]J.C. Stephenson, J. Chem. Phys. 59, 1523 (1973).
[17]High-power microwave lamps are available which produce hundreds of Watts in the portion of the spectrum required for Br^* production (Fusion Systems Corp., Rockville, Maryland).

IV. Line-tunable CO_2 laser operating in the region 2280–2360 cm^{-1} pumped by energy transfer from $Br(4^2P_{1/2})$[a]

Alan B. Petersen[b] and Curt Wittig[c]

Electrical Engineering Department, University of Southern California, Los Angeles, California 90007
(Received 2 February 1977; accepted for publication 10 May 1977)

A line-tunable CO_2 laser operating in the region 2280–2360 cm^{-1} is described. The laser is pumped by electronic-to-vibrational energy transfer from $Br(4^2P_{1/2})$ atoms, which are produced directly by the pulsed photolysis of Br_2 to CO_2 molecules. The energy-transfer process is shown to be mode specific, populating the (10^01) state of CO_2 directly and thereby providing for stimulated emission on the (10^01)-(10^00) band near 4.3 μm. The experimental arrangement provides a simple line-tunable source of laser radiation in this, as well as other, ir spectral regions. Further, the arrangement is quite convenient and easy to use since the technology involved is derived from that of flash-pumped dye and Nd lasers, and the laser gas samples do not degrade with use, allowing the system to be operated in a sealed-off mode.

PACS numbers: 42.55.Dk, 82.20.Rp, 34.50.Ez

I. INTRODUCTION

In previous publications,[1–3] the authors have reported the development of pulsed infrared molecular lasers pumped by electronic-to-vibrational (E-V) energy transfer from $Br(4^2P_{1/2})$, hereafter referred to as Br^*, to small polyatomic molecules. As a consequence of the selective nature of the excitation process, we have obtained laser oscillations in the region 3.85–16.9 μm from the species HCN, CO_2, N_2O, NO, and H_2O. In all of these experiments, Br^* was generated by the pulsed photolysis of Br_2 in the blue-green portion of the spectrum. These experiments have, for the most part, been carried out with a conventional flash photolysis apparatus, using a high-energy linear flashlamp. In this paper, we report a detailed investigation of the 4.3-μm-region CO_2 laser which is pumped by the processes

$$Br_2 + h\nu \rightarrow Br + Br^*, \tag{1}$$

$$Br^* + CO_2(000) \rightarrow Br + CO_2(10^01) - 30\ cm^{-1}. \tag{2}$$

A triaxial flashlamp arrangement was used in the present study, and this design provides significant improvement over linear flashlamp arrangements with regards to excitation rise time and prf, so that we have been able to investigate the E-V–pumped laser systems more carefully than before. In addition, the simplicity of the present design encourages duplication by other experimenters who may have use for the particular characteristics of one of the E-V–pumped molecular lasers.

II. EXPERIMENTAL

The principles of operation of the various E-V laser systems have been described in Refs. 1–3. Briefly, static gas mixtures containing Br_2 and a second molecular species are subjected to flash photolysis in the blue-green spectral region. Photodissociation of the Br_2 yields both Br and Br^*.[4] The second molecular species is unaffected by the photolysis flash, but is vibrationally excited by E-V transfer from Br^*. Lasing occurs on vibrational transitions in the second molecule.

A block diagram of the arrangement used in the present experiments is shown in Fig. 1. The apparatus differs from that used previously in that it is more compact, convenient to operate, and capable of prf's ≥ 1 Hz. In addition, the shorter rise time (0.5 μsec) of the photolysis light in this device is prerequisite to minimizing the deleterious effects of energy-transfer collisions which act to degrade the specificity of processes such as process (2). The laser itself is a triaxial device, combining a flashlamp, cooling jacket, and laser tube. A cross-sectional view of the device is shown in Fig. 2. Two pieces of commercial quartz tubing and two cylindrical stainless-steel electrodes are assembled with epoxy to form a coaxial-type flashlamp. The flashlamp annulus is 0.7 mm wide, with a diameter of 23 mm, and an arc length of 48 cm. A separate 12-mm-i.d. Pyrex tube passes through the center of the lamp. The 2-mm annulus between the Pyrex tubing and the flashlamp contains a solution of 7-diethylamino 4-methyl coumarin dye dissolved in ethanol. This solution is circulated in a closed cycle through the annulus and a water-cooled heat exchanger. The dye solution has the dual purpose of cooling the lamp and also increasing the production of Br^* because of its strong fluorescence in the blue-green spectral region.[2] The central Pyrex tube is connected to a conventional glass vacuum system and is filled with the laser gas mixtures. All vacuum connections are made with Pyrex and Viton, using a small amount of fluorinated grease, Krytox 240 AD, for lubrication. The ends of the laser tube are fitted with O-ring joints and removable Brewster windows. The flashlamp contains a static fill of ~70 Torr of xenon, supplied from a separate gas-handling system. Nominally, after a day of experiments, the lamp is evacuated and refilled. The outside of the lamp is wrapped with heavy-duty aluminum foil, serving as a current return and light reflector. A loosely fitting Lucite tube surrounds the entire flashlamp. Air is passed through the annulus space thus formed, and provides additional cooling.

Chemicals were purified as follows: Helium was passed through a trap at 77 °K. CO_2 was passed through

[a]Research supported by the U.S. Army Research Office.
[b]Present address: University of Cambridge, Physical Chemistry Dept., Lensfield Road, Cambridge CB2 1EP, England.
[c]Person to whom correspondence should be addressed.

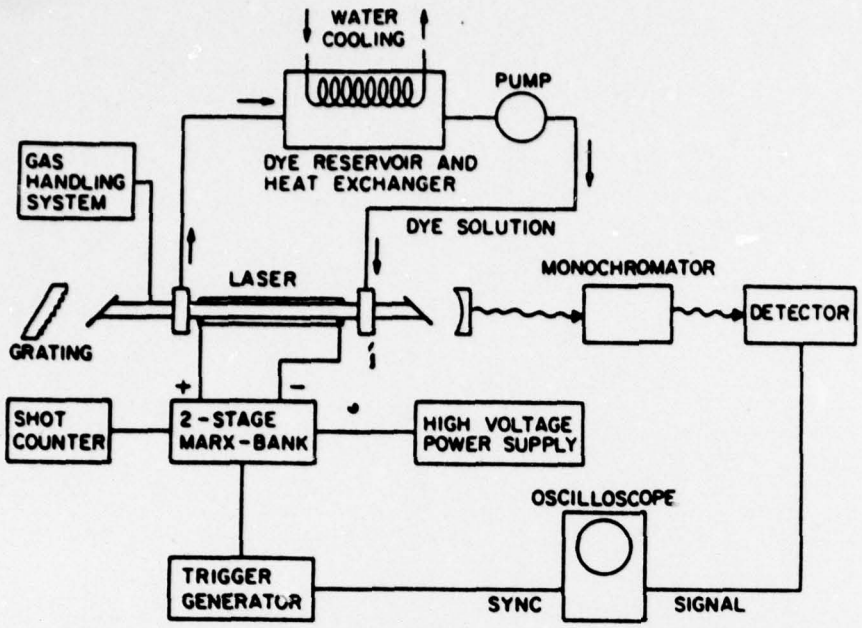

FIG. 1. Schematic drawing of the experimental arrangement.

a trap at 179 °K. Liquid Br_2 was repeatedly degassed at 233 °K.

The flashlamp is driven by a two-stage Marx-bank (Phase-R Co.), mounted in an aluminum frame. The top of the frame serves as an optical bench for the laser tube and optical components. The Marx-bank is charged by a 25-kV power supply. Maximum energy storage is 625 J, but almost all laser experiments are performed with discharge energies ≤ 400 J. Using discharge energies of 200—400 J, flashlamp output typically occurred in a burst, having a rise time of 0.5 μsec and FWHM of 1.0 μsec. This was followed by a long tail, 25% of the peak intensity, lasting 25 μsec. Xenon gas fills produced the most intense light output, followed by krypton and argon. Output from xenon was about three times greater than that from an equal amount of argon. The flashlamp has been discharge over 15 000 times in a one-month period with no observable degradation in performance.

III. RESULTS

Using this device we have investigated laser transitions in CO_2, HCN, H_2O, and NO. Results of the H_2O and NO work have been reported briefly elsewhere.[3] As with the previous laser apparatus,[2] stimulated emission from CO_2 is observed near 10.6, 4.3, and 14.1 μm. Output pulse energies of 15 mJ at 10.6 μm are obtained using laser gas mixtures containing 1:1, Br_2:CO_2 at a total pressure of ≈ 65 Torr, and 400 J of flashlamp energy. Lower energies are obtained using mixture diluted with He to a pressure of 1 atm, the limit of the apparatus.

Stimulated emission near 4.3 μm was observed during photolysis of gas mixtures containing CO_2 and Br_2 and this emission was investigated in detail. Such emission occurred in mixtures where the CO_2 content was ≤ 5%. Lasing was very persistent, and occurred at CO_2 partial pressures as low as a few mTorr in high-Q optical

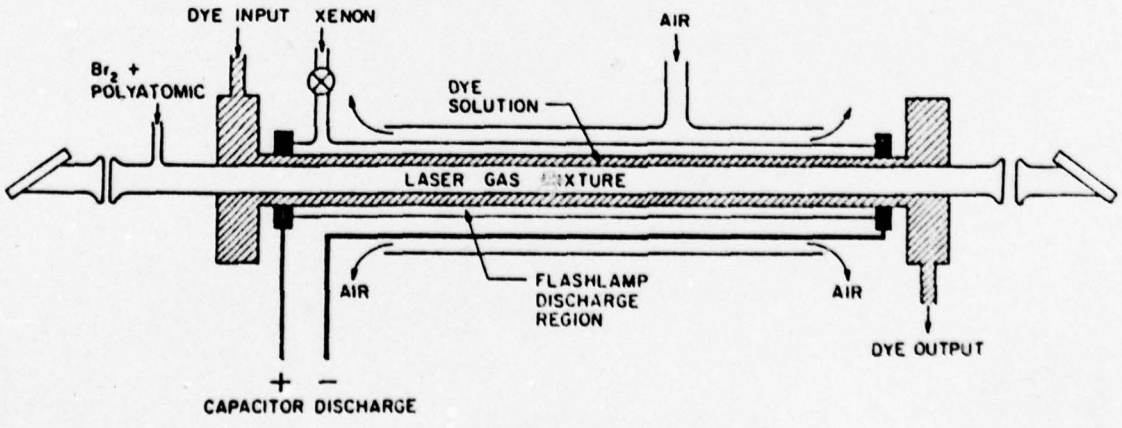

FIG. 2. Cross-sectional view of the combined flashlamp and photolysis tube.

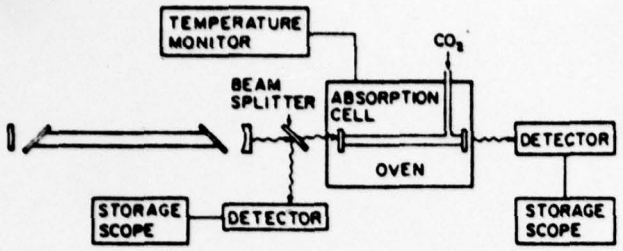

FIG. 3. Schematic drawing of the temperature-dependent absorption experiment.

cavities. Lasing generally occurred in a pulse ~5 μsec wide. The 4.3-μm emission has been assigned to the $(10^0 1)$-$(10^0 0)$ band for reasons to be described below. Stimulated emission near 4.3 μm from CO_2 was first observed by Rao *et al.* in a *Q*-switched CO_2 laser.[5] However, these oscillations occurred on the $(10^0 2)$-$(10^0 1)$ and $(02^0 1)$-$(02^0 0)$ bands and are not a consequence of a selective excitation process but rather the fast depopulation of the ν_3 mode by stimulated emission at 10.6 μm.

Strongest laser emission at 4.3 μm occurred using gas mixtures containing 50% Br_2, 1–2% CO_2, and the balance He. No lasing at 4.3 μm was observed in gas mixtures where Ar was used as a diluent in place of He. Optimum total gas pressures were 20–25 Torr. Laser pulses of 0.5 mJ were obtained using an optical cavity composed of a gold mirror and a dielectric mirror 73%*R* at 4.3 μm. Optical gain is quite high, estimated at ≥ 30% per pass, which is reasonable since the laser transitions involve the change of a single quantum of ν_3 excitation. The transition moment for $\Delta\nu_3 = 1$ transitions in CO_2 is large, allowing large optical gains to occur with relatively small inversion densities.

The laser frequency in a non-frequency-selective cavity was measured as 2304 ± 2 cm^{-1} (4.34 μm). This corresponds roughly to $(10^0 1)$-$(10^0 0)$ *P*(26), although several similar overlapping bands exist with upper levels energetically accessible to Br^*. Bands such as $(01^1 1)$-$(01^1 0)$, $(10^0 1)$-$(10^0 0)$, $(02^0 1)$-$(02^0 0)$ and $(02^2 1)$-$(02^2 0)$ were all possible, while $(11^1 1)$-$(11^1 0)$ and $(03^0 1)$-$(03^0 0)$ seemed less likely because their upper levels are several hundred cm^{-1} above the energy of Br^* (3685 cm^{-1}). Since these bands are all overlapping, it is nontrivial to make an unambiguous assignment on the basis of the many measured laser frequencies *alone*. Thus, rather than trying to measure the laser frequencies to high accuracy (we did not have a high-resolution monochromator available for these measurements) we adopted several alternate techniques that would allow us to identify the laser transitions. With a sufficiently high-resolution monochromator, it is likely that unambiguous assignments could have been made on the basis of line assignments alone.

It was noted that the laser output was strongly absorbed in a small gas cell containing CO_2 at a few Torr pressure. Taking advantage of this fact, an experiment was designed to determine which transition was responsible for lasing. The experimental arrangement is shown in Fig. 3. Output from the 4.3-μm laser was passed through a cell containing known amounts of CO_2. The degree of absorption was determined by comparing signals from two detectors. The change in this absorption was monitored as the temperature of the absorbing gas was increased.

All of the above "hot" bands, involving absorption of one ν_3 quantum, were assumed to have nearly the same transition dipole.[6] Differences in their absorption strengths would then be due mainly to thermal population of their lower levels. Using the value 2700 cm^{-2} atm^{-1} for the $(00^0 0)$-$(00^0 1)$ band strength[7] and the relative line-strength calculations of Gray,[8] the following approximate absorption coefficients were obtained:

$(00^0 0)$-$(00^0 1)$ 11.0 cm^{-1} $Torr^{-1}$

$(01^1 0)$-$(01^1 1)$ 0.45 cm^{-1} $Torr^{-1}$

$(02^0 0)$-$(02^0 1)$ 0.023 cm^{-1} $Torr^{-1}$

$(10^0 0)$-$(10^0 1)$ 0.014 cm^{-1} $Torr^{-1}$

The above values assume absorption at the center of a Doppler-broadened *P*-branch line with $J = 20$ and $T = 300\,^\circ K$. From the absorption observed in the experiment, it was immediately clear that the absorbing, and therefore lasing, transition could not be $(01^1 1)$-$(01^1 0)$. The absorption coefficient obtained, as well as its temperature dependence, indicated that the lower energy level of the transition was at 1300 cm^{-1}, a value near the $(10^0 0)$, $(02^0 0)$, and $(02^2 0)$ levels. Unfortunately, the precision of the experiment was not sufficient to distinguish among these three. The $(02^2 1)$-$(02^2 0)$ transition was ruled out, however, by other means. Using the constants given by Herzberg,[6] its band center was calculated to be 2361 cm^{-1}. Lasing at 2304 cm^{-1} would require that the transition be roughly *P*(60). That the largest optical gain would occur on such a high-*J* transition is extremely unlikely.

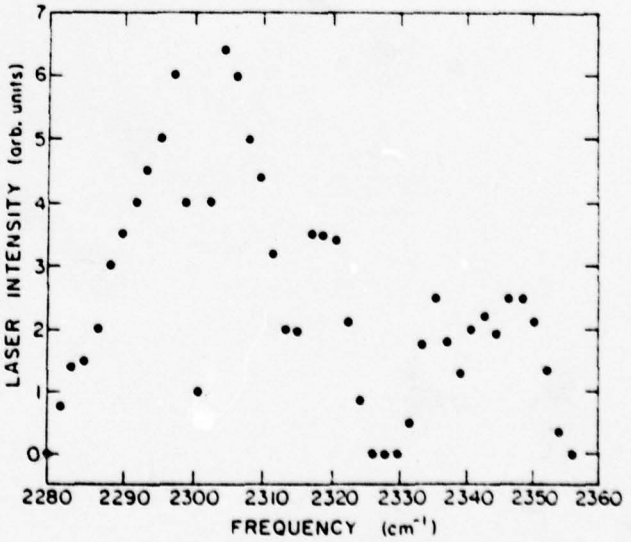

FIG. 4. Frequency spectrum of the 4.3-μm CO_2 laser obtained by tuning the intracavity grating. The circles show relative output intensity at various grating settings. Shot-to-shot fluctuations are approximately 10%.

Assignment was thus narrowed down to the (10^01)-(10^00) and (02^01)-(02^00) bands centered at 2326.59 and 2327.36 cm^{-1}, respectively. Lasing on either or both of these bands seemed quite plausible. Using the device shown in Fig. 2 equipped with an intracavity grating, laser oscillation was tuned throughout the (as yet unidentified) band and found to extend over a range of ≈ 80 cm^{-1}. This tuning range is comparable to that observed on the usual 9.4- and 10.4-μm laser bands in CO_2. A plot of stimulated emission intensity versus frequency is shown in Fig. 4. The results show a P- and R-branch profile, as expected of either of the bands, both of which are Σ-Σ bands. There are several "holes" in the laser spectrum, however, of which one, at ≈ 2300 cm^{-1}, is particularly pronounced. These "holes" and the spectrum in general were quite repeatable in successive measurements. Several explanations for these "holes" are possible, but the most likely is that there are accidental coincidences between the laser transitions and absorbing CO_2 transitions which involve unexcited CO_2 molecules. Oscillation at these frequencies is prevented because of the absorption, due to CO_2 in the atmosphere, or unexcited CO_2 in the laser tube.

To check this hypothesis, frequencies of the rotational components in the (10^01)-(10^00), (02^01)-(02^00), and (00^01)-(00^00) bands were calculated using the standard formula[9]

$$\nu = \nu_0 + (B'' + B')m + (B'' - B' - D'' + D')m^2 - 2(D'' + D')m^3 - (D'' - D')m^4. \quad (3)$$

Here ν is the calculated frequency, ν_0 is the frequency of the band center, and B and D are rotational constants of the upper and lower vibrational states, denoted by u and l. For R-branch lines, $m = J + 1$, and for P-branch lines, $m = -J$. Molecular constants given by Courtoy were used in the calculation.[10] The most striking feature emerging from this calculation is a coincidence within 0.01 cm^{-1} between (10^01)-(10^00) $P(30)$ and (00^01)-(00^00) $P(52)$ at 2300 cm^{-1}. There are no such coincidences between the (02^01)-(02^00) and (00^01)-(00^00) bands at 2300 cm^{-1}. Although the accuracy of the calculation itself may be only 0.01 cm^{-1}, it suggests, nevertheless, that lasing occurs on the (10^01)-(10^00) band. It further suggests that lasing does not occur on both bands. The pronounced variation in laser intensity with respect to frequency such as was observed at 2300 cm^{-1} would require accidental absorption coincidences in both laser bands for the same absorbing frequency, something which is very unlikely. Assignment of the 4.3-μm stimulated emission to the (10^01)-(10^00) band was further supported by observation of laser emission on the Q branch of the (10^01)-(01^11) band, which has the same upper level. This emission occurred near 711 cm^{-1}.

Lasing in HCN has also been observed in two regions near 3.85 and 3.9 μm, when using an intracavity CaF_2 prism. These transitions have been identified as the Q and P branches, respectively, of the (00^01)-(01^10) band.[1] Maximum output pulse energy at 3.85 μm is 2 mJ.

IV. DISCUSSION

Our present experimental results confirm that the (101) state of CO_2 is selectively excited by energy transfer from Br^*, and that this state is *at least one* of the major product channels. It must be cautioned that our inability to detect stimulated emission emanating from states other than (101) does not prve that other states are not excited. Although significant excitation of (021) appears unlikely on the basis of our results, states such as (210), (200), (001), etc., are not unreasonable product species. In separate experiments, we have measured the quenching of Br^* by CO_2 and have found this to proceed with a room-temperature rate coefficient of 5×10^5 sec^{-1} $Torr^{-1}$,[1,11] Since CO_2 (101) is collisionally deactivated by collisions with CO_2 (000) with a rate coefficient of 4.2×10^6 sec^{-1} $Torr^{-1}$,[12] it is clear that little energy can be stored in the (101) state, and it is only a judicious choice of operating parameters that allows us to overcome the efficient deactivation of this state. Nevertheless, a small increase in the active laser volume will make several mJ of line-tunable radiation in the 4.3-μm region conveniently available.

It should be emphasized that the E-V laser design described here is very similar to that of commerically available coaxial dye lasers. Indeed, several of the E-V–pumped laser transitions have operated well in a commercial dye laser tube (Phase-R Co. type DL-18) with only minor modification. The pulse repetition rate in our device is limited, at present, by flashlamp cooling and power supply considerations. It appears that the well-advanced flash-pumped dye laser and Nd : YAG laser technology can be applied readily to E-V laser systems. The result might be simple high-repetition-rate line-tunable laser sources, operating in spectral regions where no such sources presently exist.

[1] A. B. Petersen, C. Wittig, and S. R. Leone, Appl. Phys. Lett. 27, 305 (1975).
[2] A. B. Petersen, C. Wittig, and S. R. Leone, J. Appl. Phys. 47, 1051 (1976).
[3] A. B. Petersen, L. W. Braverman, and C. Wittig, J. Appl. Phys. 48, 230 (1977).
[4] K. R. Wilson, *Excited State Chemistry*, edited by J. N. Pitts, Jr. (Gordon and Breach, New York, 1970).
[5] D. R. Rao, L. O. Hocker, A. Javan, and K. Knable, J. Mol. Spectrosc. 25, 410 (1968).
[6] G. Herzberg, *Molecular Spectra and Molecular Structure* (Van Nostrand Reinhold, New York, 1945), Vol. II.
[7] S. S. Penner, *Quantitative Molecular Spectroscopy and Gas Emissivities* (Addison-Wesley, Reading, Mass. 1959).
[8] L. D. Gray, J. Quant. Spectrosc. Radiat. Transfer 5, 296 (1965).
[9] G. Herzberg, *Molecular Spectra and Molecular Structure* (Van Nostrand Reinhold, New York, 1950), Vol. I.
[10] C. P. Courtoy, Can. J. Phys. 35, 608 (1957).
[11] A. Hariri and C. Wittig, J. Chem. Phys. (to be published).
[12] J. Finzi and C. B. Moore, J. Chem. Phys. 63, 2285 (1975).

V.

Electronic–vibrational energy transfer from $Br(4^2P_{1/2})$ to HCN, and deactivation of HCN (001)*

A. Hariri, A. B. Petersen, and C. Wittig

Electrical Engineering Department, University of Southern California, University Park, Los Angeles, California 90007
(Received 15 March 1976)

A pulsed dye laser has been used to photolytically produce electronically excited bromine atoms in the $4^2P_{1/2}$ state in gas mixtures containing HCN. By monitoring the time resolved fluorescence from the (001) state of HCN, it was possible to determine the rate coefficient for electronic–vibrational (E–V) energy transfer from $Br(4^2P_{1/2})$ to HCN. Rate coefficients for the deactivation of HCN(001) were also measured for the collision partners HCN, Br_2, and Ar.

I. INTRODUCTION

The collisional quenching of electronic excitation in atoms and molecules, with resulting excitation of molecular vibrations, is a process that is currently under study in a number of laboratories. In general, this electronic–vibrational (E–V) energy transfer can involve a variety of inter- and intramolecular processes and can cover a wide range of excitation energies. For *low* electronic excitations, it is possible to study "near-resonant" E–V energy transfer in which only one or a few vibrational quanta are involved. Thus, several experimental studies can be found in the literature concerning E–V transfer from the $^2P_{1/2}$ states of I and Br (lying at 7603 cm^{-1} and 3685 cm^{-1}, respectively) to specific vibrational levels of small molecules.[1–7]

In this paper, we present experimental results concerning the quenching of $Br(4^2P_{1/2})$, hereafter referred to as Br^*, by HCN, with resulting excitation of the ν_3 mode of HCN [(001) state]. Although a large number of quenching channels, as shown in (1), are energetically available, the efficient and specific excitation of the (001) state results in (2) being the major quenching route:

$$Br^* + HCN(000) - Br + HCN(\text{all states}), \quad (1)$$

$$Br^* + HCN(000) - Br + HCN(001) + 374\ cm^{-1}. \quad (2)$$

Rate coefficients are determined for (1) and (2) as well as several subsequent energy exchange processes concerning the (001) state of HCN. This is the first study of the kinetics of the (001) state of HCN. HCN is an interesting molecule, and the (001) state is quite analogous to the HX vibration of the hydrogen halides. These measurements have direct bearing on several infrared HCN lasers, developed by ourselves and others, in which selective pumping is achieved by excitation of the ν_3 vibration.[3,8,9] In these devices, it is important to understand energy transfer processes concerning the (001) state since this is the upper laser level of several transitions which have been seen in stimulated emission.

II. EXPERIMENTAL

The experimental technique is straightforward. A coaxial flashlamp-pumped dye laser is used to produce laser energies of 50–100 mJ (FWHM) ~ 0.5 μsec) at approximately 485 nm when using coumarin 151 in an ethanol, H_2O solution. The dye laser is operated without a frequency selective element in the optical cavity since Br_2 absorbs continuously in the region near 485 nm. The dissociation of Br_2 in this wavelength region produces one excited atom ($4^2P_{1/2}$) and one ground state atom ($4^2P_{3/2}$) with roughly unity efficiency.[10] The entire dye laser apparatus is contained within an Al enclosure in order to minimize electrical transients produced by the flashlamp (≥ 100 J, FWHM ~ 1 μsec). The output from the dye laser is directed into a sample cell which contains a mixture of Br_2, HCN, and Ar. Because of the small absorption coefficient of Br_2 at 485 nm (1.2% $cm^{-1} \cdot torr^{-1}$), the dye laser output is reflected through the cell several times in order to produce sufficient Br^*.

Spontaneous emission is observed at right angles to the laser beam with a large area (1.2 cm^2) InSb photovoltaic detector (Spectronics). Various interference filters can be attached to the cold finger directly in front of the detector element in order to separate the different emissions and reduce the amount of background flux. Additional (room temperature) filtering is always necessary to completely block scattered laser light. The detector output is amplified and recorded with a transient digitizer (Biomation 805). Typical signals are shown in Fig. 1. Signal to noise ratio with this apparatus has been high, and signal averaging has not been necessary.

Gas samples are prepared in a Pyrex vacuum system of conventional design. All stopcocks are constructed of Pyrex and viton, and a small amount of fluorinated grease is used for lubrication. Pressures are measured with a capacitance manometer. HCN (Fumico) is purified by repeated freeze–pump–thaw cycles and distillation. Ar (Airco, 99.998%) is withdrawn from a sample held at 77 °K. Br_2 (Aristar grade from British Drug House, 99.8% pure) is the most difficult chemical to purify and requires considerable care. Repeated fractional distillation followed by slow passage over P_2O_5 is used to purify the Br_2. In addition, the glass apparatus in which the Br_2 is to be handled should be *seasoned* by exposure to Br_2, and heated under vacuum as much as possible in order to minimize the amount of H_2O on the surfaces. Having taken these precautions, there is no detectable molecular fluorescence when 20 torr of Br_2 is photolyzed in the sample cell. When 20 torr of poorly purified Br_2 is photolyzed in the cell, we readily detect spontaneous emission from H_2O and/or HBr.

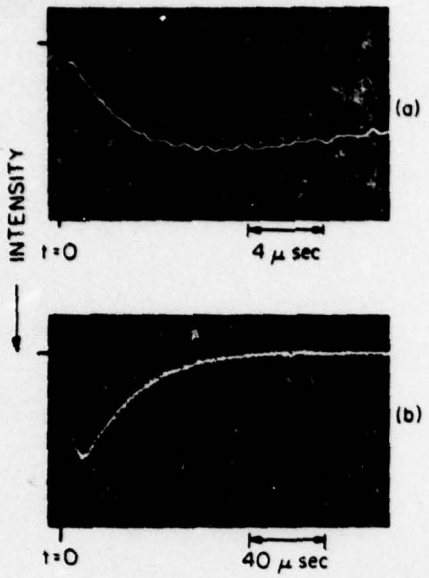

FIG. 1. Typical data from the transient recorder showing HCN(001) fluorescence from a sample containing 7 torr of a 1:3:13 mixture of HCN:Br_2:Ar. (a) and (b) show the rise and fall of HCN(001) fluorescence, respectively.

III. RATE PROCESSES

The production of Br^* by laser photolysis,

$$Br_2 + h\nu \rightarrow Br + Br^*, \tag{3}$$

takes place instantaneously on the time scale of interest in this study. Subsequent removal of Br^* then proceeds by way of

$$Br^* + HCN(000) \rightarrow Br + HCN(\text{all states}) \tag{1}$$

and

$$Br^* + Br_2 \rightarrow Br + Br_2. \tag{4}$$

Other quenching routes (e.g., $Br^* + Br$) are discriminated against experimentally in order to simplify analyses.

For small $[Br^*]$, the removal of Br^* is first order, with a decay time given by

$$\tau_{Br^*}^{-1} = k_1[HCN] + k_4[Br_2]. \tag{5}$$

Quenching of Br^* by the Ar diluent is insignificant relative to the above process.[7] Thus, it is possible to determine k_1 and k_4 by varying the mole fraction of the sample as described previously by Leone and Wodarczyk.[1] Since the buildup of HCN (001) fluorescence occurs with τ_{Br^*}, we have a convenient means of measuring k_1 and k_4. As seen in Fig. 1, the quenching of Br^* is faster than the subsequent quenching of HCN(001). Deactivation of HCN(001) can occur by the following processes:

$$HCN(001) + HCN(000) \rightarrow HCN(mn0) + HCN(pq0), \tag{6}$$

$$HCN(001) + Br_2 \rightarrow HCN(mn0) + Br_2, \tag{7}$$

$$HCN(001) + Ar \rightarrow HCN(mn0) + Ar. \tag{8}$$

Again, we have purposefully discriminated against processes that add to the complexity of the system [e.g., HCN(001) + Br]. Also, quenching of HCN(001) by Ar is inefficient, and this is discussed below. Thus, the relaxation time of HCN(001) is given by

$$\tau_{001}^{-1} = k_6[HCN] + k_7[Br_2] \ , \tag{9}$$

and k_6 and k_7 can be obtained by varying the mole fraction of the gas sample.

IV. RESULTS

Experimental results for the quenching of Br^* by HCN and Br_2 and for the quenching of HCN(001) by HCN and Br_2 are shown in Fig. 2. All of these data were obtained using a narrow-band (0.1 μm) interference filter to select fluorescence from the HCN(001) state. Each point represents an average of six data, corresponding to six different total pressures. The standard deviations from these six data points are usually smaller than could be conveniently shown in Figs. 2(a) and 2(b). The intercept at $X_{HCN} = 0$ was obtained by carefully collecting data in this region and analyzing them separately in order to insure the most accurate intercept. Good signals were obtained with X_{HCN} as low as 0.01. The laser beam was kept sufficiently diffuse in these experiments so that atom production did not affect the

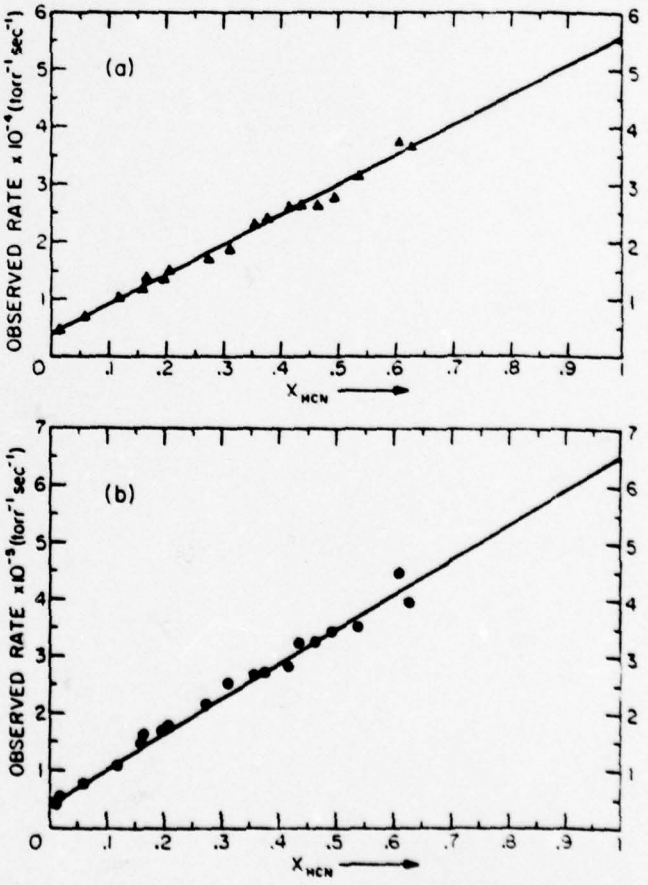

FIG. 2. Observed rate vs mole fraction. In (a), the rate of quenching of HCN(001) is given; in (b), the rate of quenching of Br^* is given. The straight lines are obtained by a least squares fit of the data.

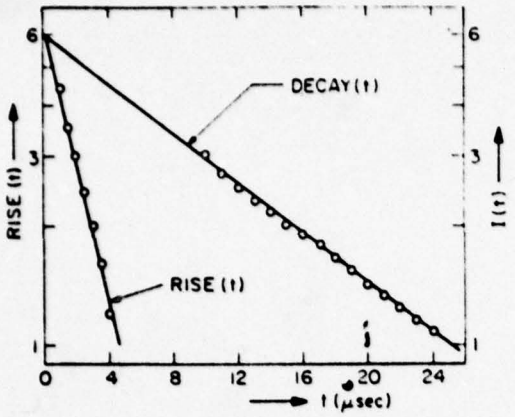

FIG. 3. Method used to obtain τ_{Br^*}. First, the decay portion of the measured fluorescence intensity, $I(t)$, is plotted in order to obtain τ_{001}. An extrapolation of these data to $t = 0$ allows τ_{Br^*} to be computed by plotting RISE(t) vs t, where RISE(t) = DECAY(t) − $I(t)$.

kinetics. This was periodically checked by changing the intensity of the beam with a lens while measuring the decay rates. At high laser intensities, where atom production was also high, it was possible to create situations where the presence of atoms resulted in *enhanced* quenching rates. No quantitative information could be obtained however, and this regime of operation was simply avoided. In Fig. 2(a), data are shown for the quenching of HCN(001). These data were obtained by analyzing the fluorescence decay at sufficiently long times to minimize effects of Br* quenching. In Fig. 2(b), the data for quenching of Br* are shown. These data are obtained as follows. First, the decay rate of HCN(001) fluorescence is determined. Next, the decaying HCN(001) density is extrapolated to short times. This provides the base line for a semilog plot of the fluorescence rise. An example of this is shown in Fig. 3.

Quenching of HCN(001) by Ar is rather inefficient, and this rate is determined as follows. With [Br_2] + [HCN] = const, Ar is added to the gas mix and the change in decay rate is observed. These data are shown in Fig. 4.

A. Absolute *E–V* rate

The absolute rate, k_2, for excitation of HCN(001) by Br* can be obtained by comparing the intensity of HCN(001) fluorescence with either the fluorescence from Br* or some molecular species whose absolute *E–V* rate is known.[1] It is required to know the spontaneous emission lifetimes of the various emitting species. The spontaneous emission lifetime of HCN(001) computed from integrated absorption data is 13.5 msec. Using this value for the HCN(001) spontaneous emission lifetime and comparing the fluorescence intensities of HCN(001) and HCl($v = 1$), which has a spontaneous emission lifetime of 33 msec,[13] we calculate that 88% of the quenching collisions result in excitation of the ν_3 mode of HCN. We estimate an uncertainty of ± 10% based on the standard deviation from six sets of data. In these intensity measurements, the molecular concentrations are kept low (0.1–0.2 torr) in order to minimize corrections due to self-absorption of the spontaneous emission. At the same time, [Br_2] is also kept low in order to minimize the corrections due to quenching of Br* by Br_2. Our previous work[3] suggests that there is little or no direct excitation of ν_2 vibrations by (1). Thus, we conclude that quenching of Br* by HCN results, almost exclusively, in the production of (001) rather than a combination state such as (011).

The essential results of the rate measurements are summarized in Table I. The quoted uncertainties are due to possible systematic as well as random errors.

V. DISCUSSION

The excitation of HCN(001) by energy transfer from Br* is an example of a fast, specific *E–V* rate process. The specificity of the excitation is not surprising in light of the similarities between HCN and the hydrogen halides, and the large *E–V* rate coefficients for the species HF[2], HCl,[1] and HBr.[1] It is interesting, however, to observe the *E–V* process in polyatomics since the different normal modes that are excited can shed light on the intermolecular forces at work during the *E–V* process.

The transfer of excitation from Br* to HCN(001) is 374 cm^{-1} exothermic. The lowest order nonvanishing term arising from the long-range multipolar field interaction is dipole quadrupole, and it is difficult to reconcile the large measured *E–V* rate coefficient on the basis of this interaction. Other *E–V* rate coefficients from Br* to small molecules are often of comparable magnitude, even when the change of more than one vibrational quantum is involved.[3,4,15] This also argues against the multipolar interaction as being the mechanism whereby energy is exchanged in these systems.

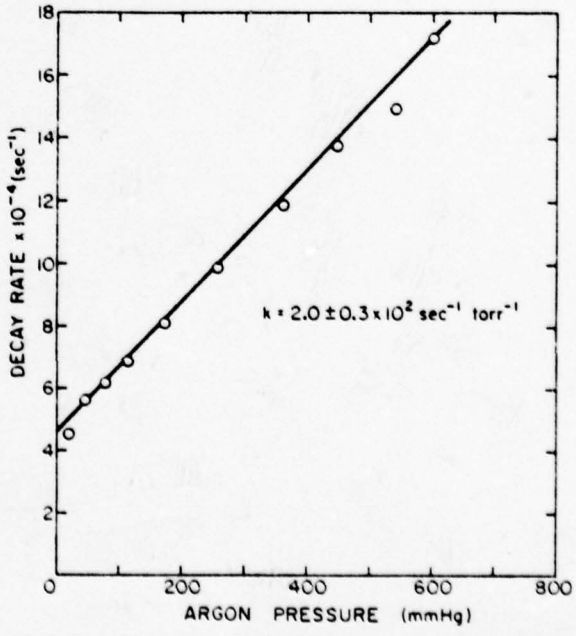

FIG. 4. Quenching of HCN(001) by Ar.

TABLE I. Results of rate measurements.

Process	Rate coefficient (295 K) This work[a]	Previous work	Reference[b]
$Br^* + HCN \xrightarrow{k_1}$ Br + HCN(all states)	$2.0 \pm 0.2 \times 10^{-11}$ $(6.5 \pm 0.7 \times 10^7)$		
$Br^* + HCN \xrightarrow{k_2}$ Br + HCN(001)	$1.8 \pm 0.4 \times 10^{-11}$ $(5.7 \pm 1.1 \times 10^7)$		
$Br^* + Br_2 \xrightarrow{k_3}$ Br + Br_2	$1.2 \pm 0.3 \times 10^{-12}$ $(3.8 \pm 1.0 \times 10^6)$	(6×10^7)	14
		$(2.6 \pm 0.3 \times 10^6)$	1
		$(1.3 \pm 0.6 \times 10^6)$	2
HCN(001) + HCN(000) $\xrightarrow{k_4}$ HCN(m=0) + HCN(n≠0)	$1.7 \pm 0.2 \times 10^{-12}$ $(5.6 \pm 0.7 \times 10^6)$		
HCN(001) + $Br_2 \xrightarrow{k_5}$ HCN(m=0) + Br_2	$1.2 \pm 0.2 \times 10^{-13}$ $(4.0 \pm 0.7 \times 10^5)$		
HCN(001) + Ar $\xrightarrow{k_6}$ HCN(m<n) + Ar	$6.2 \pm 0.9 \times 10^{-15}$ $2.0 \pm 0.3 \times 10^2$		

[a]The upper entry is in units of cm^3 molecule^{-1} · sec^{-1}; the lower entry, in parentheses, is in units of sec^{-1} · torr^{-1}.
[b]Rates measured by previous workers are given only in units of sec^{-1} · torr^{-1}.

If energy transfer occurs via short-range forces, as we are inclined to believe, then kinematics will play a large role in the excitation of the specific vibrational modes. Because of the specificity of energy transfer, the existence of a long-lived intermediate complex, (BrHCN)*, is unlikely. Obviously, further experimental work, such as the temperature dependence of the rate coefficients, will be valuable in determining energy transfer mechanism(s).

The de-excitation of the HCN(001) state by HCN, as given by (6), is efficient. We have not identified specific product channels for the deactivation process, and there are many potentially efficient inter- and intramolecular channels such as

$$\mathrm{HCN}(001) + \mathrm{HCN}(000) - \mathrm{HCN}(100) + \mathrm{HCN}(010) + 500\ \mathrm{cm}^{-1}\ . \tag{10}$$

The general willingness of the hydrogen halides to give up their vibrational quanta in collisional processes, together with the availability of channels such as (10), are consistent with our observations of a large rate coefficient for (6). De-excitation by Br_2 is also reasonably efficient. Again, there are numerous near-resonant exit channels such as

$$\mathrm{HCN}(001) + \mathrm{Br}_2(v=0) - \mathrm{HCN}(110) + \mathrm{Br}_2(v=1) + 80\ \mathrm{cm}^{-1}. \tag{11}$$

De-excitation by Ar is inefficient, as is frequently the case for the de-excitation of molecular vibrations by rare gases. A complete study of the de-excitation of the different vibrations of HCN with a number of collision partners will be published at a later date.

ACKNOWLEDGMENTS

The authors acknowledge stimulating discussions with S. R. Leone and J. R. Wiensenfeld.

*Research supported by the U. S. Energy Resource Development Agency and by the U. S. Army Research Office.

[1]S. R. Leone and F. J. Wodarczyk, J. Chem. Phys. 60, 314 (1974).
[2]F. J. Wodarczyk and P. B. Sackett, Chem. Phys. Lett. 12, 65 (1976).
[3]A. B. Petersen, C. Wittig, and S. R. Leone, Appl. Phys. Lett. 27, 305 (1975).
[4]A. B. Petersen, C. Wittig, and S. R. Leone, J. Appl. Phys. 47, 1051 (1976).
[5]R. J. Butcher, R. J. Donovan, and R. N. Strain, J. Chem. Soc. Faraday Trans. 2 70, 1837 (1974).
[6]R. J. Donovan, D. Husain, and C. D. Stevenson, Trans. Faraday Soc. 66, 2148 (1970).
[7]D. Husain and R. J. Donovan, Adv. Photochem. 8, 1 (1971). This is a review of the kinetics of electronically excited halogen atoms.
[8]G. West and M. J. Berry, J. Chem. Phys. 61, 4700 (1974).
[9]C. R. Quick, Jr. and C. Wittig (unpublished).
[10]K. R. Wilson, *Excited State Chemistry*, edited by J. N. Pitts, Jr. (Gordon and Breach, New York, 1970), p. 33.
[11]G. E. Hyde and D. F. Hornig, J. Chem. Phys. 20, 647 (1952).
[12]The absolute rate of $E-V$ transfer from Br* to HCl($v=1$) has been measured in Ref. 1.
[13]R. A. Toth, R. H. Hunt, and E. K. Plyer, J. Mol. Spectrosc. 35, 110 (1970).
[14]R. J. Donovan and D. Husain, Trans. Faraday Soc. 62, 2643 (1966).
[15]A. B. Petersen, L. W. Braverman, and C. Wittig (unpublished).

VI. Electronic to vibrational energy transfer from $Br(4^2P_{1/2})$ to CO_2, COS, and CS_2[a)]

A. Hariri and C. Wittig

Departments of Electrical Engineering and Physics, University of Southern California, University Park, Los Angeles, California 90007
(Received 27 June 1977)

In this paper, we report a study of the quenching of $Br(4^2P_{1/2})$ by CO_2, COS, and CS_2. Laser photolysis of gas samples containing Br_2 and the molecular species of interest produces $Br(4^2P_{1/2})$, and the subsequent quenching of this species results in vibrational excitation of the molecule of interest. By monitoring the time resolved ir fluorescence from $Br(4^2P_{1/2})$ and the (001) states of CO_2, COS, and CS_2, we are able to measure the quenching rate coefficients for these species as well as rate coefficients for a number of $V-V, T, R$ processes. By comparing the intensities of the $Br(4^2P_{1/2})$ and (001) state fluorescences, we measure directly the rate coefficients for electronic to vibrational ($E \rightarrow V$) energy transfer into the product states that contain at least one quantum of ν_3 vibration.

I. INTRODUCTION

The quenching of electronically excited halogen atoms in the spin–orbit state $^2P_{1/2}$ by collisions with molecular species has been studied experimentally for several decades.[1] In spite of the wealth of knowledge accumulated in early studies concerning the quenching processes, little attention was paid to product channels and it was not until 1970 that Donovan *et al.*[2] made the first direct observation of electronic to vibrational ($E-V$) energy transfer in these systems. In 1973, Leone and Wodarczyk[3] made the first direct measurement of the efficiency of $E-V$ transfer, and found that Br atoms in the $4^2P_{1/2}$ state, hereafter referred to as Br^*, produced vibrational excitation ($v=1$) in HCl and HBr on 95% and 65% of the quenching collisions, respectively. Further direct studies of $E-V$ transfer from Br^* have shown that when a molecule is an efficient quencher of Br^*, the main quenching channel is likely to be $E-V$ transfer.[4,5] In addition, when only one or two vibrational quanta are involved, the process can be highly mode specific as in the cases[5–7]

$$Br^* + CO_2(000) - Br + CO_2(101) - 30\ cm^{-1}, \quad (1)$$

$$Br^* + HCN(000) - Br + HCN(001) + 374\ cm^{-1}, \quad (2)$$

$$Br^* + H_2O(000) - Br + H_2O(100\ and/or\ 001), \quad (3)$$

where the energy of Br^* (3685 cm^{-1}) is near resonant with the vibrational product channels of Eqs. (1)–(3). Because of the selectivity of Eqs. (1)–(3), these processes have been the bases for the selective pumping of molecular lasers based on $E-V$ transer.[6,8,9] These molecular lasers oscillate on transitions that reflect the specificity of the energy transfer and thus have given rise to a number of new IR laser transitions in the region 3.85–17 μm.[6,8,9] Energy transfer studies concerning I^* have shown that $E-V$ transfer is an important process in the quenching of this species,[10,11] and one might reasonably expect that the quenching of Cl^* and F^* would also favor resonant $E-V$ channels.

The precise mechanisms whereby energy is transferred from the $^2P_{1/2}$ state to molecular vibrations are not, at this time, well understood. It has been suggested that a careful look at the different vehicles of energy transfer (multipolar forces,[12] nonadiabatic transitions,[13] etc.) may be required in order to adequately account for all of the available data.[14] In view of the uncertainty in the mechanisms for the collisonal deactivation of Br^* by small molecules, we have measured the rates of quenching and $E-V$ transfer from Br^* to the isoelectronic species CO_2, COS, and CS_2. Our results show that CO_2 is an order of magnitude more efficient than COS or CS_2 in quenching Br^*. In addition, the fraction of energy transferred from Br^* to available ν_3 excitation is larger for the case of CO_2 than COS or CS_2. These data indicate the importance of energy resonance as well as the number of quanta exchanged in the energy exchange process.

II. EXPERIMENTAL

The experimental arrangement is shown schematically in Fig. 1. Br^* is produced on a time scale which is short compared to that of the subsequent kinetic processes by the photolysis of Br_2 with the output from a flashlamp pumped dye laser

$$Br_2 + h\nu - Br + Br^*. \quad (4)$$

Both coaxial (Candela or Phase-R, 20–150 mJ, ~0.5 μs FWHM) and linear (Chromatix CMX-4, 2–8 mJ,

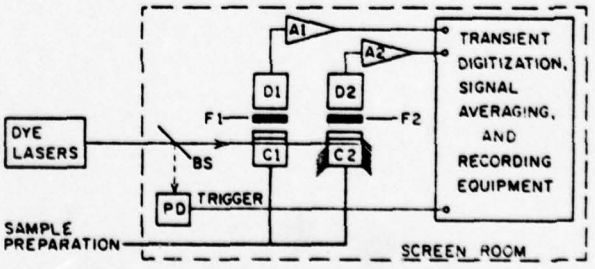

FIG. 1. Schematic drawing of experimental arrangement. *C1* and *C2* are sample cells, *F1* and *F2* are interference filters and/or gas cells, *A1* and *A2* are amplifiers matched to the detectors *D1* and *D2*. *BS* splits off a few percent of the laser beam and sends it to PD, a photodiode used to trigger the recording electronics.

[a)]Research supported by the U. S. Army Research Office under Grant No. DAAG29-76-G-0124, and by the Petroleum Research Fund administered by the American Chemical Society.

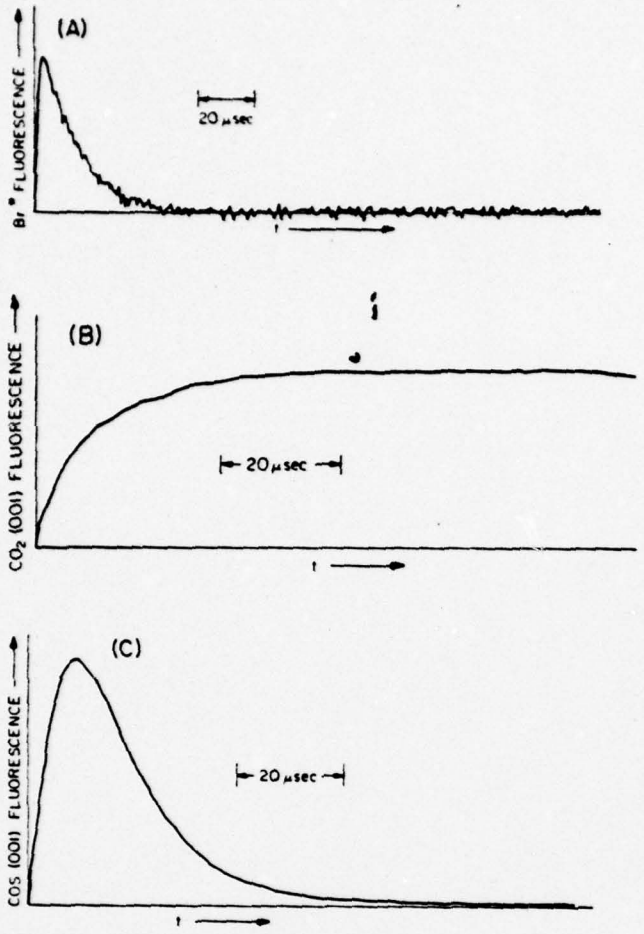

FIG. 2. Typical signal averaged fluorescence traces. (a) shows the decay of Br* when 3.12 torr of pure Br_2 is photolyzed. The laser energy is 20 mJ, and 128 shots are averaged. The finite rise time is due to the system response time of 2 μs. (b) shows the rise of $CO_2(001)$ when a sample containing 0.16 torr CO_2 and 0.10 torr Br_2 is photolyzed. The laser energy is 5 mJ, and 64 shots are averaged. The decay of $CO_2(001)$ is not discernable on the time scale shown. (c) shows the fluorescence from COS(001) when a sample containing 0.95 torr COS and 2.33 torr Br_2 is photolyzed. The laser energy is 5 mJ, and 64 shots are averaged. This is an excellent example of the situation where $\tau_{rise} \cong \tau_{fall}$.

~1.0 μs FWHM) flashlamp arrangements were used in the present study. Dye laser wavelengths of 480–500 nm were obtained with a variety of dyes supplied by Exciton (coumarin 490F, coumarin 480, LD490, LD473) dissolved in methanol/H_2O or ethanol/H_2O solutions. In the region 480–500 nm, Br_2 absorbs continuously and Eq. (4) is believed to produce approximately equal amounts of Br and Br*.[15] The output from the dye laser is directed into a screen room, which protects the detection and signal processing equipment from electrical transients. Spontaneous emission is viewed at right angles to the laser beam with large area detectors (photovoltaic InSb; photoconductive Ge:Au). Atomic and molecular fluorescence frequencies are isolated with interference filters and gas cells. When detecting fluorescence from Br*, it is necessary to use a narrow bandpass filter (FWHM = 0.12 μm at 2.7 μm and 77 °K) as well as a wide bandpass filter (FWHM = 1.0 μm at 3.0 μm) in order to completely block molecular fluorescence and scattered laser light. For a particular gas sample, we find it convenient in many experiments to use separate detectors in order to observe the Br* and molecular fluorescences simultaneously. Sample cells are constructed of pyrex, with salt or sapphire observation windows held in place with black wax (Apiezon W).[16]

Fluorescence signals are digitized (Nicolet 1090AR digital oscilloscope, 100 ns minimum gate width), averaged (Nicolet 1072 signal averager), and recorded with an *XY* plotter. Several typical data are shown in Fig. 2. Data reduction is accomplished using a variety of computer programs and the usual scientific fitting procedures. Data reduction is straightforward except for the case of a fluorescence signal with comparable rise and fall times. This is discussed below.

Samples are prepared in a pyrex vacuum system capable of 10^{-5} mm Hg. Stopcocks are constructed of pyrex, with Viton O rings which are sparingly lubricated with Krytox, a fluorinated vacuum grease. Pressures are measured with corrosion-resistant capacitance manometers (MKS).

In obtaining Br* signals, we should like to emphasize that particular care must be taken in order to avoid interference from molecular fluorescence. Because of the 1.1 s spontaneous emission lifetime of Br*, even the smallest amount of molecular fluorescence can interfere with the Br* signal. When using *only* a broadband interference filter (FWHM = 1.0 μm, centered at 3.0 μm), we can easily observe molecular fluorescence from Br_2/CO_2 mixtures in which only a trace of CO_2 is present. This molecular fluorescence is characterized by a rise time (as opposed to the instantaneous production of Br*) and a very rapid decay. The rapid rise and fall of the radiating state is consistent with previous reports of the rapid collisional deactivation of the CO_2 states in the vicinity of 3700 cm^{-1}.[17]

In the present study, we have monitored only the ν_3 vibrational modes, since our present detection system does not permit the observation of either ν_1 or ν_2 for CO_2, COS, or CS_2. Detection of ν_1 (which is only IR active in the case of COS) and the low frequency bending modes will be the subject of future experiments.

Chemicals were purified in the following manner. CO_2 (Matheson, 99.995% min) was subjected to repeated freeze–pump–thaw cycles at 77 °K. CS_2 (Baker Analyzed Reagent grade, 99.9% min) was pumped on several times at room temperature and at 223 °K. Following this, the CS_2 was distilled several times from 253 to 77 °K. Finally, the sample was degassed extensively at 163 °K to remove traces of OCS. Following purification, infrared analysis showed no sign of any impurities in either CO_2 or CS_2 samples. OCS (Matheson, 97.5% min) disproportionates to form small amounts of CO_2 and CS_2 and must be purified carefully before use. Infrared analysis of unpurified OCS samples showed 1.3% CO_2. OCS was first subjected to repeated freeze–pump–thaw cycles at 77 °K. Following this, the sample was distilled from 163 to 77 °K eight times. Infrared

analysis of the purified OCS samples showed 0.5%–0.6% CO_2 and no other impurities. These samples were always used within 24 h of purification, and we observed no disproportionation of the sample over this amount of time. Ar (Airco, 99.998% min) was passed through a trap at 77 °K and was always withdrawn from samples maintained at 77 °K. Br_2 (Aristar grade from British Drug House, 99.8% min.) was subjected to repeated distillation from 253 to 77 °K and slow passage over P_2O_5. In addition, the apparatus in which the Br_2 was to be used was *seasoned* by exposure to Br_2, and heated under vacuum as much as possible in order to minimize the amount of H_2O on the surfaces. Having taken these precautions, there was no detectable molecular fluorescence when 20 torr of Br_2 was photolyzed in the sample cell. When 20 torr of poorly purified Br_2 was photolyzed, molecular fluorescence was readily detected.

III. RATE PROCESSES

The production of Br* by laser photolysis,

$$Br_2 + h\nu \rightarrow Br + Br^*, \tag{4}$$

occurs during the laser pulse, which is $\lesssim 1$ μs FWHM in our present experimental arrangement. Thus, Br* is produced instantaneously on the time scale of interest. In the experiments reported here, photolysis was carried out at or near 490 nm. This wavelength is close to optimum for Br* production and leaves each photolysis fragment with 264 cm^{-1} of recoil energy which must be removed by momentum transfer collisions prior to energy transfer if we are to obtain room temperature rate coefficients.

Following photolysis, Br* can be quenched by the following processes

$$Br^* + Br_2 \rightarrow Br + Br_2, \tag{5}$$

$$Br^* + Ar \rightarrow Br + Ar, \tag{6}$$

$$Br^* + mol \rightarrow Br + mol^\dagger, \tag{7}$$

$$\rightarrow Br + mol\,(\nu_3), \tag{8}$$

$$\rightarrow Br + mol\,(\text{all states}), \tag{9}$$

where mol is either CO_2, COS, or CS_2, † denotes *any* vibrational excitation, and mol (ν_3) represents a molecule with at least one quantum of ν_3 excitation. The total quenching of Br* by mol, including all product vibrational states as well as the ground state of mol, is given by Eq. (9). In Eq. (5), we have paid no particular attention to the possibility of $E-V$ transfer from Br* to Br_2.

The quenching of Br* by CO_2, COS, and CS_2 proceeds via Eqs. (7)–(9). In the present study, we have monitored the ν_3 fluorescence from these molecules, in addition to Br* emission, thereby obtaining quantitative information concerning Eq. (8) in addition to the quenching rate coefficients for Eq. (9). Because the Br* energy is 3685 cm^{-1}, it is possible to excite several vibrational quanta simultaneously. For example, in separate experiments[6] we have shown that the following process is a major quenching channel in the quenching of Br* by CO_2

$$Br^* + CO_2(000) \rightarrow Br + CO_2(101) - 30\ cm^{-1}. \tag{2}$$

Since the energy transfer processes of species containing two or more quanta of excitation proceed very rapidly, it is not possible to investigate the primitive distribution of product species using our present experimental arrangement. Finzi and Moore[17] have shown that

$$CO_2(101) + CO_2(000) \rightarrow CO_2(001) + CO_2^\dagger, \tag{10}$$

as well as similar processes, proceed at rates that are near gas kinetic. Since the ν_3 quanta are preserved in such processes, it is possible to measure the production of species containing ν_3 excitation without identifying the primitive distribution from Eq. (8) precisely.

The production of vibrationally excited species in the (001) state is accompanied by the $V-V$, T, R processes which remove energy from the species under consideration

$$mol(001) + M \rightarrow mol(mn0) + M, \tag{11}$$

where M can be any collision partner. Thus, it is possible to measure rate coefficients for Eq. (11), using $E-V$ transfer as a means of preparing molecules in the (001) state.

The concentration of a particular molecular species in the (001) state following production of $(Br^*)_0$ at $t=0$, is given by

$$[mol(001)](t) = \frac{k_{E-V}(mol)(Br^*)_0}{\tau_{Br^*}^{-1} - \tau_{mol(001)}^{-1}}\left[\exp(-t/\tau_{mol(001)}) - \exp(-t/\tau_{Br^*})\right], \tag{12}$$

where τ_{Br^*} and $\tau_{mol(001)}$ are the collisional lifetimes of Br* and mol(001), respectively, for a particular experimental condition. Here, it is assumed that the rise and fall of the molecular fluorescence can be described by simple exponentials, which will be the case for sensibly first order excitation and deexcitation processes. For $\tau_{Br^*} < \tau_{mol(001)}$, the rise of the molecular fluorescence reflects the quenching of Br* and the decay of the molecular fluorescence reflects the $V-V$, T, R process that act to remove the ν_3 excitation. For $\tau_{Br^*} > \tau_{mol(001)}$, the converse is true. Thus, it is important to determine separately which processes are responsible for the observed rise and fall of the molecular fluorescence in a particular experiment. In the experiments reported here, we have monitored the decay of Br* separately, in order to avoid any ambiguity in this regard.

The Br* and mol(001) decay times are given by

$$\tau_{Br^*}^{-1} = k_9(mol) + k_5(Br_2) + k_6(Ar), \tag{13}$$

$$\tau_{mol(001)}^{-1} = k'(mol) + k''(Br_2) + k'''(Ar), \tag{14}$$

where k', k'', and k''' are the rate coefficients for quenching of mol(001) by mol, Br_2, and Ar, respectively. Deactivation by potentially efficient quenchers (Br, Br*) is discriminated against experimentally be minimizing the laser energy density. Deactivation of Br* by Ar has been shown to be very inefficient, and thus may be eliminated from Eq. (13).

Rate coefficients are obtained from Eqs. (13) and (14)

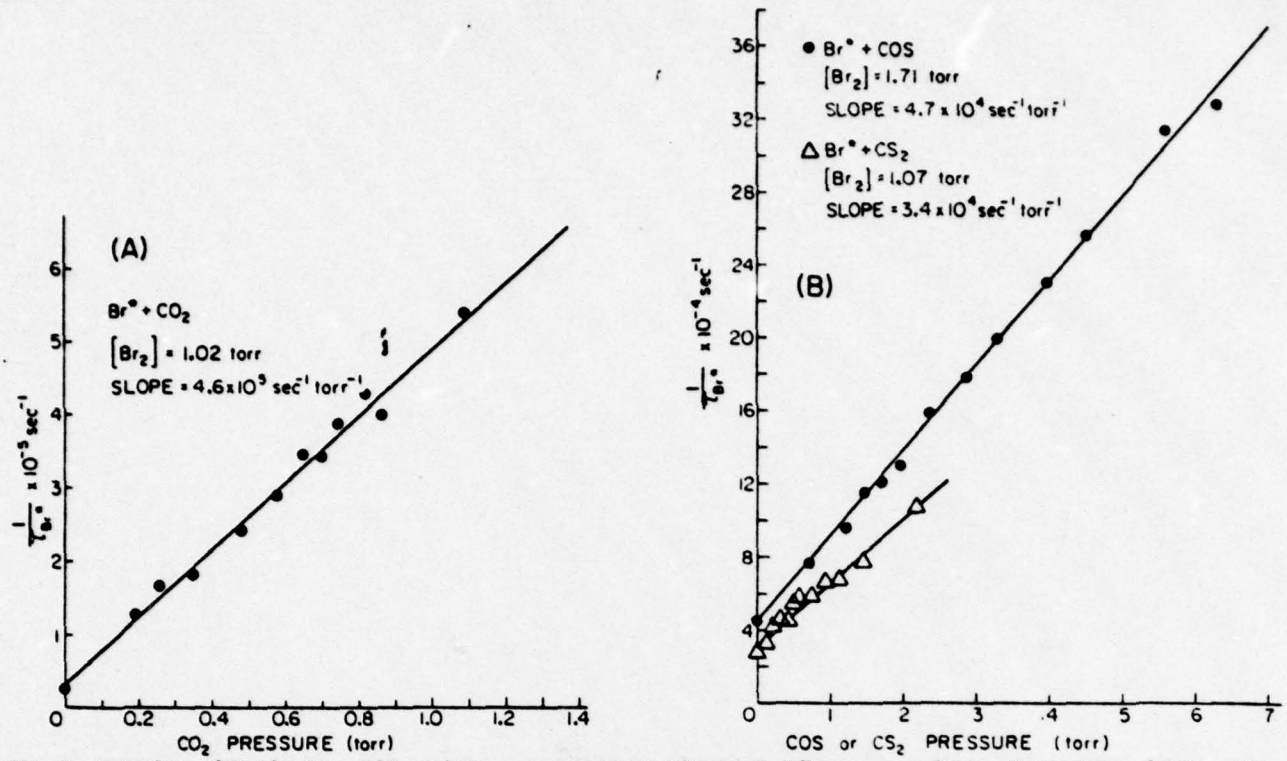

FIG. 3. Quenching of Br* by CO_2, COS, and CS_2, measured by monitoring Br* fluorescence decay. In the cases of CO_2 and CS_2, the quenching rate coefficients are the same as the slope of $(\tau_{Br^*})^{-1}$ vs concentration. In the case of COS, the quenching rate coefficient is 5% smaller than the slope due to the presence of 0.5% CO_2 in COS samples. Standard deviations are not given since other sources of uncertainty are expected to dominate. Each point represents an average of 1024 individual fluorescence signals at a laser energy of 5 mJ.

by varying the concentrations in a well-defined manner.

IV. RESULTS

Rate coefficients for the following processes:

$$Br^* + Br_2 - Br + Br_2, \tag{5}$$

$$Br^* + CO_2 - Br + CO_2 \text{ (all states)}, \tag{15}$$

$$Br^* + COS - Br + COS \text{ (all states)}, \tag{16}$$

$$Br^* + CS_2 - Br + CS_2 \text{ (all states)}, \tag{17}$$

were measured directly by monitoring Br* fluorescence while adding the appropriate molecular vapor dilute in Ar. The results of these measurements are shown in Fig. 3, and the rate coefficients are listed in Table I. Typically, 1024 fluorescence signals are averaged to obtain single curves such as the ones shown in Fig. 2(a). Each curve is then fit to an exponential decay using a least squares routine to obtain each of the data points shown in Fig. 3. The data shown in Fig. 3 were quite repeatable, and could be reproduced at will.

In obtaining rates for the Br*/COS system, we used COS samples which had been distilled less than 24 h prior to use. These samples contained 0.5% CO_2 and no CS_2. Because CO_2 is ten times more efficient than COS at quenching Br*, it was necessary to include the effect of the CO_2 impurity in the COS data reduction.

Fluorescence signals from CO_2 and COS were obtained using an InSb detector and the appropriate interference filters. These signals were very large, and it was not necessary to average more than a couple of traces in order to obtain $S/N > 20$. The $CS_2(001)$ state emits at 1523 cm^{-1} and is not accessible to the InSb detector. $CS_2(001)$ fluorescence was detected with a Ge:Au photoconductor which, although much less sensitive than InSb, was adequate for detecting molecular fluorescence. In all cases, spontaneous emission from a particular species was almost completely blocked when a 2 cm cell containing this species was placed between the detector and the laser beam, indicating that the emitting transition is (001)–(000).

Fluorescence curves were fit to the double exponential portion of Eq. (12) with a computer curve fitting routine in order to obtain τ_{Br^*} and $\tau_{mol(001)}$. By plotting $(p\tau_{Br^*})^{-1}$ and $[p\tau_{mol(001)}]^{-1}$ vs mole fraction, where $p = p_{Br_2} + p_{mol}$, it is possible to obtain the quenching rate coefficients for Br* and mol(001) by Br_2 and mol(000). Several representative data are shown in Fig. 4 and the corresponding rate coefficients are listed in Table I. In all of these experiments, [Ar] was sufficiently low that it did not contribute to the quenching of either Br* or mol(001). In many cases, such as COS, it was not necessary to use Ar at all since the Br_2/COS mix constitutes a sufficient heat bath by itself, and the rapid collisional removal of COS(001) is not affected by diffusion. From the Br* quenching data, it was possible to unambiguously

TABLE I. Quenching rate coefficients for Br* and mol (001) obtained by monitoring Br* and/or mol (001) sponanteous emission.

	Rate coefficient (295 °K)				
	This work[a]			Previous work[b]	
Process	From Br* fluorescence	From molecular fluorescence	Average		Ref.
$Br^* + CO_2 \xrightarrow{k_{15}}$	$(4.6 \pm 0.3) \times 10^5$	$(5.2 \pm 0.3) \times 10^5$	$(4.9 \pm 0.3) \times 10^5$	$(4.9 \pm 0.3) \times 10^5$	8
$Br + CO_2$ (all states)	$(1.4 \pm 0.1) \times 10^{-11}$	$(1.6 \pm 0.1) \times 10^{-11}$	$(1.5 \pm 0.1) \times 10^{-11}$		
$Br^* + COS \xrightarrow{k_{16}}$	$(4.7 \pm 0.3) \times 10^4$	$(4.5 \pm 0.4) \times 10^4$	$(4.6 \pm 0.4) \times 10^4$	$(3.9 \pm 1.1) \times 10^4$	18
$Br + COS$ (all states)	$(1.4 \pm 0.1) \times 10^{-12}$	$(1.4 \pm 0.1) \times 10^{-12}$	$(1.4 \pm 0.1) \times 10^{-12}$		
$Br^* + CS_2 \xrightarrow{k_{17}}$	$(3.4 \pm 0.3) \times 10^4$	4×10^4 [c]	$(3.4 \pm 0.3) \times 10^4$ [c]		
$Br + CS_2$ (all states)	$(1.1 \pm 0.1) \times 10^{-12}$		$(1.1 \pm 0.1) \times 10^{-12}$		
$Br^* + Br_2 \xrightarrow{k_3}$	$(2.4^{+0.3}_{-0.2}) \times 10^4$	$(2.7 \pm 0.3) \times 10^4$	$(2.6 \pm 0.3) \times 10^4$	5.2×10^3	19
				$(2.6 \pm 0.3) \times 10^4$	3
$Br + Br_2$ (all states)	$(7.3^{+0.8}_{-0.6}) \times 10^{-13}$	$(8.2 \pm 0.9) \times 10^{-13}$	$(7.8 \pm 0.9) \times 10^{-13}$	$(3.3 \pm 0.6) \times 10^4$	4
				$(2.6 \pm 0.6) \times 10^4$	18
$COS(001) + COS(000) \rightarrow$				$(4.7 \pm 0.6) \times 10^4$	20
		$(5.9 \pm 0.4) \times 10^4$		$(5.60 \pm 0.8) \times 10^4$	21
$COS(mn0) + COS(pq0)$		$(1.8 \pm 0.1) \times 10^{-12}$		$(5.5 \pm 0.5) \times 10^4$	22
				$(5.2 \pm 1.2) \times 10^4$	18
$COS(001) + Br_2 \rightarrow$		$(2.0 \pm 0.5) \times 10^4$		$(5.4 \pm 1.0) \times 10^4$	23
$COS(mn0) + Br_2$		$(6.1 \pm 1.5) \times 10^{-13}$		$(1.4 \pm 0.1) \times 10^3$	20
				71.5	21
$COS(001) + Ar \rightarrow$		$(1.0 \pm 0.3) \times 10^3$		$(1.5 \pm 0.5) \times 10^2$	22
				$(5.2 \pm 0.9) \times 10^3$	18
$COS(mn0) + Ar$		$(3.2 \pm 1.0) \times 10^{-14}$		$(4.3 \pm 0.9) \times 10^3$	23
$CO_2(001) + Br_2 \rightarrow$		$(2.6 \pm 0.2) \times 10^2$		$(2.46 \quad 0.2) \times 10^2$	24
$CO_2(mn0) + Br_2$		$(7.9 \pm 0.6) \times 10^{-15}$			
$CS_2(001) + Br_2 \rightarrow$		$(4.1 \pm 0.4) \times 10^3$			
$CS_2(mn0) + Br_2$		$(1.2 \pm 0.1) \times 10^{-13}$			

[a] The upper entry is in units of s^{-1} torr^{-1}; the lower entry is in units of cm^3 mol^{-1} s^{-1}.
[b] For comparison purposes, rates of previous workers are given in units of s^{-1} torr^{-1} only.
[c] Since $CS_2(001)$ fluorescence was only detected with Ge:Au, the S/N was not high and the more reliable quenching data are those measured directly by monitoring Br* fluorescence.

assign τ_{Br^*} and $\tau_{mol(001)}$ to either the rising or falling portions of the fluorescence curves. In the cases of CO_2 and CS_2, the quenching of Br* is much more rapid than the accompanying vibrational energy transfer processes and data reduction was quite straightforward. For the case of COS, $\tau_{Br^*} \sim \tau_{mol(001)}$ and it was necessary to use the quenching data carefully in assigning τ_{Br^*} and $\tau_{mol(001)}$ to their respective portions of the fluroescence curves. In Fig. 4 we see the difficulty of correctly ascribing the rise and fall portions of Eq. (12) to the proper rate process. By comparing the intercepts at $X_{OCS} = 1$ in Fig. 4 to the quenching rate coefficients taken from Br* fluorescence measurements, we see that the smaller rate coefficient is the one due to the quenching of Br* by OCS. Without the quenching data from the Br* fluorescence experiments, this assignment would not have been as straightforward. Considerable care must be exercised in using computer programs to extract τ's from curves such as the one shown in Fig. 2(c). We found standard fitting routines inadequate for cases such as this, and we had to write our own computer programs for the case of $\tau_{rise} \simeq \tau_{fall}$. Although computer generated curves match the experimental data very well, we find that when $\tau_{rise} \simeq \tau_{fall}$ a particular pair of τ's can be changed by $\pm 10\%$ while still achieving a reasonable fit to the data.

In addition to the information contained in plots such as those shown in Fig. 4, it was also straightforward to obtain quenching rate coefficients for the deactivation of the (001) states by various collision partners. Examples of data such as these are shown in Figs. 5 and 6. It was not the main point of the present study to measure vibrational energy transfer rates, and therefore only those (001) quenching data that are of interest to the present study are presented here. Other data of this nature will be pub-

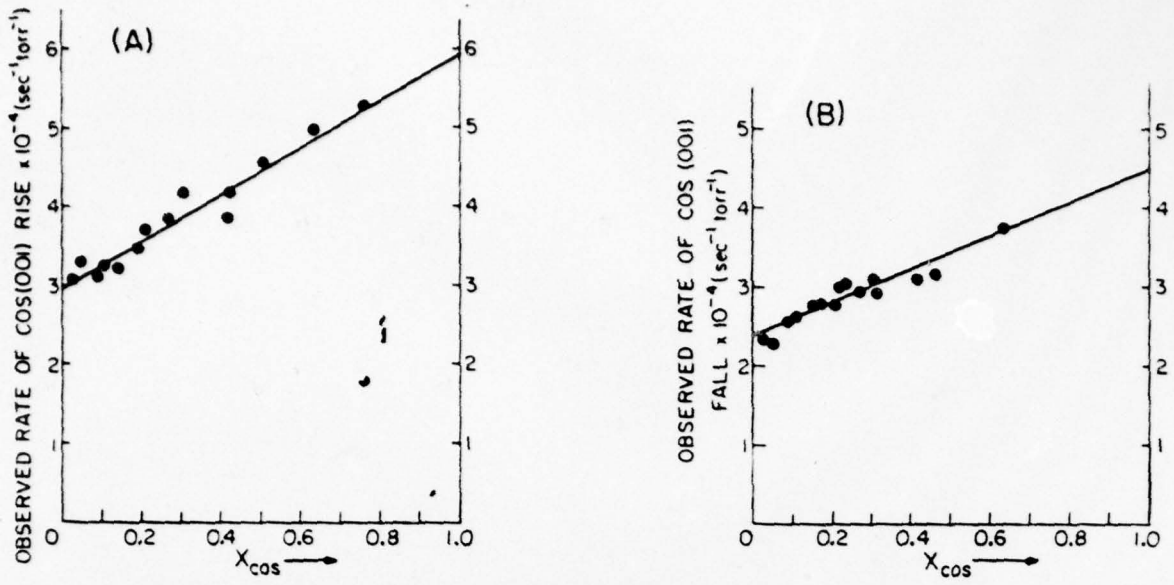

FIG. 4. Typical data for the quenching of Br* and mol (001) obtained by monitoring ν_3 fluorescence. (a) and (b) show the rate of rise and fall respectively for the case of COS. Note that the rates of rise and fall are very close here, as opposed to the cases of CO_2 and CS_2. For brevity, only data for COS are shown here. Data for CO_2 and CS_2 are *qualitatively* similar to the data for COS.

lished separately, if at all. The data shown in Fig. 5 were taken under conditions where the risetime is due mainly to the quenching of COS(001) by COS(000). Under these conditions, the addition of Ar shortens the rise time, since the quenching of COS(001) by Ar is much more efficient than the quenching of Br* by Ar. This is a further confirmation of the assignment of the rate of rise to the rate of COS(001) quenching. Figure 6 shows the deactivation of CO_2(001) by Br_2. This process is important to the operation of the Br*–CO_2 transfer laser.[6]

V. ABSOLUTE $E \rightarrow V$ RATE COEFFICIENT FOR EXCITATION OF ν_3 QUANTA

Determining the fraction of the quenching collisions that result in excitation of a particular molecular vibration is, although straightforward in principle, a difficult experimental task. Briefly, a comparison must be made between the particular molecular fluorescence(s) of interest, and a fluorescing species whose relative density is known (e.g., Br* itself, or a molecule whose abso-

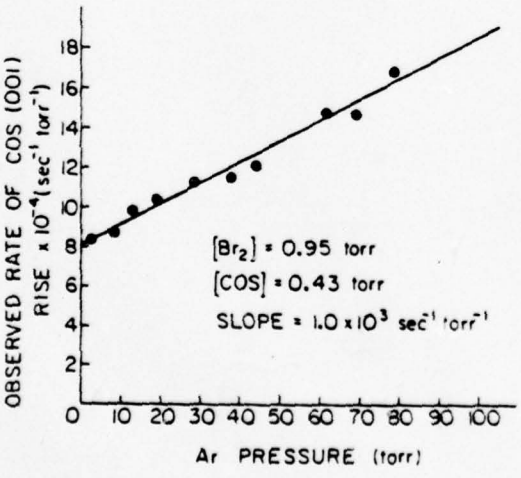

FIG. 5. The quenching of COS by Ar. By monitoring the effect of Ar on the rise and fall portions of the fluorescence, it is seen that Ar changes the rise of the COS (001) fluorescence signal, and therefore, the rise of signal is due to quenching of COS(001) by COS(000). The quenching of Br* by Ar is quite inefficient and the fall of COS(001) fluorescence is unaffected by Ar addition.

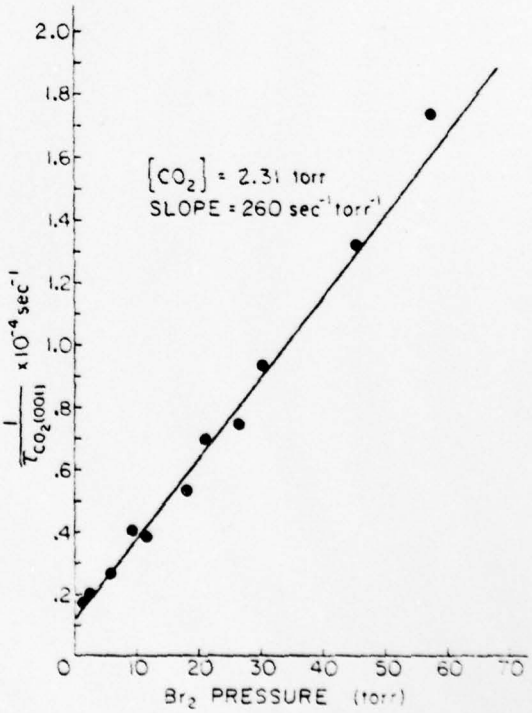

FIG. 6. The quenching of CO_2(001) by Br_2.

TABLE II. The efficiency of producing ν_3 excitation in the quenching of Br* by CO_2, COS, and CS_2.

Species	Rate coefficient for quenching Br* (295 °K, s^{-1} $torr^{-1}$)	$F(\mathrm{mol}(\nu_3))$ = fraction of Br*–mol quenching collisions resulting in excitation of one ν_3 quantum per molecule
CO_2	4.9×10^5	0.4
COS	4.6×10^4	0.2
CS_2	3.4×10^4	~0.4

lute $E-V$ rate coefficient has already been established, such as HCl). Details of the method employed here are described in the appendix. A summary of our results for CO_2, COS, and CS_2 is given in Table II. These data were obtained as follows: Fluorescence signals from CO_2(001) and COS(001) were each compared to fluorescence signals from HCl($v=1$) and Br*, as well as to each other. All of these experiments were done using a single InSb detector, and normalizing all data to the laser energy. Molecular concentrations were maintained ≤ 60 μm Hg, and the distance from the laser beam to the observation window was maintained ≤ 1 cm in order to minimize effects due to resonance absorption in the sample cell. Concentrations of the molecular species and Br_2 were varied widely and a multitude of data were collected and analyzed. All of the data agreed to within ±10%, well within the uncertainty of ±20% which includes possible systematic errors. Since CS_2(001) fluoresces at 1523 cm^{-1}, the Ge:Au detector was used for comparison purposes here. This detector is not sufficiently sensitive to detect Br* emission, so comparison was made between CS_2(001), CO_2(001), and COS(001) fluorescence. Again, there was agreement, within ±10%, between the different comparisons.

An absolute lower limit of $F(CO_2(\nu_3))=0.15$ for the case of CO_2 was established in a separate experiment. In this experiment, CO_2 laser emission was obtained on the (001)–(100) band by optically pumping a mixture of Br_2 and CO_2 contained in a 10.6 μm laser resonator.[25] The source used to optically pump the gas mixture was a dye laser operating at ≃485 nm. The intensity of the dye laser was kept low enough so that $[Br_2]$ was not affected by the laser pulse, and the amount of Br_2 dissociation could be calculated from the well known absorption coefficient of Br_2. Under these conditions, we observed that

$$\frac{\text{no. 10.6 μm laser photons emitted}}{\text{no. 485 nm photons absorbed}} = 0.15.$$

Using a branching ratio of 1:1 for the Br*:Br production at 485 nm, this result establishes a definite lower limit of 0.15 for $F(CO_2(\nu_3))$ for the case of CO_2.

Typical statistical uncertainties from repeated measurements were nominally 10%. Because of the nature of the data reduction, as described in the Appendix, we feel that systematic, rather than random errors, are the main source of uncertainty in our measurements. Whereas relative $F[\mathrm{mol}(\nu_3)]$ for CO_2, COS, and CS_2 are probably within ±20%, and the lower bound on $F(\mathrm{mol}(\nu_3))$ for CO_2 is 0.15, it would not be unreasonable for the absolute $F(\mathrm{mol}(\nu_3))$'s to be uncertain by as much as a factor of 2.

VI. DISCUSSION

Our results show that the quenching of Br* by CO_2 is more efficient, by over one order of magnitude, than the analogous quenching of Br* by COS and CS_2. If quenching were due to a nonresonant nonadiabatic transition from the electronic potential surface correlating to the $4\,^2P_{1/2}$ state, then such a pronounced effect would not have been expected. Particularly in the case of COS, the interaction of Br* with the oxygen atom is expected to be very similar to the analogous interaction in the case of CO_2.

The *origins* of the different quenching efficiencies for CO_2, COS, and CS_2 can be seen in Fig. 7, where molecular states are plotted which contain at least one quantum of ν_3 excitation. In the case of CO_2, in separate experiments, we have identified the (101) state as a major product channel by the analysis of the stimulated emission which originates from this level in a laser device pumped by $E-V$ transfer from Br* to CO_2. At this time, we do not know where the product energy states lie for the cases of COS and CS_2, so the energy defects and number of quanta involved are not known. For the species COS and CS_2, $E-V$ transfer from Br* must (a) involve a molecular state composed of more than two quanta if the process is to be resonant, or (b) involve a larger energy defect (compared to CO_2) if only two

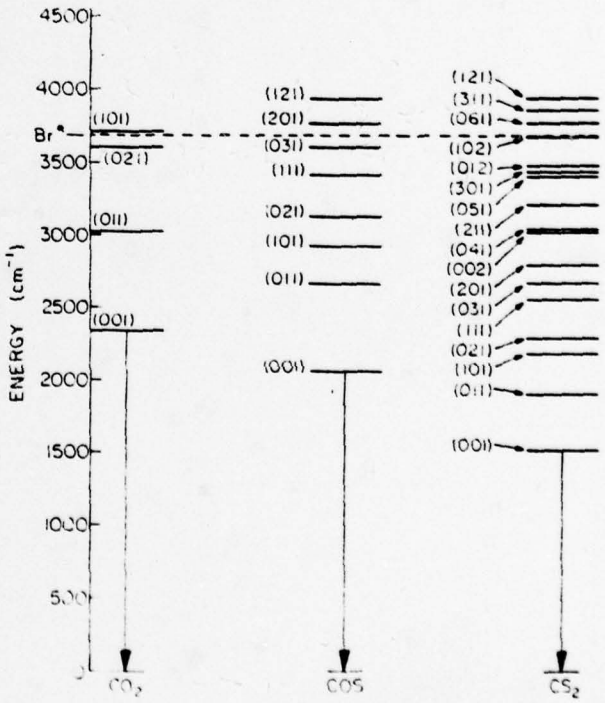

FIG. 7. Partial energy level diagram of CO_2, COS, and CS_2 showing energy states that contain at least one quantum of ν_3 excitation. The energy of Br* (3685 cm^{-1}) is also shown by the dotted line.

quanta are to be exchanged. Without information concerning the COS and CS_2 product channels, it is not possible for us to determine experimentally the respective roles of energy defect and number of vibrational quanta in contributing to the rate and efficiency of energy transfer. It is clear, however, from the results presented in this paper, that as the number of quanta required to make the quenching process near resonant ($\Delta E \sim 100$ cm^{-1}) increases, quenching becomes less efficient. It is difficult to reconcile the quenching of Br^* by CO_2, COS, and CS_2 on the basis of simply a multipolar interaction. The lowest order term in the multipolar expansion for the interaction of Br^* with CO_2 is dipole–quadrupole, and two quanta of vibrational excitation must change. For the cases of COS and CS_2, the interaction is even weaker and surely cannot account for the measured quenching rate coefficients of 4.6 and 3.4×10^4 s^{-1} $torr^{-1}$, respectively. It is possible that more than one type of interaction is important in these systems, and that a combination of multipolar interactions and nonadiabatic transitions must be considered in reconciling the rates of quenching ob Br^* by CO_2, COS, and CS_2. The dramatic change in quenching efficiency for CO_2 (with an established product channel containing two vibrational quanta 30 cm^{-1} from the Br^* energy) as compared to COS and CS_2, is very suggestive of a resonant enhancement of the quenching rate. The relatively small change in quenching efficiency of COS as compared to CS_2, where no analogous resonant states are available for either species, is also suggestive of a strong resonant effect for the case of CO_2. A study of the temperature dependencies of these rate processes should offer insight concerning these points, and these measurements are currently in progress in our lab. In the present experiments, it has not been possible to determine the primitive distribution of vibrational states because of very rapid processes such as Eq. (10) which preserve the number of quanta, but redistribute them via resonant $V-V$ transfer. In addition, we have only monitored the ν_3 fluorescence, since the other normal modes are either not IR active or fluoresce at wavelengths which are too long to be detected with our present IR detectors. Thus, even though we have measured quantitatively the branching into the vibrational product channels which contain the ν_3 vibration, it remains to measure similar $E-V$ rates for the other normal modes and this will be the subject of future study. At this point, we do not attach particular significance to the quantum yields for excitation of ν_3 vibrations as shown in Table II. Because of the experimental difficulties in measuring $F(\mathrm{mol}(\nu_3))$, the relative values of the $F(\mathrm{mol}(\nu_3))$ listed in Table II are only accurate to 20%, and the absolute values are only certain within a factor of two. Also, particular care should be exercised in drawing conclusions from these data since information concerning the $E-V$ excitation of the other normal modes for these species are not yet available. For the case of CS_2, for instance, it is energetically possible to excite two ν_3 quanta in the quenching of Br^*, where CO_2 and COS can each only receive one quantum of ν_3 excitation.

ACKNOWLEDGMENTS

The authors are very pleased to acknowledge many fruitful discussions with Steve Leone, Steve Lemont, and George Flynn, as well as a preprint of the Lemont and Flynn paper prior to its publication. We are also indebted to J. Emerson and V. Kushawaha for technical assistance.

APPENDIX

To obtain the efficiency with which the quenching process produces a specific vibrational excitation, it is necessary to compare the particular vibrational fluorescence under consideration to that of a species whose concentration is known. The total density of a particular vibrational state produced by $E-V$ transfer is obtained by integrating

$$d/dt[\mathrm{mol}(\nu_i)]_\rho = k_{E-V}[\mathrm{mol}][\mathrm{Br}^*]_0 \exp(-t/\tau_{\mathrm{Br}^*}), \quad (A.1)$$

where k_{E-V} is the particular $E-V$ rate coefficient under consideration $[\mathrm{mol}(\nu_i)]_\rho$ is the density of vibrational quanta *produced* subsequent to a single photolysis event, and the other symbols have their usual meaning. Here, we have excluded the deactivation of $\mathrm{mol}(\nu_i)$ from consideration since we are only interested in the total density of species *produced*, irrespective of their subsequent relaxation. Integration of (A.1) yields

$$[\mathrm{mol}(\nu_i)]_\rho = k_{E-V}[\mathrm{mol}][\mathrm{Br}^*]_0 \tau_{\mathrm{Br}^*}, \quad (A.2)$$

where $[\mathrm{mol}(\nu_i)]_\rho$ is now the *total* density of vibrational quanta ν_i produced by the quenching of Br^*. Since the LHS of Eq. (A.2) is proportional to the observed molecular fluorescence, we now have a basis for obtaining the absolute $E-V$ rate coefficient.

Let us take, as a basis for comparison, the fluorescence from Br^*

$$[\mathrm{Br}^*] = [\mathrm{Br}^*]_0 \exp(-t/\tau_{\mathrm{Br}^*}). \quad (A.3)$$

By comparing $[\mathrm{mol}(\nu_i)]_\rho$ to $(\mathrm{Br}^*)_0$, we have a direct measure of the efficiency with which the ν_i quanta are produced. Thus,

$$\frac{[\mathrm{mol}(\nu_i)]_\rho}{[\mathrm{Br}^*]_0} = \begin{array}{l}\text{fraction of } \mathrm{Br}^*\text{–mol quenching}\\ \text{collisions resulting in excitation}\\ \text{of a single } \nu_i \text{ quantum in the molecule}\end{array} = F(\mathrm{mol}(\nu_i)). \quad (A.4)$$

Experimentally, $[\mathrm{mol}(\nu_i)]_\rho$ can be obtained from the computer generated preexponential portion of Eq. (12), here denoted by $A_{\mathrm{mol}(\omega_i)}$. $[\mathrm{mol}(\nu_i)]_\rho$ is obtained by multiplying $A_{\mathrm{mol}(\nu_i)}$ by $|\tau_{\mathrm{Br}^*}(\tau_{\mathrm{Br}^*}^{-1} - \tau_{\mathrm{mol}(\nu_i)}^{-1}|_{\mathrm{mol}(\omega_i)}$, since $A_{\mathrm{mol}(\omega_i)}$ is given by

$$A_{\mathrm{mol}(\omega_i)} = \frac{k_{E-V}(\mathrm{mol})(\mathrm{Br}^*)_0}{|\tau_{\mathrm{Br}^*}^{-1} - \tau_{\mathrm{mol}(\nu_i)}^{-1}|_{\mathrm{mol}(\omega_i)}}. \quad (A.5)$$

In comparing the measured intensities, a number of experimental considerations must be added to (A.4) yielding

$$F(\mathrm{mol}(\nu_i)) = \frac{A_{\mathrm{mol}(\omega_i)}|\tau_{\mathrm{Br}^*}(\tau_{\mathrm{Br}^*}^{-1} - \tau_{\mathrm{mol}(\nu_i)}^{-1}|_{\mathrm{mol}(\omega_i)}}{[\mathrm{Br}^*]_0} \times \frac{A^3(\mathrm{Br}^*)}{A^3(\mathrm{mol}(\nu_i))} \frac{T_{\mathrm{Br}}}{T_{\mathrm{mol}(\nu_i)}} \frac{D^*_{\mathrm{Br}}}{D^*_{\mathrm{mol}(\omega_i)}} \frac{\lambda(\mathrm{mol}(\nu_i))}{\lambda(\mathrm{Br}^*)} \times \left(\frac{k_9[\mathrm{mol}] + k_5[\mathrm{Br}_2]}{k_9[\mathrm{mol}]}\right)[\text{trapping factor for } \mathrm{mol}(\nu_i)], \quad (A.6)$$

where A^s is the Einstein coefficient for spontaneous emission, T is the transmission of the interference filter(s), D^s is the detector response at the particular frequency on interest, λ is the wavelength of the emission, and [trapping factor for mol(ν_i)] accounts for resonance absorption, by unexcited molecules, of radiation that is emitted from the photolyzed volume. It is not necessary to account for absorption of Br^* emission because of the low density of Br atoms and the long spontaneous emission lifetime (1.1 s) of Br^*. Trapping of resonance radiation is a complex phenomenon and it is wisest to choose experimental conditions in a way that puts the trapping factor as close to unity as is possible. The term $[k_0[\text{mol}]+k_5[Br_2]]/k_0[\text{mol}]$ accounts for some of the Br^* being deactivated by Br_2 and therefore being unavailable for exciting the molecular species. The factors $A_{\text{mol}(\nu_i)}$ and $[Br^*]_0$ are taken directly from the data.

It is also possible, and sometimes very convenient, to compare the molecular fluorescence from the species under consideration to that of a molecular species whose $E-V$ rate coefficient is well known. In this regard, using the excitation of HCl to the $v=1$ state as an example, (A.6) becomes

$$\frac{F(\text{mol}(\nu_i))}{F(\text{HCl})} = \frac{A_{\text{mol}(\nu_i)}\,|\,\tau_{Br^*}^{-1} - \tau_{\text{mol}(\nu_i)}^{-1}\,|_{\text{mol}(\nu_i)}}{A_{\text{HCl}}\,|\,\tau_{Br^*}^{-1} - \tau_{\text{HCl}}^{-1}\,|_{\text{HCl}}} \times \frac{A^s(\text{HCl})}{A^s(\text{mol}(\nu_i))} \frac{T_{\text{HCl}}}{T_{\text{mol}(\nu_i)}} \frac{D^s_{\text{HCl}}}{D^s_{\text{mol}(\nu_i)}} \frac{\lambda(\text{mol}(\nu_i))}{\lambda(\text{HCl})} \times \frac{k_0^{\text{HCl}}[\text{HCl}]}{k_0^{\text{mol}}[\text{mol}]} \frac{(\text{trapping factor for mol}(\nu_i))}{(\text{trapping factor for HCl})}, \qquad (A.7)$$

where it is understood that HCl is excited to the $v=1$ state.

Whereas the use of Eq. (A.6) has the advantage of constituting more of a direct measurement than the use of Eq. (A.7), there are a number of difficulties associated with the use of Eq. (A.6). These difficulties stem mainly from the lower signal levels of Br^*, the requirement of using more than one interference filter to obtain Br^* signals, and the large change of D^s from 3685 cm^{-1} (Br^* emission) to many of the lower frequency molecular frequencies of interest. The use of Eq. (A.7) avoids these difficulties and, in addition, minimizes difficulties due to radiation trapping. In this regard, in comparing fluorescence from two molecular species with comparable spontaneous emission lifetimes (e.g., CO_2 and COS), the effects due to radiation trapping are very similar for each species, and thus do not constitute a significant source of error.

It should be cautioned that the use of Eq. (A.6) and/or (A.7) to obtain absolute $E-V$ rate coefficients is difficult, requiring considerable experimental care. The accumulation of systematic errors from the various experimental factors inevitably results in error limits of ± 20%, for the best of cases. This is the uncertainty of the relative $E-V$ rate coefficients {e.g., $F(CO_2(\nu_3))$ vs $F(COS(\nu_3))$}.

The largest sources of uncertainty in deriving *absolute* $E-V$ rates from Eq. (A.6) are the spontaneous emission lifetimes of the fluorescing species. Garstang[26,27] estimates an uncertainty of 20% for the Br^* lifetime, and similar uncertainties exist for the molecular lifetimes which are obtained from integrated absorption data. Consequently, we feel that the absolute $E-V$ rates are only certain to within a factor of two.

[1] D. Husain and R. J. Donovan, Adv. Photochem. 8, 1 (1971) and references cited therein. This is a review of the kinetics of electronically excited halogen atoms.
[2] R. J. Donovan, D. Husain, and C. D. Stevenson, Trans. Faraday Soc. 66, 2148 (1970).
[3] S. R. Leone and F. J. Wodarczyk, J. Chem. Phys. 60, 314 (1974).
[4] F. J. Wodarczyk and P. B. Sackett, Chem. Phys. 12, 65 (1976).
[5] A. Hariri, A. B. Petersen, and C. Wittig, J. Chem. Phys. 65, 1872 (1976).
[6] A. B. Petersen, C. Wittig, and S. R. Leone, J. Appl. Phys. 47, 1051 (1976).
[7] A. Hariri and C. Wittig (unpublished).
[8] A. B. Petersen, C. Wittig, and S. R. Leone, Appl. Phys. Lett. 27, 305 (1975).
[9] A. B. Petersen, L. W. Braverman, and C. Wittig, J. Appl. Phys. 48, 230 (1977).
[10] A. T. Pritt, Jr. and R. D. Combe, J. Chem. Phys. 65, 2096 (1976).
[11] G. P. Quigley and G. J. Wolga, J. Chem. Phys. 62, 4560 (1975).
[12] J. J. Ewing, Chem. Phys. Lett. 29, 50 (1974).
[13] I. H. Zimmerman and T. F. George, J. C. S. Faraday II, 71, 2030 (1975).
[14] R. J. Donovan, C. Fotakis, and M. F. Golde, J. C. S. Faraday II, 72, 2055 (1976).
[15] K. R. Wilson, *Excited State Chemistry*, edited by J. N. Pitts, Jr. (Gordon and Breach, New York, 1970), p. 33.
[16] We have been amazed by the inert character of this wax in the presence of Br_2.
[17] J. Finzi and C. B. Moore, J. Chem. Phys. 63, 2285 (1975).
[18] S. Lemont and G. W. Flynn (unpublished).
[19] R. J. Donovan and D. Husain, Trans. Faraday Soc. 62, 2643 (1966).
[20] J. K. Hancock, D. F. Starr, and W. H. Green, J. Chem. Phys. 61, 3017 (1974).
[21] B. M. Hopkins, A. Baronavski, and H. L. Chen, J. Chem. Phys. 59, 836 (1973).
[22] K. K. Hui and T. A. Cool, J. Chem. Phys. 65, 3536 (1976).
[23] D. R. Siebert and G. W. Flynn, J. Chem. Phys. 64, 4973 (1976).
[24] C. C. Davis and R. A. McFarlane, J. Chem. Phys. 65, 3709 (1976).
[25] J. Tiee and C. Wittig (unpublished).
[26] R. H. Garstang, *Forbidden Transitions in Atomic and Molecular Processes*, edited by D. R. Bates (Academic, New York, 1962).
[27] R. H. Garstang, J. Res. Nat. Bur. Stand. A 68, 61 (1964).

VII. Electronic to vibrational energy transfer, from $Br(4^2P_{1/2})$ to H_2O[a]

A. Hariri and C. Wittig

Departments of Electrical Engineering and Physics, University of Southern California, University Park, Los Angeles, California 90007
(Received 25 October 1977)

A pulsed dye laser has been used to photolytically produce excited bromine atoms in the $4^2P_{1/2}$ state in a flowing gas mixture containing Br_2, H_2O, and Ar. By monitoring the time resolved molecular fluorescence from the stretching vibrations of H_2O, it was possible to determine (1) the rate coefficient for the quenching of Br^* by H_2O, (2) the fraction of the quenching collisions which result in excitation of the (001) and/or (100) state, and (3) various V–V, R, T energy transfer rate coefficients for H_2O'. Our results indicate that energy transfer from Br^* to H_2O is a fast and mode specific process. A comparison to other Br^*–hydride systems is made.

I. INTRODUCTION

The collisional deexcitation of electronically excited halogen atoms in the $^2P_{1/2}$ state, with accompanying vibrational excitation in the molecular quencher, has become the subject of considerable experimental[1–9] and theoretical[10–12] investigation in recent years. For low electronic excitations, in which only one or two vibrational quanta are involved, such processes can be highly mode specific and there is a clear indication that resonant energy transfer is the preferred quenching route when this channel is available. Away from resonance, it is still possible to efficiently excite the vibrational degree of freedom of the quenching species, but here there are no clear propensity rules, and each case seems to be somewhat special.

The present experimental study describes the quenching of $Br(4^2P_{1/2})$, hereafter referred to as Br^*, by H_2O, with resulting excitation of the (001) and/or (100) states. Water vapor occupies a unique role in vibrational energy transfer because of the strong anisotropic forces (such as hydrogen bonding) between water molecules and a number of collision partners. H_2O is an extremely efficient, chemically stable quenching partner for species such as CO_2,[13] HF,[14] and many others. Most previous work concerning energy transfer between H_2O and other molecules was done using ultrasonic, impact tube, and shock tube techniques.[15–17]

A schematic of the H_2O and Br energy levels and energy transfer processes is shown in Fig. 1. In addition to the proximity of the (001), (100), and (020) states, there is considerable coupling of these vibrations [(001) and (100) via Coriolis interaction, (100) and (020) via Fermi interaction, and (001) and (020) via Coriolis interaction[18]].

The purpose of the present experiments is twofold. First, we require accurate rate coefficients for the Br^*–H_2O system in order to correctly determine the potential of the H_2O laser which is pumped by electronic to vibrational (E – V) energy transfer from Br^*.[19] Second, by studying energy transfer from Br^* to H_2O, we hope to contribute to an understanding of the mechanism(s) of E – V energy transfer in simple molecular systems.

II. EXPERIMENTAL

The experimental technique used in the present study is laser induced fluorescence, and our particular arrangement has been described in detail previously.[4,5] In the work reported here, H_2O dilute in Ar was injected into a flowing Br_2/Ar mix sufficiently upstream from the fluorescence cell to insure proper mixing. Pressures were measured with a corrosion resistant capacitance manometer (MKS). Since both H_2O and Br_2 were dilute in Ar, the sound velocities for the Br_2/Ar and H_2O/Ar samples were very nearly the same and no corrections to the measured partial pressures were necessary.[20] Flashlamp pumped dye lasers (Chromatix and Phase-R, 5 and 15 mJ, respectively) operating near 490 nm were used to create Br^* on a time scale short compared to that of the subsequent kinetic processes.

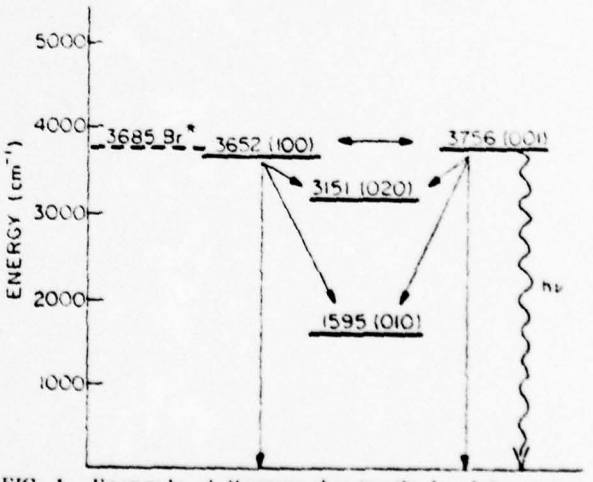

FIG. 1. Energy level diagram showing the low lying states of the $Br + H_2O$ system. The straight arrows indicate the V–V, R, T processes of the H_2O molecule. Spontaneous emission (labelled $h\nu$) is monitored on the (001) → (000) and (100) → (000) bands, with the (001) → (000) band being the stronger emitter.

[a] Research supported by the U. S. Army Research Office under Grant No. DAAG29-76-G-0124, and by the Donors of the Petroleum Research Fund, administered by the American Chemical Society.

J. Chem. Phys. 68(5), 1 Mar. 1978 0021-9606/78/6805-2109$01.00

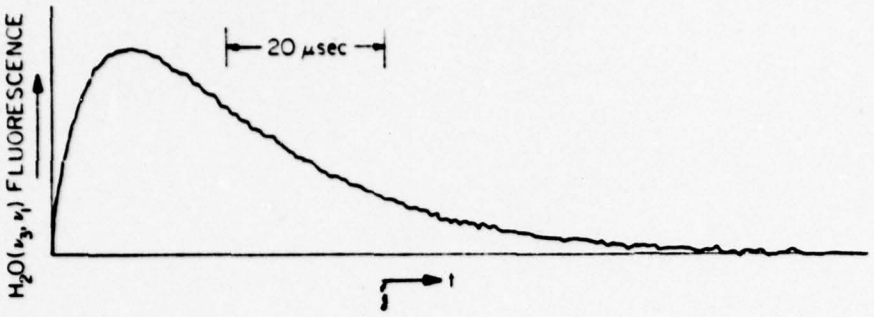

FIG. 2. Typical $H_2O^{\dagger}$ (ν_3, ν_1) fluorescence signal after averaging eight traces. Here, $[H_2O]+[Br_2]=0.61$ torr, $X_{H_2O}=0.042$, and the dye laser energy was 15 mJ.

At 490 nm, Br_2 photolysis produces Br* and Br in approximately a 1:1 ratio.[21] Mirrors were used to multiple pass the dye laser beam through the fluorescence cell thereby improving S/N. Spontaneous emission was observed at right angles to the laser beam with a large area InSb photovoltaic detector fitted with a cooled (77 °K) interference filter (FWHM = 1.0 μm centered at 3.0 μm) in order to eliminate scattered laser light and reduce the background flux incident on the detector. Signals from the detector were amplified, digitized, averaged, and recorded with an XY plotter as reported previously.[5] One such typical signal is shown in Fig. 2. Since these data are of the type where $\tau_{rise} \sim \tau_{fall}$ data analyses must be done with a computer, and this is described below. Fluorescence from Br* was strongly overlapped by $H_2O^{\dagger}$ emission and it was not possible to monitor Br* directly.

Br_2 (Aristar grade, British Drug House, 99.8%) was purified by repeated distillation from 255 to 77 °K followed by slow passage over P_2O_5. H_2O was degassed at 295 and 273 °K. Ar(Airco, 99.998%) was passed through a trap at 77 °K. H_2O/Ar and Br_2/Ar gas mixtures were prepared separately in 12 liter pyrex bulbs prior to a given run and allowed to mix thoroughly before use. In addition, the glass apparatus was seasoned by exposure to Br_2 and H_2O several hours before each experiment.

III. RATE PROCESSES

The production of Br* by laser photolysis takes place on a time scale which is short compared to that of the subsequent kinetic processes. Following photolysis, removal of Br* proceeds by way of

$$Br^* + H_2O(000) \xrightarrow{k_1} Br + H_2O(\text{all states}) \tag{1}$$

and

$$Br^* + Br_2 \xrightarrow{k_2} Br + Br_2 . \tag{2}$$

Deactivation of Br* by Ar is very inefficient[22] and does not contribute to Br* removal under our experimental conditions. Process (1) can be further separated as per the vibrational states of H_2O:

$$Br^* + H_2O(000) \xrightarrow{k_3} Br + H_2O(\nu_3, \nu_1), \tag{3}$$

$$Br^* + H_2O(000) \xrightarrow{k_4} Br + H_2O(0n0), \tag{4}$$

where $n = 0$, 1, 2, and (ν_3, ν_1) indicates one quantum of *either* ν_3 *or* ν_1 vibration. Collisional energy transfer between the (001) and (100) states:

$$H_2O(001) + H_2O(000) \xrightarrow{k_5} H_2O(100) + H_2O(000) + 104\ \text{cm}^{-1}, \tag{5}$$

is extremely rapid ($k \cong 10^7\ \text{sec}^{-1}\,\text{torr}^{-1}$ at 295 °K).[23] Due to this very strong collisional coupling of ν_3 and ν_1, we cannot treat these states separately in the experiments reported here and thus we will treat the stretching vibrations as a single energy state during much of this paper. Also, emissions from the (001) − (000) and (100) − (000) bands are strongly overlapped in frequency, preventing precise identification with interference filter resolution.

Deactivation of $H_2O(\nu_3, \nu_1)$ occurs via the following processes:

$$H_2O(\nu_3, \nu_1) + H_2O(000) \xrightarrow{k_6} H_2O(0n0) + H_2O(0n0), \tag{6}$$

$$H_2O(\nu_3, \nu_1) + Br_2 \xrightarrow{k_7} H_2O(0n0) + Br_2, \tag{7}$$

$$H_2O(\nu_3, \nu_1) + Ar \xrightarrow{k_8} H_2O(0n0) + Ar . \tag{8}$$

The $H_2O(\nu_3, \nu_1)$ density is given by

$$[H_2O(\nu_3, \nu_1)](t) = \frac{k_3[H_2O][Br^*]_0}{\tau_{Br^*}^{-1} - \tau_{\nu_3,\nu_1}^{-1}} \times \left[\exp^{(-t/\tau_{\nu_3,\nu_1})} - \exp^{(-t/\tau_{Br^*})}\right], \tag{9}$$

where $[Br^*]_0$ is the density of Br* produced by the laser, and τ_{Br^*} and τ_{ν_3,ν_1} are the lifetimes of Br* and $H_2O(\nu_3, \nu_1)$, respectively. Here, we assume implicitly that excitation is a simple process as described by (3). This of course is not the case, and (3) can be broken down to the separate processes:

$$Br^* + H_2O(000) \xrightarrow{k_{10}} Br + H_2O(001), \tag{10}$$

$$Br^* + H_2O(000) \xrightarrow{k_{11}} Br + H_2O(100) . \tag{11}$$

However, because of the very rapid equilibration of the (001) and (100) states via (5), we can take these two states to be in equilibrium with relative populations given by

$$\frac{[H_2O(001)]}{[H_2O(100)]} = e^{-\Delta E/kT} = 0.61 \tag{12}$$

at 295 °K.

Experimental conditions are maintained such that all kinetics are sensibly first order. Rate coefficients are obtained from the observed lifetimes:

$$\tau_{Br^*}^{-1} = k_1[H_2O] + k_2[Br_2], \tag{13}$$

$$\tau_{\nu_3,\nu_1}^{-1} = k_6[H_2O] + k_7[Br_2] + k_8[Ar], \tag{14}$$

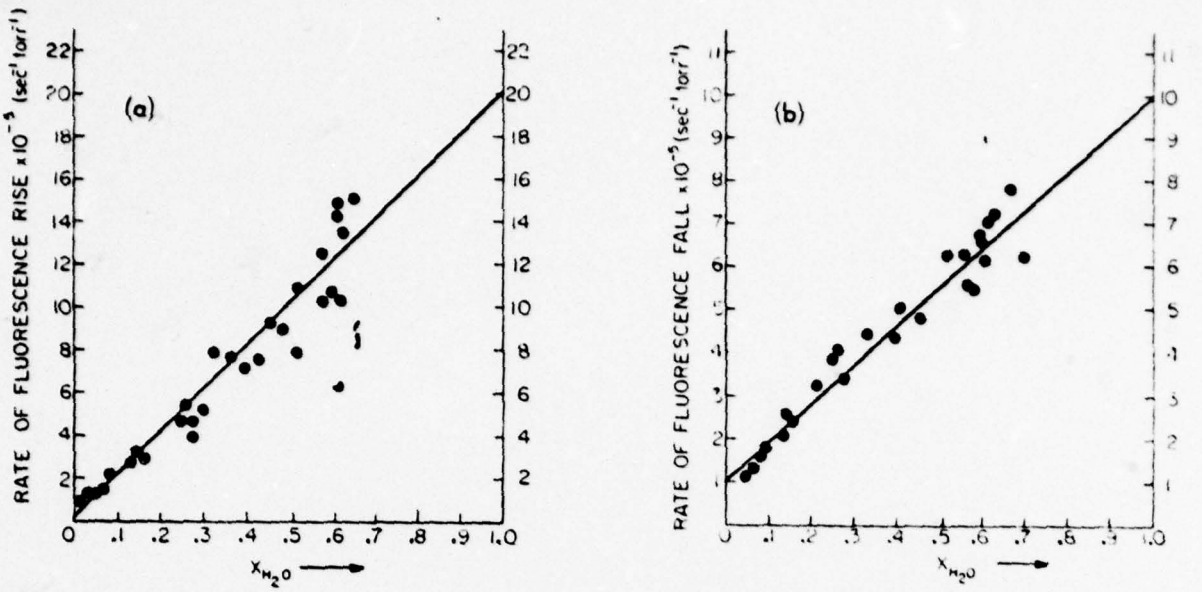

FIG. 3. Rate of fluorescence rise (a) and fall (b) as a function of sample mole fraction. Each point represents an average of nominally 128 separate traces. The straight lines are least squares fits to the data.

by the usual systematic variations of concentrations. Since the observed rise and fall times of the fluorescence signals are comparable, it was necessary to use a computer curve fitting routine to extract τ_{rise} and τ_{fall}.

IV. RESULTS

By varying the mole fraction (X) of the gas sample while measuring τ_{rise} and τ_{fall}, we obtained the data shown in Fig. 3. There is a natural ambiguity in ascribing τ_{rise} and τ_{fall} to the proper kinetic processes, and this is clear from inspection of (9). With $\tau_{Br^*} < \tau_{\nu_3,\nu_1}$, the rise time is a measure of τ_{Br^*}, while for $\tau_{Br^*} > \tau_{\nu_3,\nu_1}$, the rise time is a measure of τ_{ν_3,ν_1}. Finzi and Moore have measured energy transfer rate coefficients for the (001) and (100) states of H_2O,[23] and thus we are able to assign the $X = 1$ intercept in Fig. 3(b) to the rate coefficient for removal of the (equilibrated) stretching mode excitation. The rate coefficients (k_1, k_2, k_6, k_7) obtained from Fig. 3 are listed in Table I. In obtaining rate coefficients from the intercepts shown in Fig. 3(b), it was necessary to include the quenching of $H_2O(\nu_3, \nu_1)$ by Ar.[24] In the region near $X = 0$ in Fig. 3(a), data were collected and anlayzed separately in order to obtain an accurate intercept.[25]

The absolute rate k_3 for excitation of $H_2O(\nu_3, \nu_1)$ was obtained by comparing the fluorescence intensity of $H_2O^\dagger$ with that of HCl($v = 1$). This is an elaborate procedure, and details of the experimental technique and data analysis are given in Ref. 5 and will not be repeated here. We should like to emphasize that the largest sources of error in these measurements are systematic rather than random. In the work reported here, values of 174 and 17 $cm^{-2}\,atm^{-1}$(295 °K) for the (000) − (001) and (000) − (100) band strengths of H_2O,[26] and 135 $cm^{-2}\,atm^{-1}$(295 °K) for the 0 − 1 band strength of HCl[27] were used. The corresponding spontaneous emission lifetimes are 13.4, 145, and 29.3 msec, respectively. We feel that these values are most accurate even though other values can be found in the literature. In analyzing the data, it is necessary to include emission from (100) as well as (001):

$$I^n \propto \frac{[H_2O(001)]}{\tau_{001}} + \frac{[H_2O(100)]}{\tau_{100}}, \tag{15}$$

where I^n = fluorescence intensity, τ refers to the spontaneous emission lifetime, and we have assumed that the 104 cm^{-1} difference in emission frequencies is not important. Since collisional mixing of (001) and (100) results in an equilibrium of these states as per (12), (15) reduces to

$$I^n \propto \frac{0.38[H_2O(\nu_3, \nu_1)]}{\tau_{001}} + \frac{0.62[H_2O(\nu_3, \nu_1)]}{\tau_{100}}, \tag{16}$$

TABLE I. Summary of the rate measurements.

Process	Rate coefficients (295 °K)[a] This work[b]	Previous work
$Br^* + H_2O(0000) \xrightarrow{k_1} Br + H_2O$ (all states)	$(2.0 \pm 0.4) \times 10^{8}$ $(6.2 \pm 1.2) \times 10^{-11}$	$(3.2) \times 10^{-11}$ [c]
$Br^* + Br_2 \xrightarrow{k_2} Br + Br_2$	$(3.0 \pm 0.6) \times 10^{8}$ $(9.3 \pm 1.9) \times 10^{-11}$	[d]
Fraction of quenching collisions resulting in excitation of (100) and/or (001) states	100%	
$H_2O(\nu_3, \nu_1) + H_2O(0000) \xrightarrow{k_6} H_2O(0\nu_20) + H_2O(0\nu_20)$	$(1.0 \pm 0.3) \times 10^{7}$ $(3.1 \pm 0.9) \times 10^{-12}$	8.5×10^{-12} [e]
$H_2O(\nu_3, \nu_1) + Br_2 \xrightarrow{k_7} H_2O(0\nu_20) + Br_2$	$(5 \pm 2) \times 10^{8}$ $(1.5 \pm 0.6) \times 10^{-11}$	

[a] The upper entry is in units of $sec^{-1}\,torr^{-1}$; the lower entry is in units of cm^3 $molecule^{-1}$ sec^{-1}.
[b] The uncertainty includes the possibility of systematic as well as random errors.
[c] Reference 2.
[d] This value agrees well with previous literature values from Refs. 2–6.
[e] Reference 23.

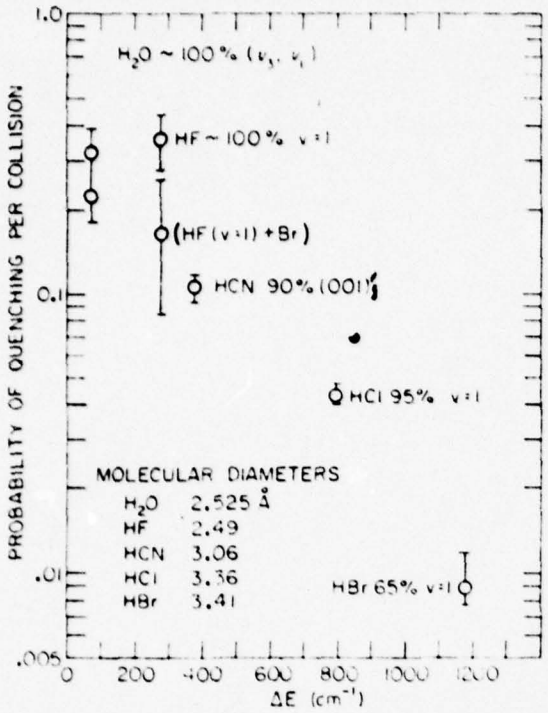

FIG. 4. Probability of quenching per collision vs energy defect for all hydrides which are known to quench Br^* via $E-V$ transfer. All probabilities are for the exothermic direction. The sources of the data are: HF(upper),[3] HF(lower),[29] HCN,[4] HCl,[2] and HBr.[2] The upper and lower circles for the case of H_2O refer to transfer into the (001) and (100) states, respectively. The measured efficiencies (k_{E-V}/k_Q) into particular product states are also listed. Molecular diameters are from Ref. 28. The diameter of Br^* is taken to be the same as Kr (3.60 Å).

where $[H_2O(001)] + [H_2O(100)] = [H_2O(\nu_3, \nu_1)]$. Since τ_{001} is an order of magnitude smaller than τ_{100}, most of the observed emission emanates from the (001) state.

Analyses of six sets of data yield an absolute rate coefficient k_3 which is 25% higher than the quenching rate coefficient k_1. It is not surprising that we measure $k_3 > k_1$, as the (001) and (100) states are not completely equilibrated during the measurement and selective pumping of (001) would produce this result. Since it is not possible to produce more than one quantum of (ν_3, ν_1) excitation per quenching collision (and given the possible systematic errors)this measurement shows that $k_3 \cong k_1$. This point is noted in Table I.

V. DISCUSSION

The excitation of $H_2O(\nu_3, \nu_1)$ via Br^* quenching is an example of a fast, resonant, mode specific energy transfer process in which electronic and vibrational degrees of freedom are coupled. Transfer to the (001) state is 71 cm^{-1} endothermic, while transfer to (100) is 33 cm^{-1} exothermic. Figure 4 compares the quenching probability of H_2O to those of other hydrides. Those species listed in Fig. 4 are *all* of the hydrides which are known to quench Br^* efficiently via $E-V$ exchange. The probabilities are shown for the exothermic direction, where detailed balance is used to make the appropriate correction for rates which are measured in the endothermic direction. In the case of H_2O, this results in two possible values for the quenching probability since we do not know whether (1) proceeds via (10) or (11).

The mode specific nature of the energy transfer process suggests that a long lived intermediate is not formed in collisions of Br^* with H_2O. Because of the high quenching probability, it is not possible to calculate this probability using standard perturbation theory techniques. We should, nevertheless, like to make a few comments concerning the two vehicles of energy transfer, multipolar interactions and nonadiabatic transitions, which may be responsible for the observed $E-V$ transfer.

The lowest order nonvanishing term arising from the long-range multipolar field interaction of Br^* with H_2O is dipole–quadrupole.[30] Rough calculations of transition probabilities, using this interaction, indicate that this interaction alone can adequately account for our observations. In these calculations, we have used first-order perturbation theory to compute the transition probabilities following Sharma and Brau.[30] We have used the integrated absorption data for H_2O[26] to obtain the transition dipole moment, and the transition quadrupole moment of $Br-Br^*$ was taken from Garstang.[31] The computed probabilities are of order unity indicating (a) that the use of perturbation theory is not valid, and (b) although an *accurate* comparison between experiment and theory is not possible, it is clear that the dipole–quadrupole interaction *can* account for our observations. Similar considerations applied to the case of $Br^* + HF$ also show that the observed $E-V$ transfer here can be explained by a dipole–quadrupole interaction. For molecules where energy transfer is much less resonant (HCN, HCl, HBr, ...), the observed quenching rates cannot be accounted for by the multipolar interaction, as the computed probabilities are very much smaller than the measured probabilities. Here, nonadiabatic transitions between the two electronic potential surfaces must be responsible for the observed energy transfer processes.

We are presently measuring the temperature dependence of the $E-V$ energy transfer rate coefficients in order to further determine the mechanisms whereby energy transfer occurs.

ACKNOWLEDGMENTS

The authors gratefully acknowledge a number of very useful discussions with J. Finzi, D. Shim, and J. Tiee.

[1] R. J. Donovan, D. Husain, and C. D. Stevenson, Trans. Faraday Soc. **66**, 2148 (1970).
[2] S. R. Leone and F. J. Wodarczyk, J. Chem. Phys. **60**, 314 (1974).
[3] F. J. Wodarczyk and P. B. Sackett, Chem. Phys. **12**, 65 (1976).
[4] A. Hariri, A. B. Peterson, and C. Wittig, J. Chem. Phys. **65**, 1872 (1976).
[5] A. Hariri and C. Wittig, J. Chem. Phys. **67**, 4454 (1977).

[6]S. Lemont and G. W. Flynn (unpublished).
[7]A. J. Grimley and P. L. Houston (unpublished).
[8]A. T. Pritt, Jr. and R. D. Coombe, J. Chem. Phys. **65**, 2096 (1976).
[9]R. D. Coombe and A. T. Pritt, Jr., J. Chem. Phys. **66**, 5214 (1977).
[10]E. A. Andreev and E. E. Nikitin, Theor. Chim. Acta (Berlin) **17**, 171 (1970).
[11]H. Zimmerman and T. F. George, J. Chem. Phys. **61**, 2468 (1974).
[12]H. Zimmerman and T. F. George, J. Chem. Soc. Faraday Trans. 2 **71**, 2030 (1975).
[13]M. I. Buchwald and S. H. Bauer, J. Phys. Chem. **76**, 3108 (1972).
[14]J. K. Hancock and W. H. Green, J. Chem. Phys. **57**, 4515 (1972).
[15]H. E. Bass, J. R. Olson, and R. C. Amme, J. Acoust. Soc. Am. **56**, 1455 (1974).
[16]P. W. Huber and A. Kantrowitz, J. Chem. Phys. **15**, 275 (1947).
[17]R. T. V. Kung and R. E. Center, J. Chem. Phys. **62**, 2187 (1975).
[18]J. M. Flaud and C. C. Peyret, J. Mol. Spectrosc. **51**, 142 (1974).
[19]A. B. Petersen, L. W. Braverman, and C. Wittig, J. Appl. Phys. **48**, 230 (1976).
[20]J. Bott, J. Chem. Phys. **61**, 8 (1974).
[21]K. R. Wilson, *Excited State Chemistry*, edited by J. N. Pitts, Jr. (Gordon and Breach, New York, 1970), p. 33.
[22]D. Husain and R. J. Donovan, Adv. Photochem. **8**, 1 (1971).
[23]J. Finzi, Ph.D. thesis, University of California at Berkeley, 1975; J. Finzi and C. B. Moore (unpublished).
[24]The rate coefficient for this process is taken from Ref. 23. Only 5×10^{-4} of the $H_2O(0_3, \nu_1)$ molecules are quenched by Ar.
[25]For the sake of brevity, these data are not shown. The rate coefficient obtained here agrees well with previous measurements by ourselves[1,5] and others.[2,3]
[26]J. A. Coakley, Jr., J. Quant. Spectrosc. Radiat. Transfer **13**, 937 (1973).
[27]R. A. Tath, R. H. Hunt, and E. K. Plyler, J. Mol. Spectrosc. **35**, 110 (1970).
[28]F. J. Zeleznik and R. A. Svehla, J. Chem. Phys. **53**, 632 (1970).
[29]G. P. Quigley and G. J. Wolga, J. Chem. Phys. **62**, 4650 (1975).
[30]R. D. Sharma and C. A. Brau, Phys. Rev. Lett. **19**, 1273 (1967).
[31]R. H. Garstang, J. Res. Natl. Bur. Stand. Sect. A **68**, 61 (1964).
[32]R. J. Donovan and D. Husain, Trans. Faraday Soc. **62**, 2643 (1969). R. J. Donovan and D. Husain, Trans. Faraday Soc. **62**, 2989 (1966).

VIII. Temperature dependence of the quenching of $Br(4^2P_{1/2})$ by CO_2 and HCl with accompanying vibrational excitation[a)]

Hanna Reisler[b)] and Curt Wittig

Department of Electrical Engineering and Physics, University of Southern California, University Park, Los Angeles, California 90007
(Received 13 December 1977)

Electronic to vibrational ($E-V$) energy transfer from excited halogen atoms in the $^2P_{1/2}$ state to small molecules has been the subject of considerable recent investigation.[1-3] Several mechanisms, such as long-range multipolar interactions,[4,5] short-range repulsive interactions, and nonadiabatic curve crossings[6] have been suggested as being responsible for this process. The determination of rate coefficients alone at a single temperature cannot distinguish between these different mechanisms. For this reason, we have measured the temperature dependence of the quenching of $Br(4^2P_{1/2})$, hereafter referred to as Br^*, by small molecules. In particular, we are interested in those systems for which $E-V$ transfer has been identified as a major quenching channel. In this communication, we report examples of such temperature dependences, for the cases of HCl and CO_2, in the temperature range 296–608 °K. The fractions of quenching collisions resulting in excitation of $HCl(v=1)$ and $CO_2(\nu_3)$ are 0.95[7] and 0.4,[1] respectively. The temperature dependence of the quenching of $I(5^2P_{1/2})$ by a number of collision partners has been reported previously.[8,9] However, vibrational excitation in the molecules was not detected in these experiments and therefore the contribution of the $E-V$ channel to the total quenching is unknown.

In the present study we have used laser induced fluorescence to measure the quenching of Br^* by HCl and CO_2, with accompanying vibrational excitation in the molecular species. The main features of the experiment have been described previously.[1,10] For the temperature dependence measurements, a fluorescence cell was constructed of an IN-3 glass tube, onto which a 2.5 cm diam sapphire window was directly fused at the center. The cell was enclosed in a copper sleeve which was wrapped with nichrome heating wire. The furnace assembly was thermally insulated by fire brick. Temperature variations during an 8-h period were $\leq \pm 2$ °K. Temperature gradients along the center portion of the cell were about 4 °K, with the window being the coolest part. To minimize temperature gradients in the sample, the laser beam passed 3 cm below the window. A flashlamp pumped dye laser (Chromatix CMX-4, 1–4 mJ, 1 μsec FWHM) operating near 490 nm was used to create Br^* atoms on a time scale short compared to that of the subsequent kinetic processes. Gas mixtures consisting of Br_2, the molecular gas, and an Ar buffer were irradiated by the dye laser in the heated fluorescence cell. Time resolved fluorescence from the molecular species was collected with a 5 cm $f1$ CaF_2 lens and directed through a narrow-band interference filter onto the InSb detector. Data were digitally averaged until $S/N > 10$ was achieved. Ar and CO_2 were purified as described previously.[1] HCl (Matheson 99.9%) was distilled from an isopentane slush (113 °K) to a vessel at 77 °K with only the middle fraction retained.

Under our experimental conditions, the rate of rise of the fluorescence curve is given by

$$\tau_{Br^*}^{-1} = k_1[Br_2] + k_2[\text{mol}] , \tag{1}$$

where τ_{Br^*} is the collisional lifetime of Br^* and k_1 and k_2 are the rate coefficients for quenching of Br^* by Br_2 and the molecular species, mol, respectively. Dividing Eq. (1) by the total pressure p we get

$$(p\tau_{Br^*})^{-1} = (k_2 - k_1)\chi_{\text{mol}} + k_1 , \tag{2}$$

where χ_{mol} is the mole fraction of HCl or CO_2. The rate coefficient k_2 was determined from a linear plot of $(p\tau_{Br^*})^{-1}$ vs χ_{mol}, which yields a slope of k_2-k_1 and an intercept of k_1. At each temperature, τ_{Br^*} was measured for at least 7 different χ_{mol} in the range 0.05–0.35, and at several different total pressures for each mole fraction. Also, a portion of each sample was directed into a second cell maintained at room temperature, and the room temperature rate coefficient was measured concomitantly to serve as a check on the purity of the samples. The room temperature rate coefficients were in good agreement with previously published values.[1,7]

A change in the temperature of the sample leads to a change in the average velocity of the molecules $\bar{v}$ and hence to a change in collision frequency. Thus, it is most germane to convert the measured rate coefficients into average cross sections ($\sigma = k/\bar{v}$) for the present discussion. The cross sections for the quenching of Br^* by HCl and CO_2 are summarized in Fig. 1.

From Fig. 1 it is clear that CO_2 exhibits a negative

3308 J. Chem. Phys. 68(7) 1 Apr. 1978 0021-9606/78/6807-3308$01.00

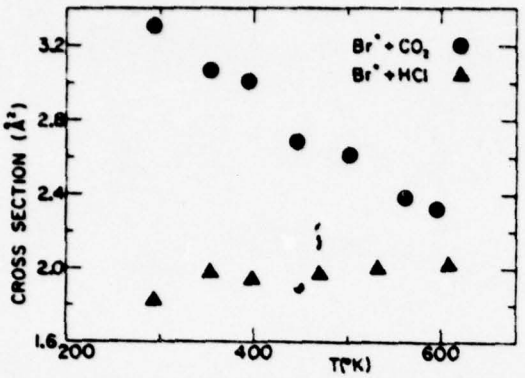

FIG. 1. Cross sections for the deactivation of $Br(4\,^2P_{1/2})$ by CO_2 and HCl. The uncertainty is ±10%. Probabilities may be obtained by dividing by the gas kinetic cross section, $\sigma_k = (\pi/4) \times (d_{Br^*} + d_{mol})^2$ where $d_{Br^*} \cong d_{Kr} = 3.60$ Å, $d_{HCl} = 3.36$ Å, and $d_{CO_2} = 3.99$ Å.

temperature dependence, a trend predicted for a long-range interaction at near resonance.[5,11] This is compatible with a major channel of the quenching of Br* by CO_2 being $E-V$ transfer to CO_2 (101) with $\Delta E = -30$ cm^{-1}, as was previously suggested.[1] We should emphasize that $E-V$ transfer to vibrational levels of CO_2 other than the (101) state may contribute to the observed cross sections since excitation of ν_3 only accounts for ~40% of the quenching.

$E-V$ transfer from Br* to HCl($v=1$) is 789 cm^{-1} exothermic, and based on comparison with $V-V$ transfer processes of similar ΔE, one would expect a positive temperature dependence. Our results show that the cross sections are almost independent of temperature in the range 300–600 °K. Also, the cross sections are too large to be accounted for by the long-range multipolar interaction as the energy transfer is quite far from resonance. It has recently been proposed[6] that for such X* + HY systems (X, Y = halogens), $E-V$ transfer proceeds via nonadiabatic transitions between crossing potential surfaces. For Br* + HCl this means crossing between the $^2A'$ surface of Br* + HCl($v=0$) and the $^2A''$ surface of Br + HCl($v=1$). Our results support this mechanism, further indicating that this crossing takes place at an energy accessible to a large fraction of the collisions even at room temperature.

In conclusion, the results presented here suggest that both multipolar long-range interactions and nonadiabatic curve crossings are important mechanisms in specific $E-V$ transfer processes. However, as the relative contributions of the various mechanisms vary with each case studied, more data are required before more general conclusions can be drawn. Such experiments are currently in progress in our laboratory.

[a]Research supported by the Army Research Office and by the Donors of the Petroleum Research Fund administered by the American Chemical Society.

[b]On leave from the Soreq Nuclear Research Center, Yavne, Israel.

[1]A. Hartiri and C. Wittig, J. Chem. Phys. 67, 4454 (1977), and references cited therein.
[2]R. D. Coombe and A. T. Pritt, Jr., J. Chem. Phys. 66, 5214 (1977).
[3]A. J. Grimley and P. L. Houston (unpublished).
[4](a) H. Zimmerman and T. F. George, J. Chem. Phys. 61, 2468 (1974); (b) J. Chem. Soc. Faraday Trans. II 71, 2030 (1975).
[5]J. J. Ewing, Chem. Phys. Lett. 29, 50 (1974).
[6]R. J. Donovan, C. Fotakis, and M. F. Golde, J. Chem. Soc. Faraday Trans. II 72, 2055 (1976).
[7]S. R. Leone and F. J. Wodarczyk, J. Chem. Phys. 60, 314 (1974).
[8]J. J. Deakin and D. Husain, J. Chem. Soc. Faraday Trans. II 68, 1603 (1972).
[9]C. Fotakis and R. J. Donovan (to be published).
[10]A. Hartiri, A. B. Peterson, and C. Wittig, J. Chem. Phys. 65, 1872 (1976).
[11](a) R. D. Sharma and C. A. Brau, Phys. Rev. Lett. 19, 1273 (1967), (b) J. Chem. Phys. 50, 924 (1969).

J. Chem. Phys. 68(7), 1 Apr. 1978 0021-9606/78/6807-3309$01.00

IX.

Temperature dependence of electronic to vibrational energy transfer from $Br(4^2P_{1/2})$ to $^{12}CO_2$ and $^{13}CO_2$[a)]

Hanna Reisler and Curt Wittig

Departments of Electrical Engineering and Physics, University of Southern California, University Park, Los Angeles, California 90007
(Received 1 June 1978)

Temperature dependent quenching cross sections for the collisional deactivation of $Br(4^2P_{1/2})$ by $^{12}CO_2$ and $^{13}CO_2$ were determined by monitoring the time resolved molecular fluorescence from the ν_3 vibrational mode of CO_2. These cross sections decrease with increasing temperature in the range 296–600°K, indicating that near resonant channels dominate the quenching processes in both molecules. The room temperature rate coefficients for the quenching of Br^* by $^{12}CO_2$ and $^{13}CO_2$ are $(5.0\pm0.2)10^3$ and $(2.3\pm0.1)10^3$ $sec^{-1}torr^{-1}$, respectively, with about half of the quenching collisions resulting in excitation of the ν_3 mode in the case of each molecule. By monitoring the amplitudes of the ν_3 fluorescence signals from $^{13}CO_2$ at different temperatures, the temperature dependence of the electronic to vibrational ($E\rightarrow V$) energy transfer cross sections into states containing ν_3 excitation was obtained. The experimental results are compared with calculations of $E\rightarrow V$ energy transfer cross sections which are based on long-range multipolar interactions.

I. INTRODUCTION

The process of electronic to vibrational ($E-V$) energy transfer from halogen atoms in the $^2P_{1/2}$ state to small molecules has recently attracted considerable attention,[1–11] and a large number of rate coefficients have been reported for $E-V$ energy transfer from $Br(4^2P_{1/2})$ and $I(5^2P_{1/2})$ to diatomic and triatomic molecules. When the number of vibrational quanta excited is small, and a near resonant channel is available, the process is often fast, efficient, and mode specific. Thus, a number of molecular lasers based on such $E-V$ energy transfer processes from $Br(4^2P_{1/2})$, hereafter referred to as Br^*, have been reported.[12–14] In cases where no resonant channels are available, the quenching rate coefficients may still be high. However, no general trends have been observed and specific details of the potential surface of the collision pair may determine the energy transfer probability. Most experimental results have been discussed in terms of two possible mechanisms: long-range multipolar interactions[15,16] and nonadiabatic curve crossings.[17] Measurements of the temperature dependence of the cross sections have proven to be very useful in elucidating mechanisms of $V-V$ energy transfer.[18] No such measurements have yet been reported for $E-V$ energy transfer.

The temperature dependence of the quenching of $I(5^2P_{1/2})$ by a number of collision partners has been reported previously.[19,20] However, vibrational excitation in the molecules was not detected in these experiments and therefore the contribution of the $E-V$ channel to the total quenching is unknown.

In a preliminary communication, we have described measurements of the temperature dependence of the quenching of Br^* by HCl and CO_2.[21] For these two systems $E-V$ energy transfer has been established as a major quenching channel at room temperature. The quenching of Br^* by CO_2 exhibits a negative temperature dependence, a trend predicted for a long-range interaction at near resonance. In the case of HCl, despite a large energy defect (789 cm^{-1}), large rate coefficients which are nearly independent of temperature in the 300–600°K range were measured. A curve-crossing mechanism may be responsible for energy transfer in this case.

In this contribution we describe further studies on the Br^*-CO_2 system. We have determined the temperature dependences of the quenching cross sections of Br^* by $^{12}CO_2$ and $^{13}CO_2$. The motivation for these measurements was to probe the importance of exact resonance in governing the magnitude and the temperature variation of the cross sections. Our results are compared to calculated energy transfer cross sections based on long-range multipolar interaction. Furthermore, in the case of $^{13}CO_2$ we have been able to determine the fraction of the quenching collisions which result in ν_3 excitation in the 300–525°K temperature range, thus establishing for the first time the temperature dependence of an $E-V$ energy transfer process.

II. EXPERIMENTAL

In the present study we have used laser induced fluorescence to measure the quenching of Br^* by $^{12}CO_2$ and $^{13}CO_2$, by monitoring the molecular fluorescence from the ν_3 mode. The experimental arrangement and procedures have been described previously.[5,21] Briefly, Br^* was produced on a time scale which was short compared to that of the subsequent kinetic processes by photolysis of Br_2 using the output from a pulsed dye laser (Chromatix CMX-4, 1–4 mJ, 1 μsec FWHM) at 490 nm. The dye laser beam was divided by a beam splitter and directed simultaneously into two fluorescence cells, one maintained at room temperature, and the other heated in an oven.[21] Gas mixtures consisting of Br_2, CO_2, and Ar were irradiated by the dye laser in the fluorescence cells. Time resolved fluorescence from the molecular species was collected with a 5 cm $f(1)$ CaF_2 lens and directed through the appropriate interference filters onto an InSb detector. For quenching rate coefficient measurements, a narrowband interference filter

[a)]Research supported by the U. S. Army Research Office.

 0021-9606/78/6908-3729$01.00

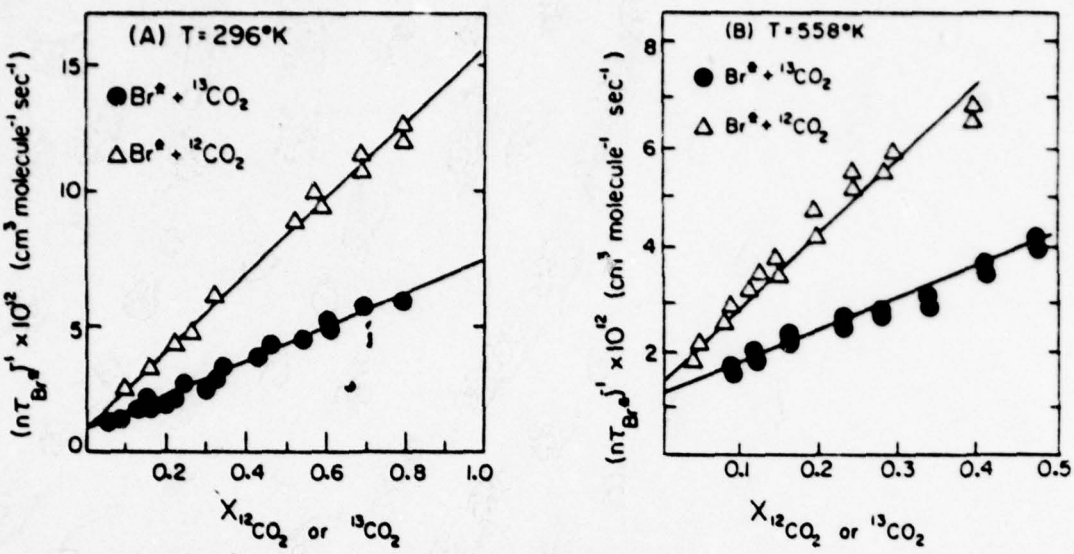

FIG. 1. Typical data for the quenching of Br* by $^{12}CO_2$ and $^{13}CO_2$ obtained by monitoring ν_3 molecular fluorescence. Quenching rate coefficients were computed from the slope and the intercept of the plots as described in the text. Typical pressures used were: Br_2 = 0.2–1.5 torr, CO_2: 0.05–0.5 torr, Ar: 10–30 torr. (a) 296 °K and (b) 558 °K.

centered at 4.35 μm with a bandwidth of 0.24 μm was used. For $E-V$ rate coefficient measurements, where the entire vibrational band must be monitored, a combination of two broadband filters giving a bandwidth of 1 μm, centered at 4.4 μm, was used.

Fluorescence signals were digitized and averaged until $S/N > 10$ was obtained (usually between 8 to 256 pulses were required).

$^{12}CO_2$ (Matheson, 99.995% min.) and $^{13}CO_2$ (Merck, Sharp, and Dohme, 95% C-13) were subjected to repeated freeze–pump–thaw cycles at 77 °K. In addition, the vacuum system was seasoned with $^{13}CO_2$ for several hours prior to its use. Ar and Br_2 were purified as described previously.[5]

III. RESULTS

A. Temperature dependences of the quenching of Br* by $^{12}CO_2$ and $^{13}CO_2$.

The rate processes which govern the rise and the decay of $^{12}CO_2$ and $^{13}CO_2$ ν_3 fluorescence are similar and have been discussed previously.[5] The number density of CO_2 molecules in the (001) state following production of Br* is given by

$$[CO_2(001)](t) = \frac{k_{E-V}[CO_2][Br^*]_0}{\tau_{Br^*}^{-1} - \tau_{CO_2(001)}^{-1}} \times \left\{ \exp\left(-\frac{t}{\tau_{CO_2(001)}}\right) - \exp\left(-\frac{t}{\tau_{Br^*}}\right) \right\}, \quad (1)$$

where τ_{Br^*} and $\tau_{CO_2(001)}$ are the collisional lifetimes of Br* and CO_2(001), respectively, $[Br^*]_0$ is the number density of Br* atoms at $t=0$, k_{E-V} is the rate coefficient for $E-V$ energy transfer from Br* to the ν_3 mode of CO_2, and the other symbols have their usual meanings. In our case $\tau_{Br^*} \ll \tau_{CO_2(001)}$. Thus, the rise of the molecular fluorescence curve reflects the quenching of Br*, and data reduction is straightforward. The Br* collisional lifetime is given, under our experimental conditions, by

$$\tau_{Br^*}^{-1} = k_1[Br_2] + k_2[CO_2], \quad (2)$$

where k_1 and k_2 are the rate coefficients for the quenching of Br* by Br_2 and by $^{12}CO_2$ or $^{13}CO_2$, respectively. Dividing Eq. (2) by the total number density, $n = [CO_2] + [Br_2]$, we get

$$(n\tau_{Br^*})^{-1} = (k_2 - k_1)X_{CO_2} + k_1, \quad (3)$$

where X_{CO_2} is the mole fraction of $^{12}CO_2$ or $^{13}CO_2$. The rate coefficients, k_2, were determined at different temperatures from linear plots of $(n\tau_{Br^*})^{-1}$ vs X_{CO_2} either by extrapolating to $X_{CO_2}=1$, or from the slope (k_2-k_1) and the intercept (k_1). Examples of such plots are given in Fig. 1 at 296 and 558 °K. A portion of each sample was directed into the second cell maintained at room temperature and the room temperature rate coefficient was measured concomitantly to serve as a check on the purity of the samples.

Special attention has been paid to the room temperature rate coefficient for the quenching of Br* by $^{13}CO_2$ which has not been previously determined. The value obtained from the plot in Fig. 1, corrected for the presence of 5% $^{12}CO_2$, is $(2.3 \pm 0.1)10^5$ torr^{-1} sec^{-1}, as compared with a rate coefficient of $(5.0 \pm 0.2)10^5$ sec^{-1} torr^{-1} for the quenching of Br* by $^{12}CO_2$.

A change in the temperature of the sample leads to a change in the average velocity of the molecules, $\bar{v}$, and hence to a change in collision frequency. Thus, it is most germane to convert the measured rate coefficients into average cross sections ($\sigma = k/\bar{v}$) for the present discussion. The cross sections for the quenching of Br* by $^{12}CO_2$ and $^{13}CO_2$ over the temperature range 296–600 °K are summarized in Table I. The *statistical* uncertainties from repeated measurements ranged from

TABLE I. Quenching cross sections of Br^* by $^{12}CO_2$ and $^{13}CO_2$.

$^{12}CO_2$		$^{13}CO_2$	
T (°K)	σ (Å^2)	T (°K)	σ (Å^2)
296	3.3 ± 0.2[a]	296	1.56 ± 0.15
354	3.1 ± 0.3	356	1.5 ± 0.2
398	3.0 ± 0.3	398	1.4 ± 0.2
448	2.7 ± 0.3	454	1.3 ± 0.2
500	2.6 ± 0.3	509	1.2 ± 0.2
558	2.4 ± 0.4	556	1.2 ± 0.2
593	2.3 ± 0.4	600	1.1 ± 0.2

[a]Previous work: σ (Å^2) = 3.2 ± 0.2[5].

±5% at room temperature, to ±15% at the highest temperature. *However, the trend of decreasing cross sections with increasing temperature was reproducible in every instance.*

From the intercepts of plots such as the ones shown in Fig. 1, the rate coefficients for the quenching of Br^* by Br_2 can be obtained. Although no special attention has been devoted to this low X_{CO_2} region, rough analyses of the data indicate that the quenching cross sections of Br^* by Br_2 are only weakly dependent on temperature in the range 300–600 °K.

B. Absolute $E \rightarrow V$ rate coefficients for excitation of ν_3 quanta.

The fraction of the quenching collisions that result in excitation of the ν_3 mode, $F(CO_2)$, has been obtained at room temperature by comparing the intensities of $^{12}CO_2$ and $^{13}CO_2$ fluorescences with that of HCl fluorescence generated by energy transfer from Br^*. Although the method, which has been described in detail previously,[5] is straightforward, and the scatter in the data is usually not larger than ±10%, great care should be exercised in eliminating possible systematic errors. The measured fluorescence intensities should be corrected for differences in detector response, filter transmission, radiative lifetimes, and self-absorption. This latter phenomenon is the most difficult to estimate and therefore it is imperative to work at low molecular concentrations in order to minimize its effects. In our experiments, CO_2 pressures have been kept between 30 and 100 mtorr and the CO_2 fluorescence is compared with that of the same pressure of HCl. Equal Br_2 pressures have also been used in both mixtures. Under these experimental conditions, a plot of $\ln(I_{CO_2}/I_{HCl})$ (where I is the observed molecular fluorescence amplitude) vs molecular pressure gives a straight line. Extrapolation to zero molecular pressure gives fluorescence intensity ratios corrected for self-absorption which are then used to estimate $F(CO_2)$. By taking $F(HCl) = 0.95$,[2] we get $F(^{12}CO_2) = 0.42$ and $F(^{13}CO_2) = 0.50$, or $F(^{13}CO_2/F \times (^{12}CO_2) = 1.2$. This value for $F(^{12}CO_2)$ is in very good agreement with the value of 0.4 obtained previously.[5] Although the absolute values may be subject to systematic errors as discussed before, we feel that the ratio $F(^{13}CO_2)/F(^{12}CO_2)$ is accurate to ±20% since the correction factors used for the two molecules are very similar.

The measurement of $F(CO_2)$ at the higher temperatures involves additional complications. The responsivity of the detector has to be determined as a function of the ambient temperature. This was accomplished by directing chopped 4.3 μm radiation (obtained from a blackbody–narrow bandpass filter combination) through the oven and monitoring its intensity with the InSb detector as the temperature of the oven was varied. It was found that the detector responsivity was constant over the temperature range 300–525 °K. In addition, at high temperatures the InSb detector had to be located 15 cm above the heated fluorescence cell in order to keep it cool. In the case of $^{12}CO_2$, this created a serious problem due to the temperature dependent self-absorption of ν_3 fluorescence by air. Therefore, only results for $^{13}CO_2$, whose ν_3 fluorescence is not significantly absorbed by the atmosphere, are reported. The procedure used in these experiments was as follows. Gas mixtures containing Br_2, $^{13}CO_2$, and Ar were first admitted into the two fluorescence cells at room temperature. The cells were irradiated simultaneously and the ν_3 fluorescence amplitudes generated in the two cells were compared. One cell was then heated to the desired temperature and the fluorescence intensity ratio between the two cells was measured again. The procedure was repeated over a wide pressure range, maintaining the same $^{13}CO_2$ number density in both cells. However, since the absorption coefficient at line center is temperature dependent through its dependence on the linewidth, the observed intensity ratios were again plotted as a function of $^{13}CO_2$ density and extrapolated to zero concentration. It was found that at the molecular pressures used in this experiment (< 150 mtorr) the intensity ratios were independent of pressure.

Our results show that, within experimental error (±20%), the fraction of the quenching collisions which produce ν_3 excitation in $^{13}CO_2$ is independent of temperature in the range 296–525 °K.[22] The uncertainties quoted reflect the scatter in the data at each temperature. The observed average fractions obtained at different temperatures did not show any systematic trend. Therefore, we feel that despite the rather large scatter in the data, our results demonstrate that the fractions that go into ν_3 excitation are indeed independent (within ±20%) of temperature. Consequently, the temperature dependence of the total quenching cross section is similar to that of the cross section for $E - V$ transfer to the ν_3 state, although the latter takes place only in about 50% of the quenching collisions.

C. Calculation of $E \rightarrow V$ energy transfer cross sections due to long-range interactions.

The quenching cross sections for Br^* by $^{12}CO_2$ and $^{13}CO_2$ exhibit negative temperature dependences, a trend predicted by the theory for near resonant energy transfer processes based on long-range multipolar interactions. We have used an approximate version of this treatment, based on the Sharma–Brau treatment of

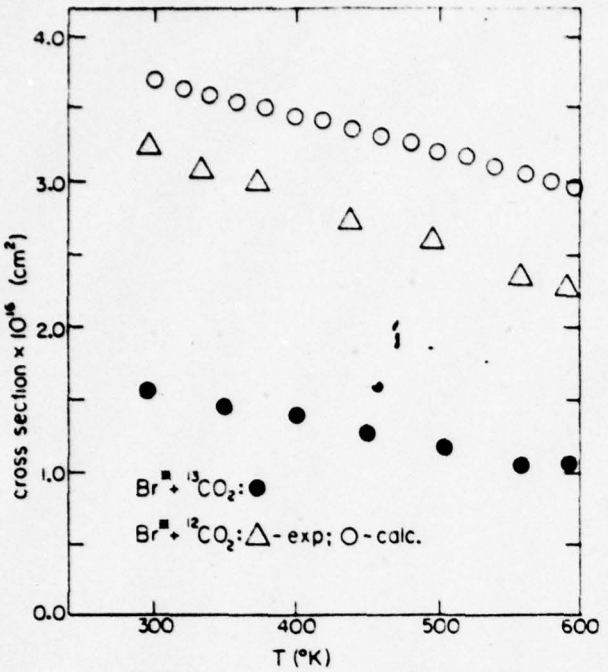

FIG. 2. Cross sections for the quenching of Br* ($4^2P_{1/2}$) by $^{12}CO_2$ (△) and $^{13}CO_2$ (●) over the temperature range 296–600 °K. Probabilities may be obtained by dividing by the gas kinetic cross section, $\sigma_g = \frac{\pi}{4}(d_{Br} + d_{CO_2})^2$ where $d_{Br} \cong d_{Kr} = 3.60$ Å, and $d_{CO_2} = 4.0$ Å. The calculated cross sections for the $E - V$ energy transfer channel for $^{12}CO_2$ are given by the open circles (see text).

$V - V$ energy transfer,[23] to see if this simple theory can account for our experimental observations. For the Br*–CO_2 case, the first nonvanishing term in the multipolar expansion of the interaction potential is due to the dipole–quadrupole interaction. The rms, angle-averaged form of this potential[24] was used in our calculations. The integrated absorption for the (101) – (000) transition of $^{12}CO_2$[25] was used to estimate the transition dipole moment ($\langle\mu\rangle^2 = 9.4\ 10^{-40}$ stat c^2 cm^2), which was assumed to be the same for $^{12}CO_2$ and $^{13}CO_2$. The transition quadrupole moment of Br – Br* was taken from Garstang[26] ($\langle q\rangle^2 = 2.63\ 10^{-51}$ esu^2 cm^4). First order perturbation theory was used to estimate the probabilities of $E - V$ energy transfer, $P(\Delta E, b, v)$ (where b is the impact parameter and v is the relative velocity), for transitions involving $\Delta J = \pm 1$ which are dipole allowed. To obtain the cross sections, $\sigma_J(\Delta E, v)$, the calculated probabilities were integrated over impact parameters, b. In the region $d < b < \infty$ (the collision diameter $d = \frac{1}{2} \times (d_{Br^*} + d_{CO_2}) = 3.8$ Å[27]) the integral was evaluated exactly following Gait.[28] In the region $0 < b < d$ it was assumed that $P(b, v) = P(d, v)$. The probabilities should also be properly averaged over the velocity distribution. However, for the purpose of our calculations we simply used the average thermal velocities $\bar{v} = (8kT/\pi\bar{M})^{1/2}$, where $\bar{M}$ is the reduced mass and k is the Boltzmann constant.

Due to the Boltzmann distribution of rotational levels in the ground state of CO_2, each observed cross section is, in effect, given by a sum over rotational levels, J.

$$\sigma(T) = \sum_J \sigma_J(T) N_J(T) , \tag{4}$$

where T is the temperature and $N_J(T)$ is the relative population of the Jth rotational level in the ground vibrational state at a temperature T. The calculated cross sections, σ, thus obtained for $E - V$ energy transfer from Br* to $^{12}CO_2$ are presented in Fig. 2 along with the experimental results. Considering the assumptions inherent in the theory and the approximations used in the calculations, the agreement between the calculated and the experimental results is satisfactory, especially as it correctly predicts the temperature dependence. It should be emphasized, however, that whereas the experimental curve gives the total quenching cross section, the calculated curve describes only the $E - V$ energy transfer channel to the (101) level of $^{12}CO_2$.

Carrying out similar calculations for $E - V$ energy transfer from Br* to $^{13}CO_2$ yielded cross sections which were an order of magnitude smaller than the observed values and showed a positive temperature dependence.

IV. DISCUSSION

Our results show that the quenching cross sections of Br* by $^{12}CO_2$ and $^{13}CO_2$ exhibit similar negative temperature dependences (Fig. 2). However, the cross sections for quenching by $^{12}CO_2$ are larger than those for the case of $^{13}CO_2$ by more than a factor of 2. At room temperature, about half of the quenching collisions give rise to excitation of the ν_3 mode in both molecules, and this fraction remains the same for $^{13}CO_2$ at higher temperatures. Thus, the probability for $E - V$ energy transfer from Br* to the ν_3 mode of $^{13}CO_2$ has a negative temperature dependence as well. Based on the similarities between the Br*–$^{12}CO_2$ and the Br*–$^{13}CO_2$ systems in all respects except the magnitude of the cross section, it is probable that the $E - V$ energy transfer channel in $^{12}CO_2$ exhibits a negative temperature dependence similar to that of $^{13}CO_2$.

In separate experiments it has been shown[13] that the process Br* + $^{12}CO_2$(000) – Br + $^{12}CO_2$(101) is a major quenching channel. Assuming that an analogous process is important in the quenching of Br* by $^{13}CO_2$, the energy defects associated with the $E - V$ transfer channels in both systems are very similar, being, -30[29] and $+52$ cm^{-1} [30] for $^{12}CO_2$ and $^{13}CO_2$, respectively. However, if we take into account the Boltzmann distribution of rotational levels within the CO_2 ground state and assume, in accordance with the long-range multipolar interaction theory, that those J levels for which the energy defect is minimized have a dominant contribution to the cross section and that only transitions with $\Delta J = \pm 1$ are allowed, then the number of near resonant channels is larger for $^{12}CO_2$ than it is for $^{13}CO_2$. This effect is illustrated schematically in Fig. 3 where the relative intensities of the possible vibration rotation transitions are plotted as a function of the transition energy. For example, transitions involving the most populated rotational level at $T = 600$ °K ($J = 24$) are only 8 cm^{-1} away from resonance for $^{12}CO_2$ whereas the analogous number for $^{13}CO_2$ is 35 cm^{-1}. A possible explanation for the difference in cross sections between $^{12}CO_2$ and $^{13}CO_2$

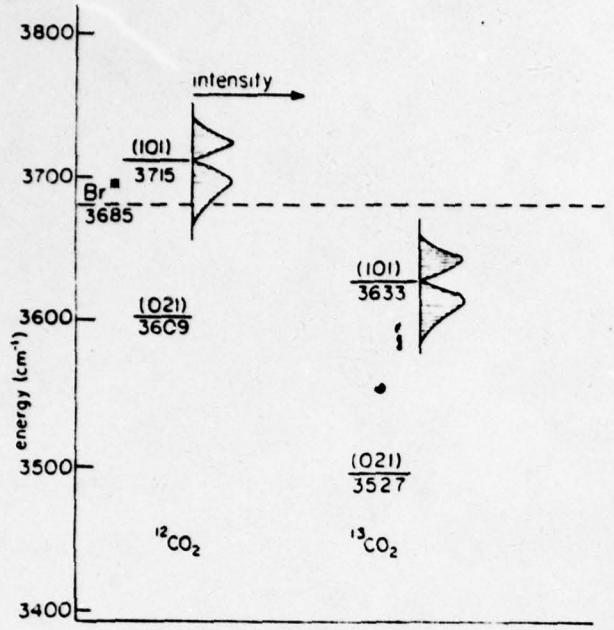

FIG. 3. Partial energy level diagram of $^{12}CO_2$ and $^{13}CO_2$ showing molecular vibrational levels which are near the Br* electronic state at 3685 cm^{-1}. The relative intensities, at room temperature, of possible rotational transitions with $\Delta J = \pm 1$ in the (101) – (000) vibrational band as a function of frequency, are indicated schematically. A Boltzmann distribution of rotational levels in the ground state was assumed. Spectroscopic constants were taken from Refs. 23 and 24. The relative line intensities increase in the direction indicated by the arrow.

may thus involve the difference in the number of participating channels.

The quenching cross sections of Br* by $^{12}CO_2$ and $^{13}CO_2$ exhibit negative temperature dependences, a trend predicted by the long-range multipolar interaction theory for a near resonant energy transfer process. Our approximate calculations based on this theory show that whereas satisfactory agreement is obtained for the case of $^{12}CO_2$, the theory predicts a nonresonant behavior for the Br*–$^{13}CO_2$ case, i.e., small cross sections and a positive temperature dependence. Evidently, for the less resonant case of $^{13}CO_2$, the theory cannot adequately describe the experimental results. It appears that the system can accommodate larger energy discrepancies than suggested by the simple theory. This may occur either through inclusion of higher multipoles which allow transitions with $\Delta J > \pm 1$, or through coupling of rotation to translation, as has been suggested for $V-V$ energy transfer.[31] If we include the next possible transitions (those involving $\Delta J = \pm 3$ which are octupole allowed) the number of near resonant channels in $^{13}CO_2$ becomes comparable to that in $^{12}CO_2$ and a negative temperature dependence is obtained. The transition moments may be smaller than those for $\Delta J = \pm 1$ transitions, thus accounting for the smaller cross sections observed for $^{13}CO_2$. It must be borne in mind, however, that for these shorter range collisions several of the assumptions inherent in the treatment of multipolar interactions by first order perturbation theory are no longer justified.

We would like to point out that although the total quenching rate coefficient of Br* by $^{13}CO_2$ is smaller than that by $^{12}CO_2$, the fraction of the quenching collisions that goes into ν_3 excitation is very similar for both cases. Thus, the mode specificity of the energy transfer process has been retained. A similar phenomenon has been observed for the near resonant $E-V$ energy transfer from I*[7] and Br*[5] to H_2O. $E-V$ transfer is the dominant channel in both cases, despite a much smaller quenching rate coefficient for the I*–H_2O system than for the Br*–H_2O system. It should also be noted that about half of the quenching collisions in the Br*–CO_2 system proceed via channels other than excitation of the ν_3 mode. At present we do not know the nature of the other deactivation channels since information concerning $E-V$ excitation of the other normal modes is not yet available.

Comparison with other $E-V$ energy transfer processes such as deactivation of Br* by H_2O[10] and HF[3] suggests that long-range multipolar interactions can account for the experimental observations for these near resonant channels as well. However, away from resonance other collision mechanisms should probably be invoked to explain the observed deactivation rates and their dependence on temperature. In the case of quenching of Br* by HCl for example, the mode specificity of the energy transfer process and the large rate coefficients and their temperature dependence[21] are consistent with a nonadiabatic curve crossing mechanism. The very weak temperature dependence observed in this work for the deactivation of Br* by Br_2 may be explained in terms of quenching via collision complex formation, as suggested by Hofmann and Leone.[11]

V. CONCLUSIONS

The excitations of the ν_3 modes of $^{12}CO_2$ and $^{13}CO_2$ via $E-V$ energy transfer from Br* are fast, mode specific energy transfer processes. About half of the quenching collisions produce excitation of vibrational modes containing ν_3 quanta in both molecules. However, $^{12}CO_2$ is about twice as efficient as $^{13}CO_2$ in quenching Br*. The cross sections have a negative dependence on temperature for both molecules, a trend typical of a near resonant, long-range interaction. A simple $E-V$ energy transfer theory based on long-range multipolar interactions gives satisfactory agreement with the experimental results for the Br*–$^{12}CO_2$ system, while a modified version might be needed to account for the experimental observations in the case of $^{13}CO_2$.

Our results, as well as the results of other investigators, indicate that in near resonant $E-V$ energy transfer processes involving halogen atoms in the $^2P_{1/2}$ state, long-range multipolar interactions are of major importance.

[1] R. J. Donovan, D. Husain, and C. D. Stevenson, Trans. Faraday Soc. 66, 2148 (1970).
[2] S. R. Leone and F. J. Wodarczyk, J. Chem. Phys. 60, 314 (1974).
[3] F. J. Wodarczyk and P. B. Sackett, Chem. Phys. 12, 65 (1976).

[4]A. Hariri, A. B. Petersen, and C. Wittig, J. Chem. Phys. **65**, 1872 (1976).
[5]A. Hariri and C. Wittig, J. Chem. Phys. **67**, 4454 (1977).
[6]S. Lemont and G. W. Flynn (unpublished work).
[7]A. J. Grimley and P. L. Houston, J. Chem. Phys. **8**, 3366 (1978).
[8]A. T. Pritt, Jr. and R. D. Coombe, J. Chem. Phys. **65**, 2096 (1976).
[9]R. D. Coombe and A. T. Pritt, Jr., J. Chem. Phys. **66**, 5214 (1977).
[10]A. Hariri and C. Wittig, J. Chem. Phys. **68**, 2109 (1978).
[11]H. Hofmann and S. R. Leone, Chem. Phys. Lett. **54**, 314 (1978).
[12]A. B. Petersen, C. Wittig, and S. R. Leone, Appl. Phys. Lett. **27**, 305 (1975).
[13]A. B. Petersen, C. Wittig, and S. R. Leone, J. Appl. Phys. **47**, 1051 (1976).
[14]A. B. Petersen, L. W. Braverman, and C. Wittig, J. Appl. Phys. **48**, 230 (1977).
[15]H. Zimmerman and T. F. George, (a) J. Chem. Phys. **61**, 2468 (1974); (b) J. Chem. Soc. Faraday II **71**, 2030 (1975).
[16]J. J. Ewing, Chem. Phys. Lett. **29**, 50 (1974).
[17]R. J. Donovan, C. Fotakis and M. F. Golde, J. Chem. Soc. Faraday II **72**, 2055 (1976).
[18]See for example C. Bradley Moore, Adv. Chem. Phys. **23**, 41 (1973) and references cited therein.
[19]J. J. Deakin and D. Husain, J. Chem. Soc. Faraday II **68**, 1603 (1972).
[20]C. Fotakis and R. J. Donovan, Chem. Phys. Lett. **54**, 9 (1978).
[21]H. Reisler and C. Wittig, J. Chem. Phys. **68**, 3308 (1978).
[22]The temperature range in these experiments was limited by the need to use a broadband filter to encompass the whole band envelope. Above 525 °K the thermal radiation level reaching the detector became too high.
[23]R. D. Sharma and C. A. Brau, (a) Phys. Rev. Lett. **19**, 1273 (1967); (b) J. Chem. Phys. **50**, 924 (1969).
[24]H. Margenau, Rev. Mod. Phys. **7**, 1 (1939).
[25]S. S. Penner, *Quantitative Molecular Spectroscopy and Gas Emissivities* (Addison–Wesley, Reading, MA, 1959), p. 23.
[26]R. H. Garstang, J. Res. Natl. Bur. Std. Sec. A **68**, 61 (1964).
[27]The molecular diameter of CO_2 (4.0 Å) has been taken from J. O. Hirschfelder, C. F. Curtiss, and R. B. Bird, *Molecular Theory of Gases and Liquids* (Wiley, New York, 1954). The diameter of Br^* is taken to be the same as Kr (3.60 Å).
[28]P. D. Gait, Chem. Phys. Lett. **35**, 72 (1975).
[29]C.-P. Courtoy, Can. J. Phys. **35**, 608 (1957).
[30]C.-P. Courtoy, Ann. Soc. Sci. Bruxelles **73**, 5 (1959).
[31]J. C. Stephenson and C. Bradley Moore, J. Chem. Phys. **56**, 1295 (1972).

X. COLLISIONAL ENERGY TRANSFER FROM $I_2(B^3\Pi_{0u^+})$ TO CO_2[a]

M.A. Capote, H. Reisler, and C. Wittig
Department of Chemistry
University of Southern California
Los Angeles, California 90007

ABSTRACT

Electronic to vibrational energy transfer from $I_2(B^3\Pi_{0u^+})$ to the ν_3 vibrational mode of CO_2 is reported. Only 4±2% of the collisions in which CO_2 quenches $I_2(B^3\Pi_{0u^+})$ result in $CO_2(\nu_3)$ excitation. This efficiency does not vary markedly with excitation wavelength in the region 575-620 nm, suggesting the absence of resonant contributions to the quenching process.

[a]Research supported by the U.S. Army Research Office under Grant No. DAAG29-76-G-0124, and by the Donors of the Petroleum Research Fund, administered by the American Chemical Society.

I. INTRODUCTION

The quenching of electronically excited diatomic halogens, which is often accompanied by dissociation of the excited molecule, has recently been the subject of considerable research.[1-13] The collisional redistribution of energy within the electronically excited vibration-rotation manifold has been studied in the cases of Br_2,[1-2] I_2,[3-7] BrCl,[8] and BrF.[9] In the case of $I_2(B^3\Pi_{0u^+})$ (referred to hereafter as I_2^*) collisional quenching cross sections have been measured in both steady state[3-5] and time resolved[10] experiments. These studies have demonstrated that the quenching cross sections vary markedly with excitation energy as well as the quenching species involved. A simple model which invokes Van der Waals forces between I_2^* and the quenching species is in very reasonable agreement with these data.[12] Not surprisingly however, the quenching cross sections for *molecules* are consistently larger than for *atoms* even though the Van der Waals model does not predict this difference.[14] Additional energy disposal channels which become available via the vibrational and rotational degrees of freedom of molecules may account in part for this difference.

Although studies of the collisional quenching of electronically excited atoms by molecules have demonstrated that such quenching is often characterized by high electronic to vibrational (E→V) energy transfer efficiencies,[15-17] the disposal of excited state energy via the quenching of electronically excited diatomic molecules has received little attention. Only recently, have Hsu and Lin[11] shown that in the quenching of I_2^* and ICl* by CO, vibrational excitation of CO is a minor quenching channel. In the present communication, E→V energy

transfer from I_2^* to the ν_3 mode of CO_2 is reported. The E→V transfer efficiency was determined by comparing the amount of CO_2 containing one quantum of ν_3 excitation, hereafter referred to as $CO_2(\nu_3)$, that results from the quenching of I_2^* by CO_2, with the amount of $CO_2(\nu_3)$ produced from the quenching of $Br(4^2P_{\frac{1}{2}})$, hereafter referred to as Br*, by CO_2.[15] Our experiments show that only 4±2% of the collisions in which CO_2 quenches I_2^* result in excitation of a quantum of ν_3 vibration in CO_2.

II. EXPERIMENTAL

The experimental arrangement is shown schematically in fig. 1. The fluorescence cell and vacuum system were described elsewhere.[15a] A flashlamp pumped dye laser (Chromatix CMX-4, 1.0 μs FWHM, ~3 cm^{-1} FWHM) was used to produce I_2^*. Time resolved $CO_2(\nu_3)$ fluorescence was monitored at right angles to the laser beam with a large area InSb photovoltaic detector (1μs risetime). To minimize self-absorption of the fluorescence, the laser beam was situated as close to the cell's window as possible. An interference filter was used to isolate $CO_2(\nu_3)$ fluorescence at the detector. Digital signal averaging was used to obtain signal to noise ratios >10. The laser energy was monitored simultaneously with the fluorescence signal with a photodiode which had been calibrated against a thermopile. In order to assure the reproduceability of the laser energy measurements, the laser beam was diffused prior to detection. Typically, the pulse to pulse variation in laser energy was ≤±10%. Signal averaged CO_2 fluorescence signals were reproducible to within ±5%.

Gases were premixed before introduction into the cell. I_2 was maintained in a sidearm connected to the mixing bulb and its

pressure was determined from the temperature of the sidearm.[7] The cell and vacuum system were seasoned with the appropriate halogen before experiments. CO_2 and Br_2 were purified as described previously.[15a] Reagent grade I_2 was purified under vacuum by distillation and fractionation at room temperature. To measure the amount of energy absorbed by I_2, a 49 cm cell, to which a cold finger had been attached, was employed. The laser beam was passed through this I_2 vapor filled cell, and the laser energy was monitored with a photodiode.

III. RESULTS AND DISCUSSION

Details of the kinetics which describe the quenching of electronically excited species by CO_2 have been published elsewhere.[15a] I_2^* is produced only during the laser pulse, and is removed via several processes, one of which is collisional energy transfer to CO_2 with concomitant excitation of the ν_3 vibration. The predominant mechanism whereby I_2^* is quenched by CO_2 is known to produce two ground state iodine atoms.[13] In this case, since the photon which produces I_2^* is ~16,000 cm^{-1} and the dissociation energy to form two ground state iodine atoms is 12,450 cm^{-1}, the excess energy is sufficient to excite only one ν_3 quantum in CO_2. Considering the small fraction of collisions which excite ν_3 vibrations in CO_2, the quenching of I_2^* by CO_2, producing $I_2(X^1\Sigma_g^+)$ and $CO_2(mnp)$ with $p>1$, cannot be ruled out.

The time varying concentration of $CO_2(\nu_3)$ can be described in a straightforward manner.[15a] Since the I_2^* radiative lifetime $\simeq$1 μs, the $CO_2(\nu_3)$ concentration is characterized by a risetime <1 μs,

followed by a much slower decay. At high CO_2 pressures (e.g. 100 torr) almost all of the quenching of I_2^* is via collisions with CO_2 molecules and other quenching processes do not play an important role. At these pressures, radiation from the 001 state of CO_2 is almost completely trapped, so that photons which arrive at the detector emanate from a state that is not connected to 000. The most likely candidate is 011, but other states such as 021 and 101 may also contribute. For the purposes of our measurements, it is not necessary to monitor 001 directly since we compare intensities measured at the same CO_2 concentrations. In our experiments, species such as CO_2(mnp) undergo very rapid energy transfer processes, *in which* ν_3 *quanta are preserved.* These processes occur instantly on the time scale of interest.[19] At $t>2$ μs, $[CO_2(\nu_3)]$ is given by

$$[CO_2(\nu_3)](t) = \frac{k_2}{k_3} [I_2^*]_0 \, e^{-t/\tau} \tag{1}$$

where $[I_2^*]_0$ is the concentration of I_2^* produced by the laser pulse, τ is the lifetime of $CO_2(\nu_3)$, and k_2 and k_3 are rate coefficients for the collisional processes

$$I_2^* + CO_2 \xrightarrow{k_2} CO_2(\nu_3) + 2I \text{ (or } I_2) \tag{2}$$

$$I_2^* + CO_2 \xrightarrow{k_3} CO_2(\text{all states}) + 2I \text{ (or } I_2) \tag{3}$$

Implicit in (2), is that processes which produce CO_2(mnp) transfer vibrational energy efficiently but preserve ν_3 excitation. Since the fluorescence signal is proportional to $[CO_2(\nu_3)]$, an extrapolation gives

$$I_{\nu_3}^{I_2^*}(0) = C[CO_2(\nu_3)](0) = C[I_2^*]_0 \, F_{\nu_3}^{I_2^*} \tag{4}$$

where $I_{\nu_3}^{I_2^*}$ is the fluorescence signal, C is a constant, and $F_{\nu_3}^{I_2^*}=k_2/k_3$ is the probability of exciting a ν_3 quantum in an I_2^* - CO_2 collision. Within experimental uncertainty, self-absorption of $CO_2(\nu_3)$ fluorescence was found to be constant over the range of pressures employed, thus allowing self-absorption to be incorporated into the constant C.

We find in our experiments that $I_{\nu_3}^{I_2^*}(0)$ depends on the wavelength of the I_2^* excitation. In tuning the dye laser through the region 575-620 nm, we observe eleven $CO_2(\nu_3)$ fluorescence signal maxima which correspond, within experimental uncertainty, to the locations of I_2 absorption bands.[10] The most intense $CO_2(\nu_3)$ fluorescence occurs with the dye laser tuned to 591.7 nm. This excitation wavelength was chosen for comparison with the Br^* + CO_2 system.

To eliminate the need to determine C, which includes the detector sensitivity, filter response, $CO_2(\nu_3)$ self-absorption, etc., values of $I_{\nu_3}^{I_2^*}(0)$ can be compared to similar values obtained from the quenching of Br^* by CO_2. An equation similar to eq. (4) can be written from a consideration of the kinetics of Br^* + CO_2, and this equation can be combined with eq. (4) yielding:

$$F_{\nu_3}^{I_2^*} = \frac{I_{\nu_3}^{I_2^*}(0)}{I_{\nu_3}^{Br^*}(0)} \frac{[Br^*]_0}{[I_2^*]_0} F_{\nu_3}^{Br^*} \qquad (5)$$

where $I_{\nu_3}^{Br^*}(0)$ is the fluorescence signal (extrapolated to t=0) for Br^* + CO_2, $[Br^*]_0$ is the concentration of Br^* produced by the laser pulse, and $F_{\nu_3}^{Br^*}$, the probability of transferring a ν_3 quantum in a Br^* - CO_2 collision, is taken as unity.[20] $[Br^*]_0$ can

be determined from published Br_2 absorption coefficients[21] and the efficiency of Br* formation.[22]

The absorption of the laser beam by I_2 does not follow the Beer-Lambert law in the region 575-620 nm.[23,24] For our purposes $[I_2^*]_0$ could be determined from an empirical function of the variables which affect absorption, $A(\lambda,[I_2],L,P_{total})$, so that

$$[I_2^*]_0 = [\langle n \rangle_t]\, A(\lambda,[I_2],L,P_{total})\, f_{I_2^*} \qquad (6)$$

where $[\langle n \rangle_t]$ is the time integrated photon density in the laser beam, L is the length of the absorbing medium, P_{total} is the total pressure in the cell which includes absorbing and non-absorbing (but line broadening) species, and $f_{I_2^*}$, the efficiency of forming I_2^*, = $0.9^{+0.1}_{-0.2}$ at ≈591.7 nm.[23] Ideally, A should be determined in the fluorescence cell using the actual experimental pressures and path lengths. However, the absorption under these conditions was too small to be measured reliably. Therefore, the dependence of A at 591.7 nm on the product $(L)[I_2]$ was measured using the 49 cm cell, and A was extrapolated to the fluorescence cell $(L)[I_2]$ values. These data are shown in fig. 2. Because of the small amount of absorption, there is large uncertainty (±40%) in the values of A obtained by this extrapolation. As fig. 3 demonstrates, pressure broadening did not have a significant effect on A at CO_2 pressures up to 100 torr.

Sixteen values of $I^{I_2}_{\nu_3}(0)$ and $I^{Br^*}_{\nu_3}(0)$ were obtained at CO_2 pressures ranging from 65 to 100 torr. Using eq. (5), these data gave $F^{I_2^*}_{\nu_3}$ = 0.04±0.02 at 591.7 nm.

The cross section for the quenching of I_2^* by CO_2 is known to increase by almost a factor of two as the wavelength increases from 580 nm to 620 nm. In order to estimate the wavelength dependence of $F_{\nu_3}^{I_2^*}$, values of $I_{\nu_3}^{I_2^*}(0)$ were obtained for each of the eleven $CO_2(\nu_3)$ fluorescence maxima. By normalizing the literature values of the wavelength dependence of the I_2 absorption coefficient[23] to the value of A we obtained at 591.7 nm, the wavelength dependence of A was obtained. From this approximate wavelength dependence of A, and the value of $F_{\nu_3}^{I_2^*}$ obtained at 591.7 nm, the wavelength dependence of $F_{\nu_3}^{I_2^*}$ shown in fig. 4 was obtained. Fig. 4 indicates that there is not a *marked* wavelength dependence of $F_{\nu_3}^{I_2^*}$.

The data indicate that E→V energy transfer to the ν_3 mode of CO_2 is not a major channel in the quenching of I_2^* by CO_2. If quenching collisions simply induce a non-adiabatic transition to a dissociative I_2 potential surface, then vibrational excitation of CO_2 will be small. Such vibrational excitation may be mode specific in the sense that certain collision geometries may facilitate the non-adiabatic transition, and therefore, forces on the CO_2 molecule will be directed so as to excite specific normal modes. Also, vibrational modes with weak restoring forces will be an easier prey to the external forces on the CO_2 molecule than those modes with stronger restoring forces. A measurement of ν_2 excitation in CO_2 as a consequence of I_2^* quenching may illuminate this point, but this is a rather difficult experiment.

In the present investigation, the precision of the fluorescence signal comparison method for obtaining E→V energy transfer

efficiencies was limited primarily by the uncertainty in the absorption of I_2. This large uncertainty did not affect the major conclusions, however, since only a very small amount of energy was found in the ν_3 mode. The intensity comparison method is easily adaptable to many other systems making it possible to obtain energy transfer efficiencies for systems which are characterized by faster rise times than the detection system can discern. The only requirement is that a value of F_{ν_3} be known for another system employing the same quencher.

The authors are indebted to Eric Weitz for illuminating discussions regarding self-absorption.

REFERENCES

1. G.A. Capelle, S. Sakurai, H.P. Broida, J. Chem. Phys. 54 (1971) 1728.
2. F. Zaraga, N.S. Nogar, C.B. Moore, J. Mol. Spect. 63 (1976) 564.
3. R.L. Brown, W. Klemperer, J. Chem. Phys. 41 (1964) 3072.
4. J.I. Steinfeld, W. Klemperer, J. Chem. Phys. 42 (1965) 3475.
5. R.B. Kurzel, J.I. Steinfeld, J. Chem. Phys. 53 (1970) 3293.
6. S.R. Jeyes, A.J. McCaffery, M.D. Rowe, Mol. Phys. 36 (1978) 31.
7. R. Clark, A.J. McCaffery, Mol. Phys. 35 (1978) 617.
8. M.A.A. Clyne, I.S. McDermid, Trans. Far. Soc. 74 (1978) 807.
9. M.A.A. Clyne, I.S. McDermid, Trans. Far. Soc. 74 (1978) 644.
10. G.A. Cappelle, H.P. Broida, J. Chem. Phys. 58 (1973) 4212.
11. D.S.Y. Hsu, M.C. Lin, Chem. Phys. Lett. 56 (1978) 79.
12. J.E. Selwyn, J.I. Steinfeld, Chem. Phys. Lett. 4 (1969) 217.
13. E. Rabinowitch, W.C. Wood, J. Chem. Phys. 4, (1936) 358.
14. Plotting the quenching cross sections given in ref. 10 against the parameters given in ref. 12 indicates that for a given excitation energy, separate but parallel lines can be drawn through the points corresponding to atoms and molecules.
15. (a) A. Hariri, C. Wittig, J. Chem Phys. 67 (1977) 4454.
    (b) A.B. Petersen, C. Wittig and S.R. Leone, Appl. Phys. Lett. 27 (1975) 305.
    (c) A.B. Petersen, C. Wittig, and S.R. Leone, J. Appl. Phys. 47 (1976) 1051.
    (d) A.B. Petersen, L.W. Braverman and C. Wittig, J. Appl. Phys. 48 (1977) 230.

(e) A. Hariri, A.B. Petersen, and C. Wittig, J. Chem. Phys. 65 (1976) 1872.

(f) A.B. Petersen and Curt Wittig, J. Appl. Phys. 48 (1977) 3665.

16. A.J. Grimley, P.L. Houston, J. Chem. Phys. 68 (1978) 3366.

17. A.J. Grimley, P.L. Houston, J. Chem. Phys. 69 (1978) 2339.

18. L.J. Gillespie, L.H.D. Fraser, J. Am. Chem. Soc. 58 (1936) 2260.

19. J. Finzi and C.B. Moore, J. Chem. Phys. 63 (1975) 2285.

20. In previous work,[15a] we estimated $F_{\nu_3}^{Br^*}=0.4$. This number was surprisingly low in light of the very rapid and mode selective nature of the transfer of energy from Br* to CO_2. Recently, E. Weitz at Northwestern University has carefully measured the self-absorption of CO_2 at low pressures (~10 mtorr). Using his data, our revised estimate of $F_{\nu_3}^{Br^*}$ is very close to unity.

21. D.J. Seery and D. Britton, J. Chem. Phys. 68 (1964) 2263.

22. T.G. Lindeman, J.R. Wiesenfeld, J. Chem. Phys. 70 (1979) 2882.

23. J. Tellinghuisen, J. Chem. Phys. 58, (1973) 2821.

24. D.H. Burde, R.A. McFarlane, J.R. Wiesenfeld, Chem. Phys. Lett. 32 (1975) 296.

FIGURE CAPTIONS

1. Schematic drawing of the experimental arrangement: D-diffuser, PD-photodiode, InSb-infrared detector.
2. I_2 absorption at 591.7 nm vs. optical density. Absorption is defined as (outgoing energy)/(incoming energy). The square datum is the average of the data shown in Fig. 3. The *fluorescence* experiments were performed in the region $(L)[I_2] = 0.2\text{-}0.3\times10^{-7}$ mole/cm^2. The dashed lines indicate the large uncertainty in the slope (±40%).
3. Absorption vs. CO_2 pressure at $(L)[I_2]=10^{-7}$ mole/cm^2. Here the total pressure is approximately the pressure of CO_2. The error bar shown is typical.
4. Dependence of $F_{\nu_3}^{I_2*}$ on excitation wavelength. The error bar shown is typical.

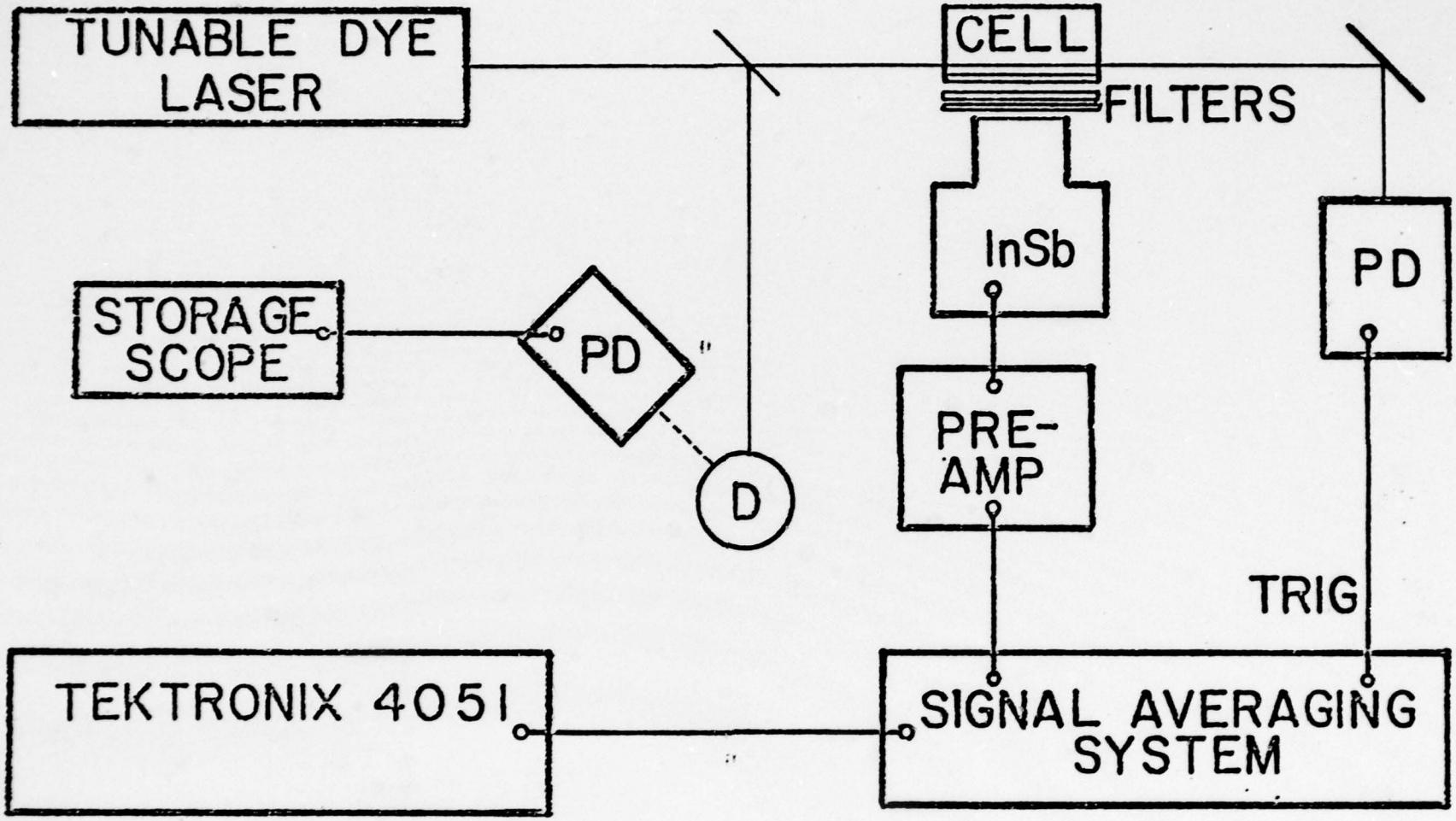
TUNABLE DYE LASER
CELL
FILTERS
InSb
PD
STORAGE SCOPE
PD
PRE-AMP
D
TRIG
TEKTRONIX 4051
SIGNAL AVERAGING SYSTEM

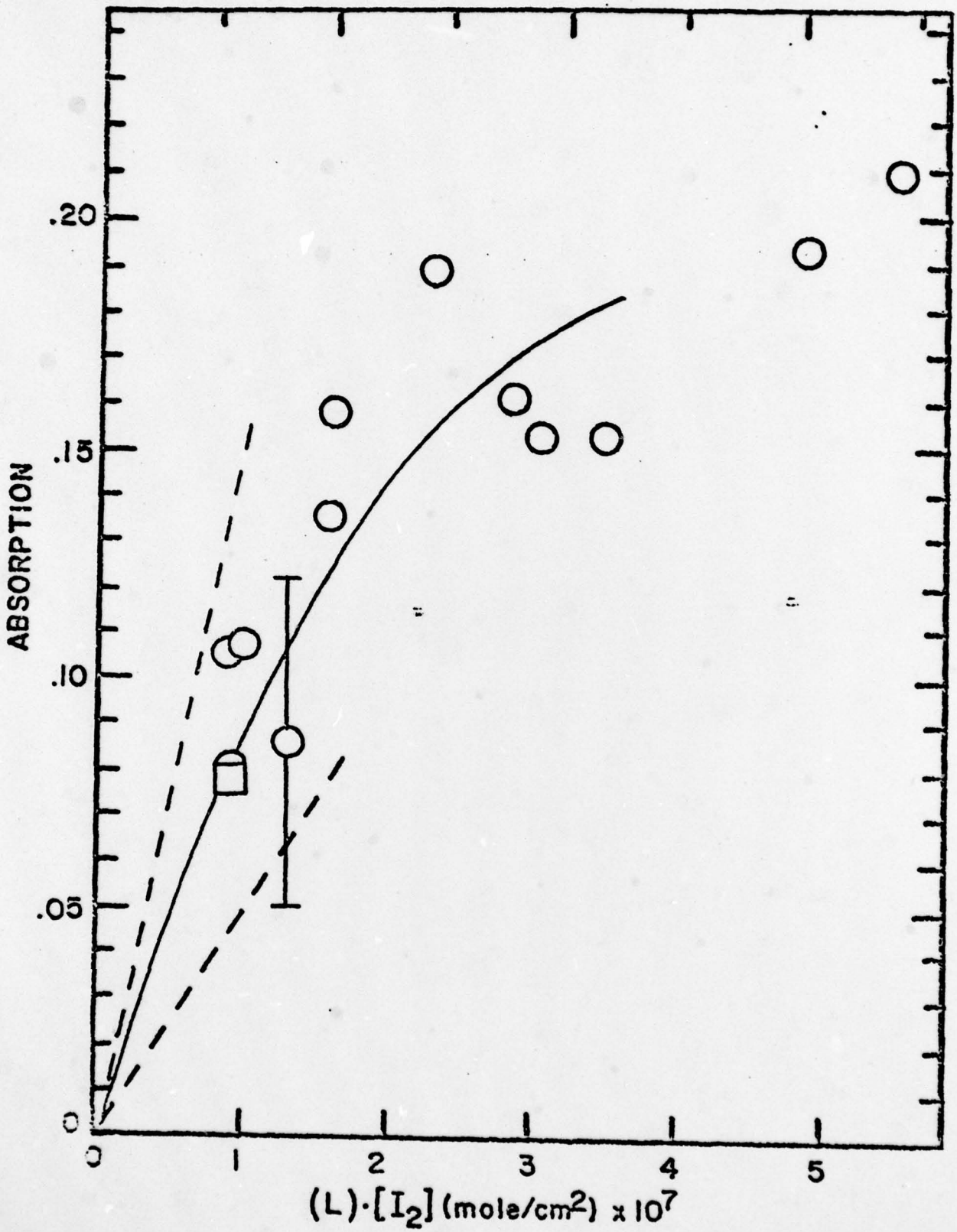
ABSORPTION
.20
.15
.10
.05
0
0
1
2
3
4
5
(L)·[I2] (mole/cm2) x 10^7

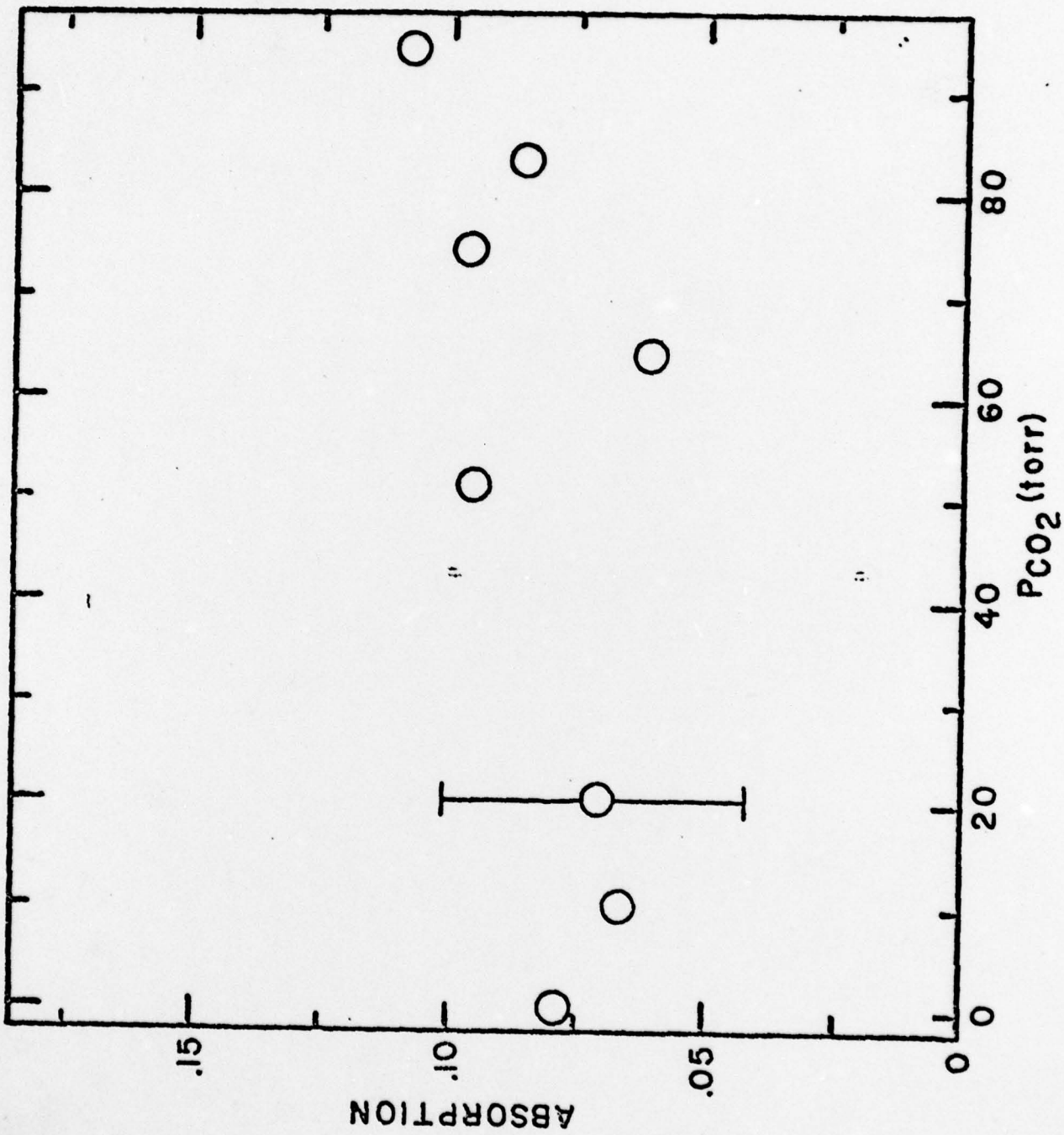
ABSORPTION
.15
.10
.05
0
0
20
40
60
80
P_{CO_2} (torr)

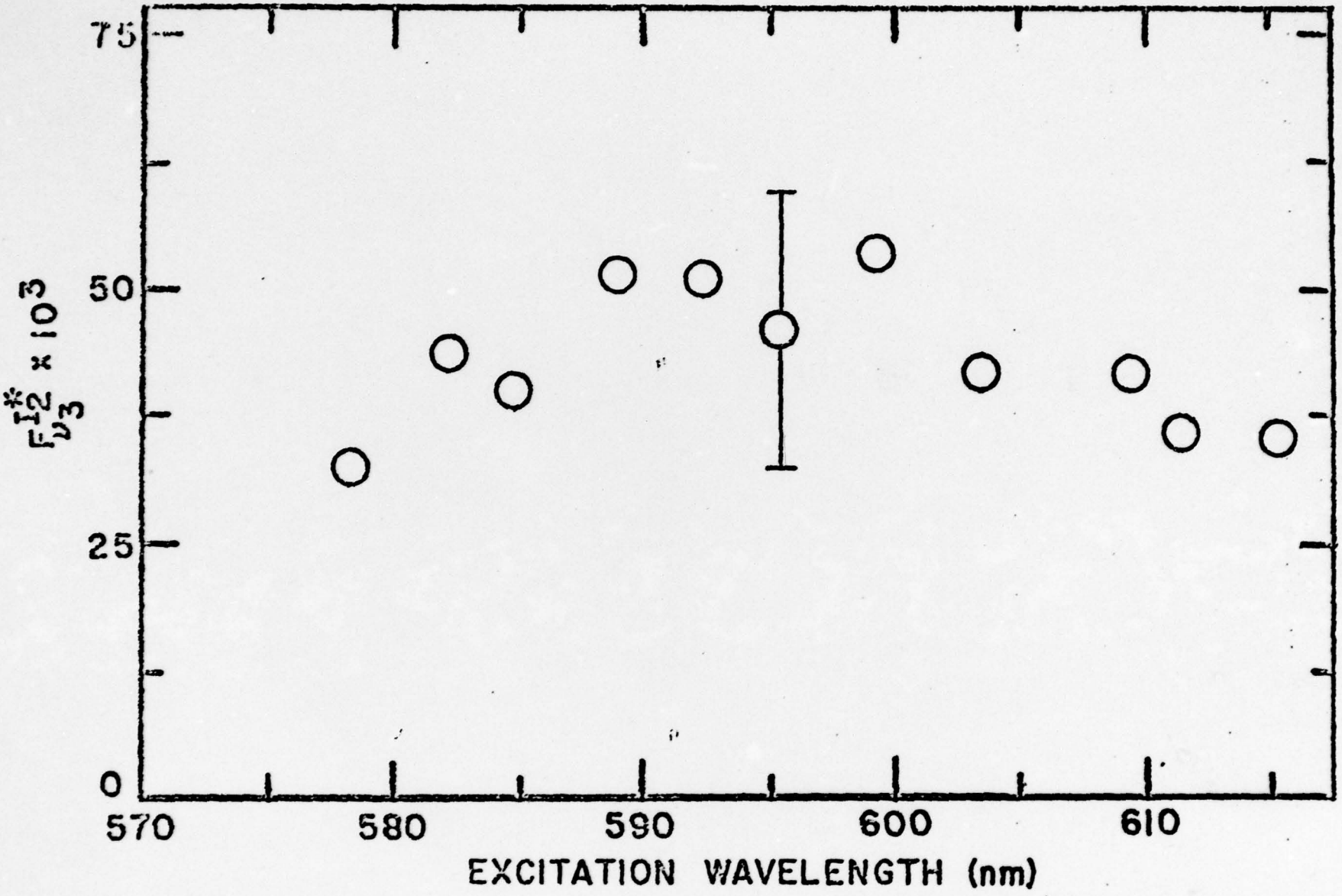
75
50
25
0
$F_{D3}^{*F2} \times 10^3$
570
580
590
600
610
EXCITATION WAVELENGTH (nm)